Synthesis of Graphite/SiC Microcomposites and their influence on MgO-C Refractories

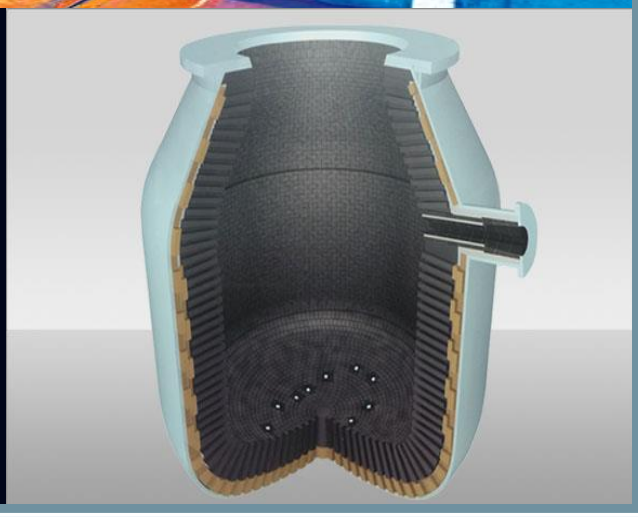

RAJU MULA

National Institute of Technology

Rourkela -769008

Synthesis of Graphite/SiC Micro-composites and their influence on MgO-C Refractories

A Thesis Submitted in Partial Fulfillment of the

Requirements for the Degree of

MASTER OF TECHNOLOGY (RESEARCH)

In

Ceramic Engineering

By

Raju Mula

(Roll No: 612CR604)

Under the guidance of

Prof. Debasish Sarkar

Department of Ceramic Engineering
National Institute of Technology, Rourkela

August 2015

National Institute of Technology

Department of Ceramic Engineering

Rourkela, INDIA

CERTIFICATE

This is to certify that the thesis entitled "**Synthesis of Graphite/SiC Micro-composites and their influence on MgO-C Refractories**" being submitted by **Mr. Raju Mula**, for the degree of **Master of Technology** (Research) in **Ceramic Engineering** to the National Institute of Technology, Rourkela, is a record of bonafide research work carried out by him under my supervision and guidance. His thesis, in my opinion, is worthy of consideration for the award of the degree of Master of Technology (Research) in accordance with the regulations of the institute.

The results embodied in this thesis have not been submitted in any other university/ institute for the award of any Degree or Diploma.

Dr. Debasish Sarkar
Associate Professor
Department of Ceramic Engineering
National Institute of Technology
Rourkela -769008

Declaration

I hereby declare that my M.Tech (Research) thesis is entitled as "**Synthesis of Graphite/SiC Micro-composites and their influence on MgO-C Refractories".** This thesis is my own work and has not been submitted in any form for another degree or diploma at any university or other institution of tertiary education. Information derived from the published and unpublished work of others has been acknowledged in the text and a list of references given in this thesis.

Raju Mula

_____ _____

Date Signature

TABLE OF CONTENTS

3. Experimental Work

4. Results and Discussion

SECTION-I

Synthesis of Graphite-SiC Microcomposites from Natural Flake Graphite and Microfine Silica at different conditions

Acknowledgements

It is with the most sincere thanks to who helped me to make this thesis possible.

I wish to express my deep, sincere gratitude to advisor Prof. Debasish Sarkar for assigning me the project and for his inspiring guidance, constructive criticism and valuable suggestion throughout this research work. I would also like to thank Prof. Himadri Sekhar Maiti, Former Director, CGCRI- Kolkata, currently INAE Distinguished Professor, Govt. College of Engineering and Ceramic Technology, Kolkata for the continuous suggestion to achieve the research objective.

I am extremely thankful to the TSD group of Department of Science and Technology (DST), New Delhi for providing me the financial support throughout my research period. I would like to express my gratitude to Dr. Sukumar Adak (Ex.VP Technology, TKRL, Belpahar) for allowing me to carry out my project work TRL Krosaki Refractories Limited.

I express my sincere thanks to Prof. Swadesh Pratihar, Head of the Department, Ceramic Engineering for providing me all the departmental facilities required for the completion of the project work. I am also thankful to all other faculty members of the Department of Ceramic Engineering, NIT Rourkela for their constructive suggestions and encouragement at various stages of the work.

I am also thankful to Dr. M. Sathiya Kumar (AGM, TKRL), Tapas Mahata, for their valuable suggestions and encouragements at various stages of the work.

My sincere thanks to all non-teaching staffs in Department of Ceramic Engineering for providing full of high- spirited delight in the lab and helping me throughout this project.

My sincere indebted to my senior research colleagues Sanjay Kumar Swain, Jayarao Gorinta, Abhisek Choudhary, Sambi Reddy Bhemavarapu, Sangeeta Adhikari, Mayaluri Zefree Lazarus for their unconditional support and constant motivation whenever needed. I am very grateful my friends Prtiva Adhikari, Venus, Sarath Chandra, Sowjanya, Soumya, Abhinay, Venkatesh, Sreenivasulu and Satyananda Behera who have given me their friendship, put up with my odd hours, and provided me with lifts and practical help.

Last but not least, I would like thank to my dear parents & family members and friends who have patiently extended all kinds of help for accomplishing this work.

Raju Mula

Abstract

The magnesia carbon (MgO-C) refractory is a classical choice for the working lining of steel making furnaces because of slag corrosion and thermal shock resistance. However, the poor oxidation resistance of carbon beyond 900^{o}C eventually damage the brick, and subsequent necessities of reinstallation enhance the cost of steel. Hence, minimization of carbon content without compromising of existence properties of MgO-C brick is one of the prime research areas. The present investigation aims to replace a part of the carbon (mostly graphite flakes) with graphite-SiC microcomposite (C/SiC). The latter non-oxide SiC is known to have excellent high temperature strength, better oxidation resistance, high abrasion resistance and moderate thermal conductivity. The basic objective of this dissertation is to carry out systematic laboratory and pilot industrial scale preparation of composites and understand the effect of microcomposites on MgO-C refractory properties. The micro-composite has been synthesised by a simple carbothermal reduction of microfine silica (SiO_2) in presence of graphite flakes in the temperature range of 1600 - 1650^{o}C under a reducing atmosphere created by packing the reactants within petroleum coke in raising hearth furnace (RHF)/ tunnel kiln (TK) or either controlled atmospheric furnace (CAF). It has been observed that two different morphologies of the SiC phase namely fibre/rod and ribbon developed based on the specific condition of synthesis. A different grade of MgO-C bricks has been prepared through the addition of a different percentage of synthesized graphite-SiC composites at an optimum processing condition and evaluated their physical, thermo-mechanical, oxidation and slag corrosion behaviour. An optimum content of SiC present in the synthesized graphite – SiC microcomposite exhibits better oxidation resistance, hot modulus of rupture and slag corrosion properties compared to the only graphite content brick or addition of equivalent amount of free commercial grade β- SiC containing MgO-C brick.

Keywords: Magnesia carbon refractory, Graphite-SiC micro-composite (C/SiC), β- SiC

List of Figures

List of Tables

Chapter -1

Introduction

1.1. Introduction Overview

Refractory materials are defined by the ASTM, are supposed to heat resistant and can be exposed to different degrees of mechanical and thermal stress and strain. Apart from this, they are also resistant towards corrosion /erosion from solid, liquid and gas diffusion, and mechanical abrasion at various temperatures [1]. These refractory materials are used in various high-temperature process applications like steel and iron making, cement industries, non-ferrous metal, cement, glass, chemical industries, etc. They are commonly used in high-temperature furnaces, kilns, boilers, regenerators, etc.

In general, refractories are chemically classified into three major groups;

a) Acidic (Fireclay, Silica, Zircon, etc.)
b) Basic (Magnetite, Dolomite, Magnesia-carbon, Magnesia-chrome, Alumina-Magnesia-Carbon, etc.)
c) Neutral (Alumina, Carbon, Silicon carbide, Mullite, etc.) [2].

Iron and steel industries are the major consumers of refractories. The world steel association provided recent figures in 2013; the total crude steel production was 1607.2 million tonnes (MT). China is currently the biggest steel producing country, which accounted for 48.5% of the world steel production in 2013. With the rapid rise in production, India has become a 4th largest producer of the crude steel and the maximal producer of sponge iron in the world in 2013. India produced 81.2 MT crude steel production in 2013, and it is targeted to 300 million tonnes per annum capacity by 2025. The 12th plan has projected that the crude steel capacity in the county is likely to be113.3 million tonnes by 2016-17. The national steel policy had set a production targeted to 130 million tonnes by 2019-20 if all requirements are effectively met. The proposed assessment expansion plans are implemented according to the schedule; India may become second largest crude steel producer in the world by 2020 [3]. In the recent years, the production of refractory has also increased to reach the growing demand for steel production. The capacity utilization, however, currently stands at around 11.5-12 lakh tonnes per annum. Also, there has been an extraordinary change in refractory technology to fulfil the demand of high-quality steel production

From the global stock, steel industries (75%), cement industries (12%), non-ferrous industries (5-6 %) and glass industries (3%) are the major consumers of refractories, which had been shown in the Figure 1.1. Refractories are mostly used (70%) in basic metal industries whereas iron and steel industries are the primary consumers of refractories.

Therefore, refractory production is in tuned with the demand of iron and steel industries. In steel making furnaces, particularly basic nature refractories are using because of the basic reaction takes place during steel making process [4].

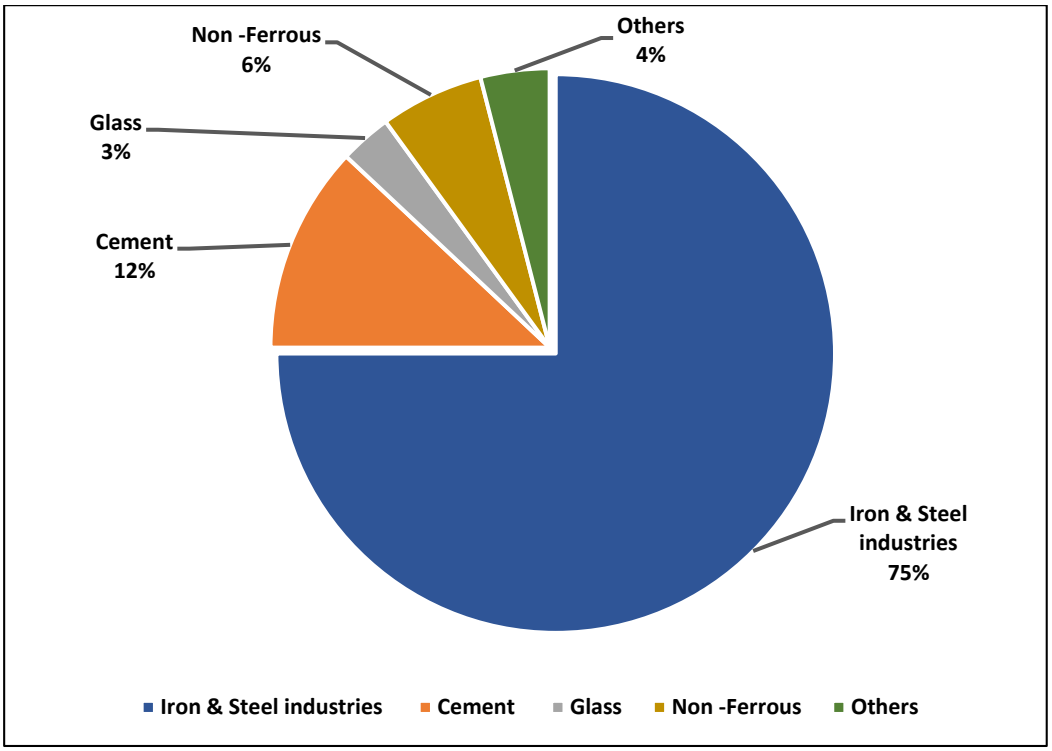

Figure 1.1: Consumption of refractory industry wise

MgO–C refractories are particularly used in basic oxygen furnaces (BOF), electric arc furnaces (EAF) and steel ladles. These refractories have excellent slag resistance, good thermal shock resistance and high thermo-mechanical strength. MgO-C bricks dominates the slag zone in steel production for at least a decade as they possess superior slag penetration resistance (chemical corrosion resistance) and excellent thermal shock resistance at elevated temperature because of the non-wetting properties of graphitic carbon. Since, carbon has low wettability and excellent thermal shock resistance at operating temperature. Therefore, the slag does not get wet and enhanced the MgO-C brick service life [5, 6]. In continuation of the steel production increment, both refractory manufacturers and users to resume interest in the further improvement of thermochemical and thermo-mechanical properties of MgO-C refractories [7].

1.2. Features of MgO-C Brick

Magnesia carbon (MgO-C) brick is a composite material. It is a combination of magnesia (MgO) and Carbon (C) and bonded with high carbon-containing pitch or resin with some metallic powder as anti-oxidants to protect the carbon. MgO-C bricks are made by using a high capacity press. These refractories exhibit excellent resistance slag corrosion and thermal shock resistance at operating temperatures. Magnesia carbon bricks (MgO-C) are widely used in steelmaking furnaces like basic oxygen furnaces, electric arc furnaces and steel ladles, etc.[1]

The approximate operating temperature of the basic oxygen furnace is 1650^{o}C-1700^{o}C during steel making process. However, the BOF slag containing equal portions of CaO and Fe_2O_3. But, metallurgical phase diagram shows, the BOF slag containing 50wt.% of iron oxide at operating temperature. The molten slag is a universal solvent, so it can easily react with any oxide material except MgO and Cr_2O_3. This useful property of MgO and Cr_2O_3 is subject to beneficial for the use of slag zone applications in metallurgical converters. However, Cr_2O_3 has lower melting point compare to MgO, and hence, MgO-C is the best choice for slag line refractories. Here, MgO-FeO phase diagram shows in Figure 1.2, where the MgO can tolerate without the formation of liquid phase when it is used in slag zone applications.

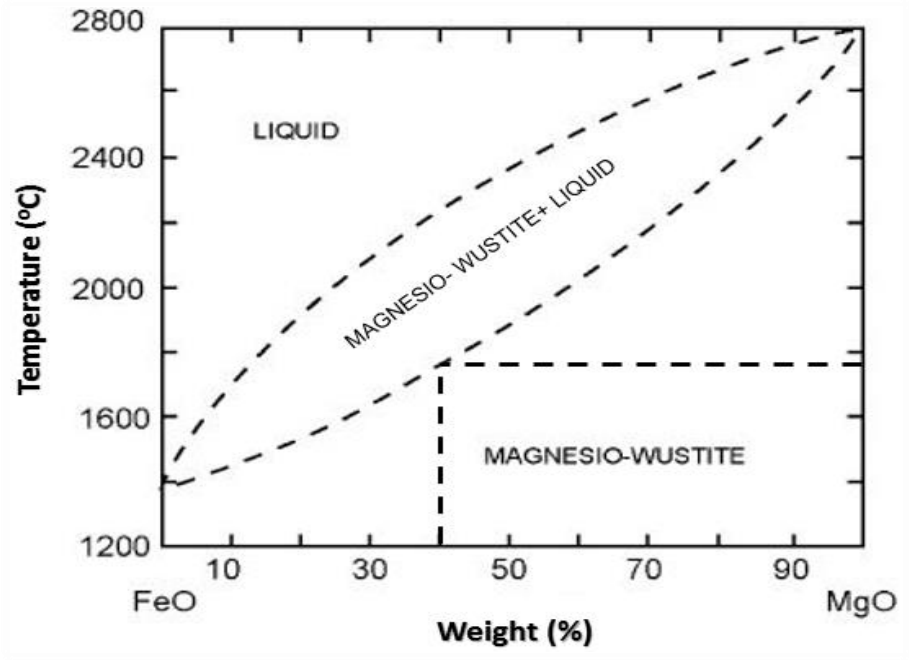

Figure 1.2: MgO-FeO phase diagram [8]

The temperature lines in the MgO-FeO-Fe_2O_3 phase diagram shown in Figure 1.3 indicates the melting point of the MgO-C brick composition. Here, the phase diagram describes the behaviour of MgO-C brick when contacting with FeO and Fe_2O_3 containing slag. The MgO does not form liquid phase below 1600°C until the composition consumes more than 80% iron oxide. Because of this advantage, the MgO-C brick performs the better role in the slag lines.

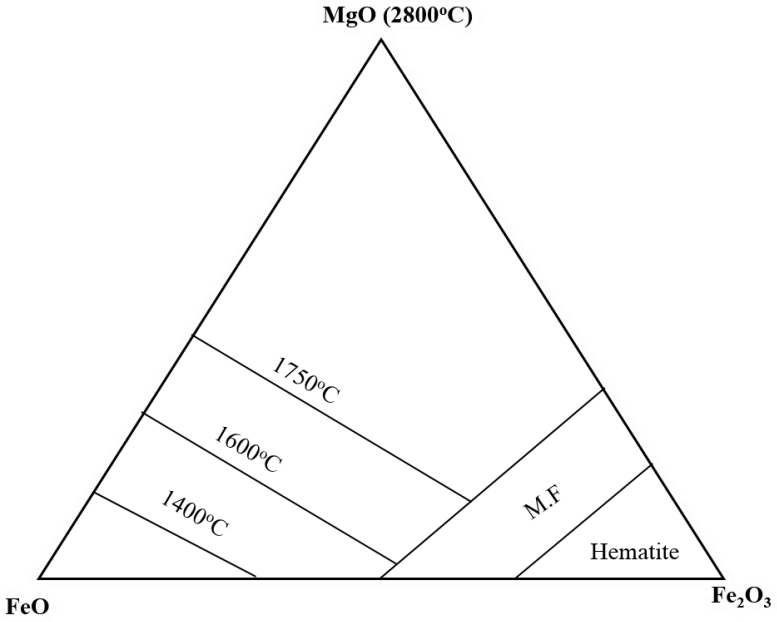

Figure 1.3: Schematic MgO-FeO-Fe_2O_3 phase diagram

Moreover, MgO – FeO phase diagram depicts that, the maximum operating temperature of basic oxygen furnace can be extended up to 1800°C. Interestingly, the MgO-C refractory can withstand without forming any liquid phase up to 60wt% consumption of iron oxide into the brick structures. However, beyond 60wt% absorption, the iron oxide supposed to follow solid solution and subsequent liquid phase reaction [8].

MgO-C bricks have the following features [9]:

- Poor wettability with molten slags and metal because of non-wetting nature property of carbon.
- It can resist rubbing action of liquid metal.
- It has high thermal shock resistance due to high thermal conductivity and low thermal expansion characteristics.
- It has high refractoriness.

- The depth of the slag infiltration and permeability of gases during operation is low.

- It will reduce the iron oxide (FeO) from the metallic iron during metal purification.

  Without carbon $CaO{\cdot}FeO{\cdot}SiO_2$ ---------- Eutectic ~ 1300°C

  In presence of carbon $CaO{\cdot}SiO_2$ + Fe ----------Eutectic > 1650°C

- It increased the lifetime of metallurgical converters lining
- It increases the viscosity of the slag.

1.3. Limitations of Graphite

The carbon has poor oxidation resistance as one of the drawbacks thus higher carbon content in MgO-C refractory tends to oxidize at higher temperatures. After the oxidation of carbon, the structure of magnesia–carbon brick is destroyed, and the slag can penetrate into the structure. Due to this problem the brick lining gets eroded and the brick loses its strength [4, 5].

❖ The Graphite based MgO-C brick has relatively low mechanical strength. In order to emphasize the mechanical response of MgO-C brick, we have highlighted different mechanical properties to compare without carbon containing MgO brick given in below Table 1.1.

Table 1.1: Comparing mechanical Properties of MgO and MgO-C bricks [10, 11].

Properties	MgO Brick	MgO-C Brick
CCS (MPa)	60	32
RUL ($t_a{}^oC$)	1720	---
MOR (MPa)	23	12

❖ The higher carbon content magnesia carbon refractories lead to decrease quality of steel. In actual, several mechanisms are needed to encounter during BOF operation process like slag chemistry, temperature, oxygen blowing, charging Impact and converter motion. According to 1970's Zonal concept [12, 13], 15- 18 % carbon containing MgO-C bricks are using in slag zone area to minimize the slag penetration into the brick structure and to improve the lifetime of converter lining. However, now a day's majority

of the steel plants are like to adopt 5-10% carbon containing MgO-C bricks for bottom zone and metal zone to improve the productivity of high-quality of steel [14]

To overcome these drawbacks, several research works are going on to reduce the carbon content including MgO-C refractories life improvement.

1.4. Application of the MgO-C brick

1.4.1. Basic Oxygen Furnace (BOF)

A typical top-blown basic oxygen furnace is a refractory lined vertical cylindrical vessel with a closed bottom and an open upper cone through which a water-cooled oxygen lance can be raised and lowered. The basic oxygen furnace (BOF) is a vessel used to convert pig iron, of about 94 percent iron and 6 percent combined impurities such as carbon, manganese, and silicon, is reduced to varying levels below 1% depending on the product specifications. The oxygen initiates a series of intensively exothermic (heat releasing) reactions, including the oxidation of such impurities as carbon, silicon, phosphorus, and manganese. The wear factors of the refractory lining are due to either the individual and combined effects of the following reasons [15, 16].

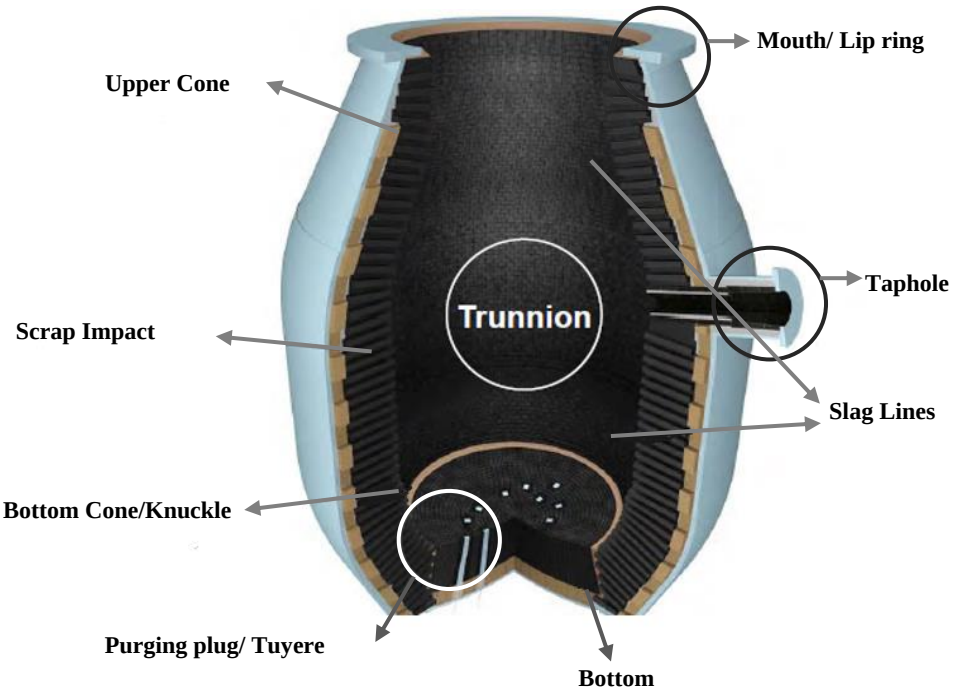

Figure 1.4: Different zones of basic oxygen atmospheric furnace (BOF)

- ✓ Corrosion due to chemical attack of slag
- ✓ Temperature
- ✓ Oxidizing atmosphere
- ✓ Impact and Abrasion
- ✓ Mechanical damage during deskulling

MgO-C refractory bricks are widely used in slag lines of BOF (Basic Oxygen Furnace) because of their superior slag-corrosion resistance. By using of MgO-C bricks, clean steel can be produced with a minor amount of refractory consumption [17].

Table 1.2: BOF area wear conditions and recommended materials [15]

Area of application	Wear Conditions	Recommended refractories
Cone	Oxidizing atmosphere Mechanical abuse Thermo-mechanical stress High temperature	Pitch-bonded magnesia brick Resin-bonded low-carbon refractories with anti-oxidants
Trunnions	Oxidizing atmosphere Slag corrosion Slag and metal erosion	Premium-quality magnesia–graphite refractories containing fused MgO and anti-oxidants.
Charge Pad	Mechanical Abrasion from scrap and hot metal	Pitch-impregnated burned magnesia brick Standard-quality, high-strength magnesia–graphite refractories containing antioxidants.
Tap Pad	Slag erosion High temperature Mechanical erosion	High-strength, low-graphite magnesia carbon brick with metallic additives.
Turn-down slag lines	Severe slag corrosion High temperature	Magnesia- graphite bricks (premium quality) containing fused magnesia with antioxidants.
Bottom Stadium	Erosion by moving metal, slag and gases Thermo-mechanical stresses as a result of the expansion.	High-strength standard-quality magnesia–graphite refractories containing anti-oxidants. Magnesia–graphite refractories without metallic additives characterized by low thermal expansion and good thermal conductivity

1.4.2. Electric Arc Furnace (EAF)

Electric arc furnaces (EAF) are used to produce molten steel from scrap steel. EAFs are used to produce carbon steels and alloy steels primarily by recycling ferrous scrap. Operation of electric arc furnace has traditionally involved refining of phosphorus, sulphur, aluminum, silicon, manganese and carbon from the steel [18].

- ✓ Long arc operation
- ✓ Water cooled wall and roof panel (withstand to TSR)
- ✓ Foamy slags formation
- ✓ Oxy-fuel burner
- ✓ Inert gas removing
- ✓ Eccentric bottom tapping

The slag line area blows the water cooled panels are lined with refractories that are like to withstand slag and molten steel and resist the opening of brick joints and spalling. In ancient days, fusion cast magnesia chrome bricks and fired dolomite & magnesite bricks were used, but at present, magnesia carbon bricks are widely used. These bricks are particularly used in hot zones, furnace bottom zones and slag line applications. The current days, they have also used for the bottom blowing plugs, the sleeves of furnace bottom tap holes and furnace bottom [19].

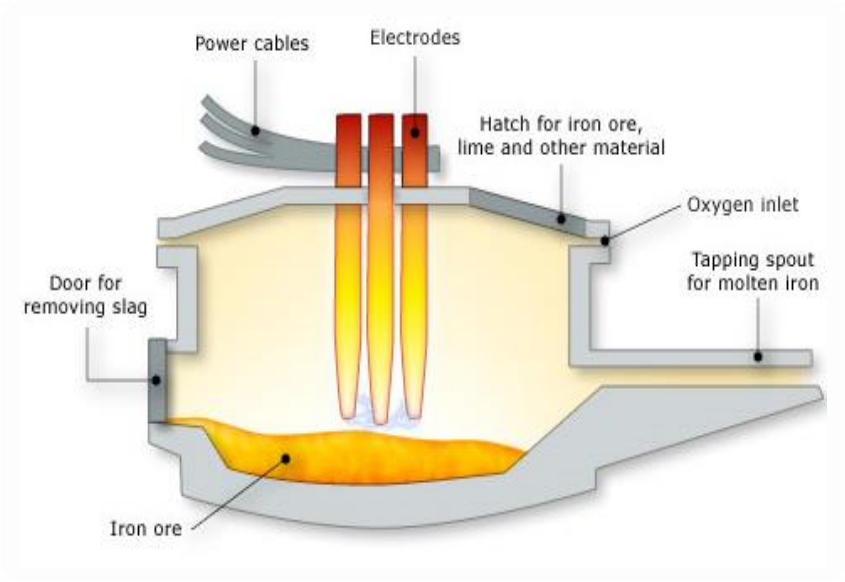

Figure 1.5: Structure of Electric arc furnace (EAF) and their zones

1.4.3. Steel Ladle

A steel ladle is a container with refractory lining for transporting molten steel tapped from the electric arc furnaces or converter up to the casting shop, reserving the steel during casting and occasionally during secondary refining of the steel. The below-mentioned factors are considered to be the most influencing objects in the lining life of steel ladles [20]:

- ✓ Slag basicity and fluidity of molten steel
- ✓ Long holding time with hot molten steel
- ✓ Stirring action of molten steel
- ✓ Thermal spalling from temperature.
- ✓ Fluctuation & Ladle handling method
- ✓ Ladle structural design & Tap conditions
- ✓ Lining/repairing method, etc.

The area mostly corroded in steel ladle is the slag zone. The reasons for corrosion are; a chemical reaction with metal & slag, erosion by stirring, oxidation at high temperature and thermal spalling due to temperature changes. At the earlier stage, mag-chrome brick was used, but it was not very successful in achieving higher life because these bricks corroded very fast with the high basicity of slags. Later on, magnesia carbon bricks were found as most suitable for the slag area, and performance was satisfactory, but to get higher life above 80 heats with one repair [21, 22, 23].

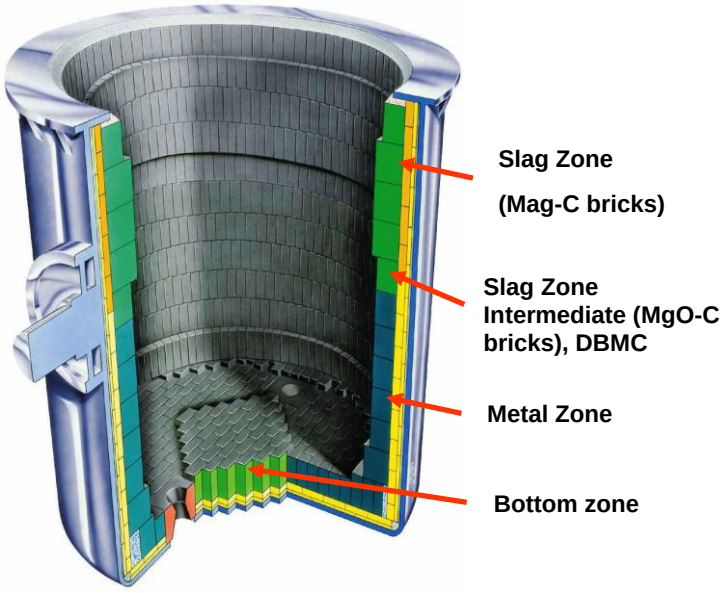

Figure 1.6: Structure of Steel ladle and their different zones.

The MgO-C refractories used in steel ladle lining is divided into several zones, including slag zone, slag intermediate zone, metal zone and bottom zone shown in Table 1.2

Table 1.3: Zone of application of the MgO-C refractory in steel ladle.

Steel Ladle zone	Type of bricks used	Basic slag resistance	Abrasion resistance	Spalling resistance	Hot strength
Slag Zone	MgO-C Refractory	Most important	Moderate	Most important	Most important
Metal Zone		Moderate	Moderate	Important	Important
Bottom Zone		Moderate	Most important	Important	Most important

MgO–C bricks considering that most important refractory materials applied in the ladles and basic oxygen furnace slag line. One of the crucial problem of slag attack during the operational process of such equipment is to adjust the liquid composition in order to attain dual saturation (with respect to CaO–MgO) or at least the MgO. The MgO content required for liquid saturation is a function of the slag basicity and temperature. The slag conditioning practice provides important benefits to the steel making processes, including ladle refractory life improvement, better control of metal recovery, lower flux cost/additions among other benefits with using of MgO-C bricks [24].

References:

[1] Refractories Handbook, edited by Charles A. Schacht Consulting Services Pittsburgh, Pennsylvania, U.S.A (2004).

[2] W.D. Kingery, H.K. Bowen, and D.R. Uhlmann, “Introduction to Ceramics”. John Wiley and Sons, New York, (1976).

[3] http://steel.nic.in/overview.htm

[4] A.S. Gokce, C. Gurcan, S. Ozgen, S. Aydin, The effect of antioxidants on the oxidation behaviour of magnesia–carbon refractory bricks. Ceramics International (34) 323–330 (2008).

[5] A Figueiredo, N Bellandi, A Vanola, and I Zamboni , “Technological evolution of magnesia–carbon bricks for steel ladles in Argentina,”Iron and steel technology, vol.1 pp.42-47 (2004).

[6] G. Buchebner, L. Sampayo, V. Samm, P. Blondot, S. Peruzzi and S. Boulanger ANKERSYN “A new generation of carbon- bonded magnesia carbon bricks”, RHI Bulletin, pp.24-27 (2008).

[7] S. Chatterjee and R. Eswaran, “Continual improved performance MgO-C refractory for BOF”, Proc.UNITCER’09, Salvador, Brazil, Article ID.136 (2009).

[8] E. Prestes, A. S. A. Chinelatto, W. S. Resende, “ Post mortem analysis of burned magnesia-chromite brick used in short rotary furnace of secondary lead smelting”, Ceramica (55) 61-66 (2009) .

[9] Mörtl et al. Berg- und Hüttenmännische Monatshefte 137 pp-196 (1992).

[10] LIU Bo, SUN Jia-lin, TANG Guang-sheng " Effects of Nanometer Carbon Black on Performance of Low-Carbon MgO-C Composites" Journal of Iron and Steel Research, International. 17(10), 75-78 (2010).

[11] http://www.tataref.com/product-basket/basic.html.

[12] Michael et al. "Magnesite-Carbon Refractories" Patent no: US 4912068.

[13] Dody, Julie, A "Method of Protecting Ladle Linings" Patent no: EP0755329 B1

[14] Steelmaking Refractories D. H. Hubble, Chief Refractory Engineer, R. O. Russell, Manager, Refractories, LTV Steel Co (1998).

[15] D. H. Hubble, R. O. Russell, H. L. Vernon, R. J. Marr, Manager, " Steel making refractories" The AISE Steel Foundation pp.227-290 (1998).

[16] http://ispatguru.com/refractories-for-basic-oxygen-furnace/

[17] G.D.Pickering, J.D.Batchelor, "Carbon –MgO Reactions in BOF Refractories, pp.611-614, Vol. 50, No.7, (1971).

[18] http://www.indiamart.com/tata-refractories-limited/iron-and-steel.html.

[19] C.G Aneziris, D. Borzov, and J. Ulbricht, "Magnesia carbon bricks-a high-duty refractory material", Intr. Ceram Refract. Man., pp.22-27 (2003).

[20] http://ispatguru.com/ladle-metallurgy/.

[21] Sune Jansson "A study on Molten Steel/Slag/Refractory Reactions during Ladle Steel Refining." ISRN KTH Stockholm (2005).

[22] P. Blumenfeld, S. Peruzzi, S. Puillet, and J. de Lorgeril, "Recent improvements in Arcelor Steel Ladles", La Revue de Metallurgie CIT, 3, pp.233-239 (2005).

[23] A.P. Luza, F.C. Leite, M.A.M. Brito, V.C. Pandolfelli, "Slag conditioning effects on MgO–C refractory corrosion performance". Ceramics International (39) 7507–7515 (2013).

Chapter-2

Literature Review & Objective of the Present Work

2.1 Historical developments of MgO-C Refractories

Carbon in any form plays a vital role in minimizing the penetration of steelmaking slags into the microstructure of magnesia carbon refractories. The addition of carbon in oxide refractory materials started since early 1950's. Carbon, which is known to have very high thermal conductivity and non-wettable surface property, has been considered as an excellent additive to oxide refractories leading to significant improvement in thermal and chemical properties. It enhances the life of the refractory lining particularly in steel melting furnaces and ladles [1]. The carbon-containing refractories have been accepted for many different applications. At present MgO-C bricks are extensively used as an important lining material for basic oxygen furnaces (LD converters), electric arc furnaces (EAF) and also in ladle metallurgy for steel making and refining [2].

Barthel et al. contrasted the wear in basic oxygen furnace test panels between burned magnesia brick and the same brick had been pitch-impregnated. Even though, the initial rate of wear was more in the carbon-free refractory and lesser in the case of pitch-impregnated magnesia brick. The main importance of carbon is minimizing the slag attack [3]. Another undesirable impurity found is boron oxide (B_2O_3). Researchers in the 1960s and 1970s found that one of the major dead-burned Grecian magnesite had a dramatic effect on the increased life of pitch-impregnation. The Burned MgO brick manufactured from this material was used in the impact pads of basic oxygen furnaces. Because, due to its inheriting low boron content that is less than 0.005 wt.% of MgO and 97% magnesia grain having lime to silica ratio of 2 to 3 [4]. In 1980's, development of resin bonded magnesia-graphite refractories with higher carbon content and also the addition of antioxidants to preserve the carbon content. [5]. The effect of binder type, as well as graphite and magnesia particle size distribution on the porosity of MgO-C refractory, was studied. The addition of various additives like metals, alloys, and inorganic compounds started to achieve better oxidation resistance, hot strength and corrosion resistance. These metals or metallic alloys (such as Al, Si, Mg, or Mg/Al alloy) function as antioxidants and improves the oxidation resistance [6, 7]. It was reported that Al in addition to Si metal containing samples had the best oxidation resistance and high temperature strength. Whereas, the Mg alloy containing samples had the maximum slag corrosion resistance and hydration resistance properties [8]. After 1980s silicon carbide (SiC), was used in manufacturing the initial magnesia-carbon refractories. Aluminium, magnesium, and silicon metals and their alloys quickly replaced this compound.

These materials are predominantly in use till today. Lately, some boron compounds, such as B_4C, CaB_6, ZrB_2, and TiB_2 have been introduced [9].

In recent, the effect of TiO_2 and ZrO_2 nanopowder together with Al as an antioxidant in the MgO-C system was studied, where thermal shock resistance is found to be improved. It attributed to the formation of dumbbell shaped Al_4C_3 whiskers in the carbonaceous matrix and the generation of a stress-induced surface due to the nano-scale dispersion of the oxide phase [10]. Magnesium aluminates spinel ($MgAl_2O_4$) possess unique properties, such as high melting point, high strength at elevated temperatures and excellent thermal shock resistance. Also, the spinel does not expand under alternating temperature and oxygen partial pressure conditions. Moreover, the use of the spinel with magnesia can lead to refractory products with improved impact strength and slag corrosion resistance. Finally, the formation of carcinogenic compounds in contact with calcium contaminants is not a problem with this raw material [11].

A study on nano carbon addition in MgO-C refractory shows that even a small amount can also reduce the overall carbon content without affecting the other properties. Nano carbon addition increases the oxidation resistance and the packing density as well as strength. The high thermal conductivity of graphite is caused by greater energy loss through MgO-C brick lining. In order to reduce the energy consumption due to loss of heat, it is preferred to have relatively low carbon content in MgO-C refractories [12]. However, this leads to less thermal shock resistance because of the formation of a glassy phase with poor mechanical properties, during carbonization of the phenolic resin binder. In recent years, the reduction of carbon content has been attempted through the addition of nanometer-sized carbon black, which leads to the formation of nanoporous MgO grains with reduced probability of catastrophic failure. It has been reported that only 1.5% nano carbon particles showed thermal spalling resistance equivalent to that of existing refractories containing 18% graphite [13, 14]. The addition of nanometer size carbon black results in a significant enhancement of hot modulus of rupture (HMOR) and cold crushing strength (CCS) [15, 16]. Synthesis of Al_2O_3-SiC composite is relatively cheap raw materials like kaolinite or pyrophyllite has been used for sometimes. Recently, this composite used as an additive to MgO-C refractory in order to reduce the carbon content and encouraging results were reported [17,18]

2.2. Corrosion mechanisms of MgO-C refractory

In the steel making process, the MgO-C refractory lining directly contacts with the slag resulting different corrosion mechanisms takes place. Corrosion of carbon bonded refractories follows the following mechanisms. The open pores and microcracks the main channels for initial slag penetration into the refractory.

- ✓ The formation of decarburized layer due to oxidation carbon by FeO in the slag or oxygen in the furnace atmosphere.
- ✓ The slag infiltration into decarburized layer and erosion of the MgO grains by slag penetration aided by high temperature softening point intergranular silicate bond and reaction and dissolution of the MgO grain into slag and molten steel [19].
- ✓ The MgO grains reduction at high temperature (~1600^{o}C) reaction with carbon, it causes further erosion.

The magnesia carbon refractories contain MgO grains and carbon in the form of graphite and as well as various phases derived by addition of different antioxidants. The graphite makes a high wetting angle with slag, so it more difficult to penetrate into pores and cracks in the refractory, is shown in Figure 2.1. Once the carbon has gone out, the effect of wear on the grain phase of the corresponding magnesia. Diffusion of slag into the refractory material causes to change the physical properties [20].

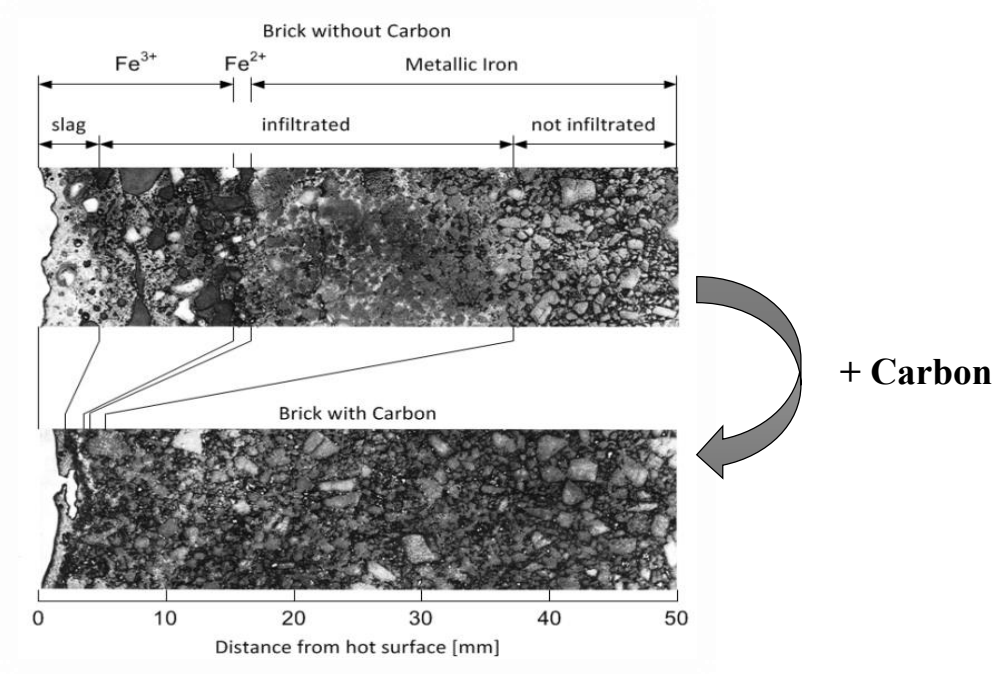

Figure 2.1: Wear factors on MgO-C refractory in metallurgical converters [21]

The diffusion mechanism causes to infiltrating slag into the structures of refractory. The infiltrating depth was also affected by the temperature gradient in the brick. The temperature gradients cause, the viscosity of the slag to increase with increasing distance into the refractory matrix, thereby decreasing the infiltration depth will get a decrease. Here several reactions may occur and lead to the generation of vapor spices. The thermodynamic situation is thus rather complex and may vary depending on location in the brick. Whether the hot face is being considered or the inside of the brick away from liquid penetration [22, 23].

Magnesia carbon refractory slag penetration mechanisms are

- ✓ Three consecutive steps govern **dissolution** at refractory interface:
    - **Transport** of reactants from the melt to the refractory interface**.**
    - **Chemical reaction** at the refractory interface.
    - **Transportation** of products from the refractory interface to the melt
- ✓ **Penetration** is caused corrosion of the refractory wall due to its volume expansions and contractions between refractory and slag and then after the slag can easily penetrate into the brick structure.
- ✓ **Erosion** is caused by the mechanical action of a fluid and velocity of gases that comes in contact with the refractory material.

2.3. Raw materials for MgO-C refractory

The raw materials are playing a vital role in the performance and life of the refractories. Several research works had been channeled out to find out the outcome of different raw materials based on purity, crystallite size, porosity and other parameters of various new materials along the final properties of MgO-C refractories. The main raw materials used for the preparation of MgO-C refractory are magnesia, graphite, antioxidants and binders like resin, powder resin and pitch. Details of the raw materials used in present work; described below [24, 25, 1].

2.3.1. Magnesia

The Magnesia is the primary reinforcement material for the MgO-C brick, it contains around 80-90 wt% of the total batch. Three different types of magnesia raw materials are used to produce MgO-C brick.

Fused magnesia produced by magnesia fusing in an electric furnace

Seawater magnesia produced by magnesium hydroxide extracted from seawater and then after fired at high temperature

Sintered magnesia produced from natural magnesite sintered at high temperature

Various research reports have been put out on the effect of magnesia aggregates on the corrosion and abrasion resistance of MgO-C brick. The quality of magnesia grain has the most significant impression on the corrosion resistance. Magnesia grain contains various impurities (such as SiO_2, Al_2O_3, Cr_2O_3, Fe_2O_3, FeO, B_2O_3 and CaO) which provide a silica bonding phase

(i) Large periclase crystal grain to reduce the extent of grain boundary [26].
(ii) High ratio of CaO/SiO2 (>2) and small content of B_2O_3 [27, 28]
(iii) High purity and minimum impurity of magnesia.

2.3.2. Graphite

The carbon source for MgO-C refractory from natural flake graphite which is available in nature, it plays a very vital role by providing non-wetting nature to the refractory. Carbon gets oxidized in the oxidizing atmosphere which results in a porous structure with very poor strength. So, resistance to oxidation is very important as the carbon source. Again, due to the flaky nature, it imparts higher thermal conductivity and lower thermal expansion, resulting in very high thermal shock resistance. It has been reported that fine graphite particles are more effective to improve the corrosion resistance of refractory [29]. The Properties of MgO-C refractory like porosity, bulk specific gravity, and cold crushing strength are not affected significantly by the particle size of graphite. The strength of MgO-C brick, particularly during heat treatment has also been reduced by the bigger particle size of graphite. The Purity of graphite is also an important factor. The Impurities present in the graphite is reacting with MgO and form low melting phase, resulting in less corrosion resistance and also lower hot strength [30].

Graphite role in MgO-C bricks:

i. Graphite covers the pores in between magnesia grains and fills the porous brick structure.
ii. The liquid penetration to the refractories is limited because of the non-wettable nature of carbon.

iii. Graphite increases the productivity of steel.

iv. Graphite makes a high wetting angle with metallic slags on the grounds, so it prevents the slag penetration into the brick structure.

v. At the service temperature, magnesium oxide is decomposed to pure magnesium by carbon and the gaseous magnesium comes to the brick surface and again oxidized with atmospheric oxygen to become magnesia. The formation of this dense layer of MgO and CO at the slag and brick interface prevents further penetration of oxygen into the brick [31].

$$MgO + C \rightarrow Mg + CO\uparrow \quad \text{..... (2.1)}$$

$$Mg + \frac{1}{2}O_2 \rightarrow MgO \quad \text{..... (2.2)}$$

vi. Graphite addition improves the thermo-mechanical properties and spalling resistance of the brick because of its high thermal conductivity and low thermal expansion.

vii. Slag containing Fe_2O_3 has higher corrosive action than that of containing FeO. Carbon reduces Fe_2O_3 to FeO, and further reduction of FeO produces metallic iron, enriches the production of steel.

$$Fe_2O_3 / FeO + C \rightarrow Fe + CO_2\uparrow \quad \text{..... (2.3)}$$

2.3.3. Binders

The raw materials are added to the ceramic, mixed blends to hold the different aggregates and network particles together in a structure that can be taken care of with less breakage. A few bonds are temporary, intended for green strength to handle from presses after forming, while drying or curing, and stacking for firing in furnaces; other bonds have sufficient green strength to be handled after shaping and then develop additional strength after curing or tempering [32].

The binders can be classified into following types;

Inorganic binders: This group includes materials such as various clay minerals, including montmorillonites, soluble sulphates and sulphuric acid, sodium silicates, and calcium aluminate cement.

Organic binders: This category includes materials such as pitches, resins, lignins and lignosulfonates, dextrins and starches, celluloses, waxes, and polyvinyl alcohol. The two major organic binders are pitch and resin.

In MgO-C refractory manufacturing process generally pitch or resins are used because of graphite has flaky morphology and non-wetting characteristics of low viscous binder, and hence it is obvious to add high viscous and strong adhesive binder say liquid resin to achieve high dense compact while pressing.

In initial days, the pitch was used as a binder for MgO-C refractory. Pitches are derived from either coal or petroleum. But during operating conditions, pitch releases large amounts of volatile matters, it causes swelling of the brick [33, 1]. The volatile matter is very tox due to their high content of polycrystalline aromatic compound (PAC) like benzo alpha-Pyrenes. The pitch bonded MgO-C mixtures were needed hot pressing. So, the resin was found to be the best binder for MgO-C refractories due to this following property.

- The ratio of fixed carbon is high; it maintains high strength on carbonization. Phenolic resins are the preferred binder for carbon-containing refractories
- It gives high adhesion and green body strength
- It is a thermosetting resin system whose strength on curing is high, and the size and stability of the resulting refractory component are good.
- At curing temperatures (~ 200^{o}C) resin polymerizes, which gives isotropic interlocking structure
- The harmful properties and industrial environmental issues are lower than those associated with the use of pitch binder.

Two major thermosetting phenolic resins are used in the refractories industry, those are novolacs and resoles. Novolacs require the addition of hexamethylenetetramine for polymerization during curing but resoles contain a built-in catalyst. The resins feature 60 wt% carbon contains volatile matter, but resol resin having 70 wt% carbon contains volatile matter. Only very mild elevated temperatures (~200 –300^{o}C) are required to control over polymerization during production, so using resins saves energy over the use of pitches. Powder novalac resin can be used to overcome this type of difficulty. Compressibility during pressing improves with the increase in resin content and consequently the CCS of the tempered samples increase. The resol type resin is best as a binder among various resin types. Because of its moderate viscosity and lower content of volatile species the samples containing resol resin had the less porosity after heating at high temperature [6].

2.3.4. Antioxidants

The primary drawback of carbon-containing refractories was the oxidation of the carbon. The oxidations of carbon in MgO-C refractories happen in two ways. [4, 34, 35].

(a) Direct oxidation: the oxidation takes place below 1400°C and carbon is oxidized directly by atmospheric oxygen.

(b) Indirect oxidation: the oxidation occurs above 1400°C and carbon is oxidized by the oxygen from MgO or slag.

To prevent the oxidation of carbon in MgO-C refractory, the different non-oxide anti-oxidants like metal powders (Al, Si) metallic alloys (Mg/Al) and non-oxide materials (SiC, B_4C, etc.) are effectively used. However, the Al and Si anti-oxidants are mostly used in refractory industries because of low cost and high effective protection on the bulk refractory specimen [36].

If there is no antioxidant in the MgO-C refractory, the life of the brick will be reduced due to loss of graphite through oxidation. This reaction is given in (Eqn. 2.4). But, the addition of an antioxidant like aluminium prevents the graphite loss by forming alumina (Eqn. 2.5) [37].

$$2C(s) + O_2(g) \rightarrow 2CO(g) \quad \text{..... (2.4)}$$

$$\Delta G^o = -223426 - 175.30 \left(\frac{j}{mol}\right) \qquad T < 932\ ^\circ K$$

$$2Al\ (s) + \frac{3}{2}O_2\ (g) \rightarrow Al_2O_3(s) \quad \text{..... (2.5)}$$

$$\Delta G^o = -1675100 + 313.95 \left(\frac{j}{mol}\right) \qquad T < 932\ ^\circ K$$

Oxidation of aluminium and carbon at a temperature less than 932 ^{O}K has shown in the above equations with standard molar free energy of reaction data. With the addition of aluminium (antioxidant) reduces the graphite loss below the particular temperature. This is due to the tendency of aluminium to react with oxygen to form alumina is more compared to the carbon to form carbon monoxide. This is because of the variation in the standard molar Gibbs free energy for the formation of two oxides at the respective temperature and pressure. Thermodynamically, this can be explained by the following Figure 2.2. At every temperature, standard molar Gibbs free energy of reaction (ΔG^o) for the formation of alumina (Al_2O_3) is

much less than the formation of CO. Thus, the reduction of oxidation carbon by alumina has negative standard free energy change (ΔG^o) than CO because, where aluminium favoured forming alumina under the respective conditions.

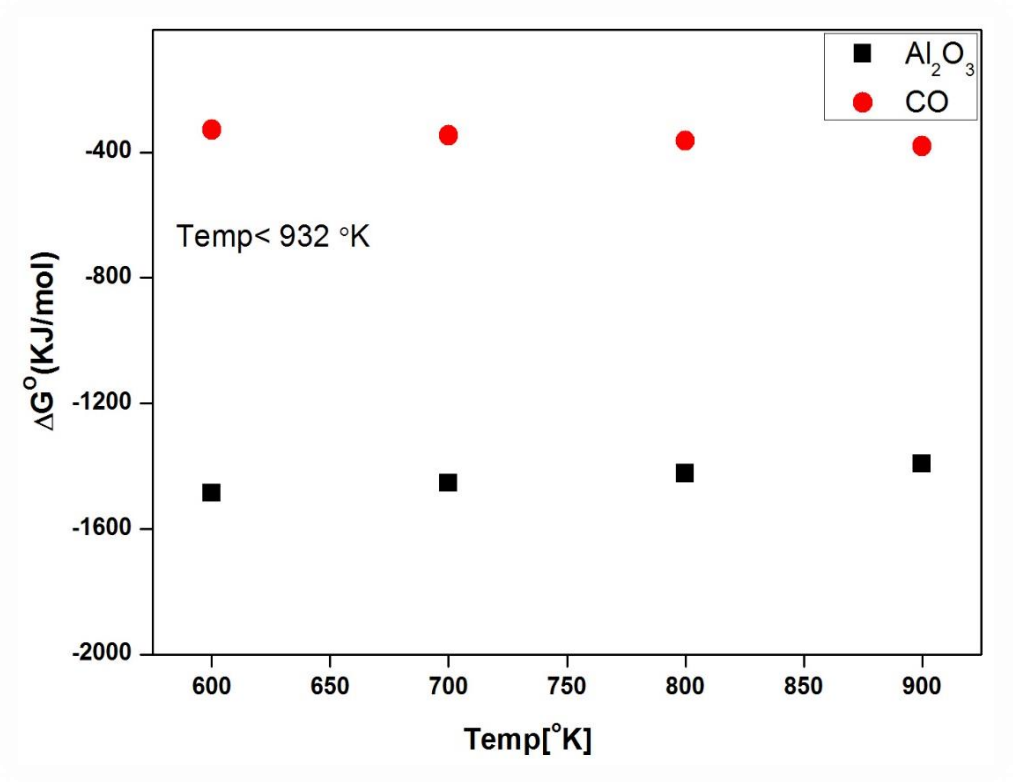

Figure 2.2: Standard molar gibbs free energies of alumina and carbon monoxide

In service condition, the Al metal powder melts at 660°C following that form a thin Al_2O_3 layer that can hold the liquid aluminum for a while until the oxide layer breaks and release the molten aluminium [31, 37]. The Al reacts with C to form Al_4C_3 (Eqn. 2.7), then the Al_4C_3 reacts with CO (carbon is oxidized by the air diffused into the brick) to form Al_2O_3 (Eqn. 2.8), which further reacts with MgO to form $MgAl_2O_4$ (Eqn. 2.9).

$$4\,Al\,(s) + 3O_2\,(g) \rightarrow 2Al_2O_3\,(s) \text{ ------ (2.6)}$$

$$4\,Al\,(l) + 3C(s) \rightarrow Al_4C_3\,(s) \text{ ------- (2.7)}$$

$$Al_4C_3\,(s) + 6CO\,(g) \rightarrow 2Al_2O_3\,(s) + 9C(s) \text{ ------- (2.8)}$$

$$Al_2O_3\,(s) + MgO\,(s) \rightarrow MgAl_2O_4\,(s) \text{ ------- (2.9)}$$

$$Al_4C_3\,(s) + 12H_2O\,(g) \rightarrow 3CH_4\,(g) + 4Al(OH)_3(s) \text{ ------- (2.10)}$$

In a similar way, Si metal reacts with carbon to form SiC at temperature > 1100°C. Between 1100°C and 1500°C Si reacts with CO and carbon deposition takes place (Eqn. 2.10 & 2.11) [31].

$$Si\ (s) + CO\ (g) \rightarrow SiO\ (g) + SiC\ (s) \text{ ---------- } (2.11)$$

$$SiC\ (s) + CO\ (g) \rightarrow SiO_2\ (s) + 2C\ (s) \text{ ---------- } (2.12)$$

Above 1500°C, silica reacts with MgO and forsterite formation takes place (Eqn. 2.13) [38].

$$2MgO\ (s) + SiO_2\ (s) \rightarrow 2MgO\text{-}SiO_2 \text{ ---------- } (2.13)$$

The formation of Al_4C_3 and SiC opposes oxidation of the carbon. B_4C reacts with the CO forms B_2O_3. The form B_2O_3 on reaction with MgO transforms to a liquid phase compound $MgO.B_2O_3$ [39]. The liquid phase boron compound comes to the refractory surface as a protective layer, thus preventing oxygen to comes in contact with the refractory material [40].

2.4. Silicon carbide properties

Silicon carbide is composed of tetrahedra of carbon and silicon atoms with strong covalent bonds in the crystal lattice. This produces a very hard and strong material. Silicon carbide is not attacked by any acids or alkalis or molten salts up to 800°C. In the air, SiC forms a protective silicon oxide coating at 1200°C, and it can be used up to 1600°C. The high thermal conductivity coupled with the low thermal expansion and high strength gives this material exceptional thermal shock resistant qualities. Silicon carbide ceramics with little or no grain boundary impurities maintain their strength at very high temperatures, approaching 1600°C with no strength loss [41].

- ✓ Silicon carbide is a structural material having low density.
- ✓ It can sustain high temperature, excellent resistance to oxidation, wear and creep.
- ✓ It has great strength and elastic modulus because high industrial applications.
- ✓ Single-crystal Silicon carbide has a high dissociation temperature of about 2600°C.
- ✓ It does not have any congruent melting point. At the dissociation temperature, it decomposes into graphite and molten silicon.
- ✓ Excellent thermal shock resistance.
- ✓ Superior chemical inertness
- ✓ Low thermal expansion

Table 2.1: Comparison of the physical properties of graphite and SiC.

Material Properties	Silicon carbide	Graphite
Density (gm/cc)	3.21	2.09 - 2.25
Hardness (GPa)	28.0	1.5
Oxidation Resistance (^oC)	1000	600
Elastic Modulus (GPa)	450	34
Thermal Conductivity (W/m^oK)	120	400(II), 16($\perp$)
Non-wettable nature	low	High

The SiC has excellent hardness, elastic modulus and oxidation resistance, but moderate thermal conductivity when compared to graphite.

2.5. Importance of SiC whiskers and rods in microcomposite

The nano SiC whiskers (fibers) or rods are played a vital role to improve the material properties. Silicon carbide (SiC) whiskers have high mechanical strength, good thermal and chemical properties. They are used as a reinforcement material for high-strength, lightweight composite materials and damage-tolerant refractory ceramic–matrix composites [42, 43].

Mechanical properties: It's highly dependent on the orientation and volume fraction of fibers or rods. The silicon carbide (SiC) whiskers have given good reinforcement to the structure. So that, it has been extensively used several hi-tech applications because of their good mechanical properties like high tensile strength, high elastic modulus, excellent shock and degradation resistance [42].

Thermal properties: They reduce the thermal conductivity, thermal shock failures chemical stability, etc. and its attracting attention in property improvements observed with the incorporation of SiC whiskers. These properties are very critical to apply as a flow channel insert as a low thermal conductivity is required to reduce the temperature losses adequately [43, 44].

The ß-SiC whiskers are produced by different solid state reaction methods. Those are chemical vapor deposition (CVD) and carbothermal reduction reaction by using various starting materials.

2.6. Different synthesis routes for preparation of SiC

2.6.1. Acheson process

The charge usually consists of silica, finely ground petroleum coke and sawdust. The silica is normally added in the form of sand. The sawdust is added to create porosity, which is needed for the SiC crystals to grow [45]. In this process, the raw materials are mixed then fired in an Acheson graphite electric resistance furnace nearly 24 - 48 hours. In this process, a solid-state reaction between silica sand and petroleum coke at very high temperature (more than 2500°C) leads to the formation of silicon carbide (SiC). Which is still used for the production of polycrystalline SiC.

The below equation (Eqn. 2.14) shows the overall reaction in the Acheson process. The silica is either a solid or liquid, depending on the temperature at the time of reaction. As the temperature exceeds the melting point of silica is 1700°C, so the SiO_2 melts, becoming glassy and highly viscous.

$$SiO_2(s,l) + 3C(s) \rightarrow SiC(s) + 2CO(g) \quad \text{(2.14)}$$

The reaction becomes thermodynamically favorable above 1500°C. As long as the temperature is below 1700°C the main product from this reaction will be β-SiC. If the temperature increases, there may formation of α-SiC [46].

2.6.2. Chemical vapor deposition (CVD)

The SiC powders were prepared through the vapor-phase (CVD process) chemical reaction method by using gaseous mixtures [47]. In this process fine amorphous SiC powder synthesized particles are prepared with Silane (3 mole% SiH_4 in H_2) and propane (0.3 mole % C_4H_8 in H_2) are used as sources of silicon and carbon respectively. Firing temperature ranges 1100°C to 1600°C in air atmosphere. The mean particle size of the powder is approx. 0.1-0.2mm.

The following reaction has taken place in the during reaction

$$2SiH_4\,(g) + C_2H_2\,(g) \rightarrow 2SiC\,(s) + 5H_2\,(g) \quad \text{---------- (2.15)}$$

2.6.3. Carbothermal reduction

In recent, silica sol and sugar was used in the wide range molar ratio of 0.96 – 1.02 to prepare the SiC. The sugar dissolved solution was freeze dried and preheated at 800^{o}C in flowing Ar gas to protect the furnace from hydrocarbon condensate liquids while conversion of sugar to the carbon at high temperature. Pre-treated mass further carbothermally reduced in the temperature range of 1550 to1800°C. Impurity carbon was removed by oxygen flow and obtained pure SiC in the presence of additional Fe powder [48].

Yang Zhong et.al prepares silicon carbide nanopowders prepared by using silica fume and graphite. The materials were ball milled in a high energy ball mill to get a uniform mixture, which was then subjected to carbothermic reduction to get SiC nanopowders in a tube furnace at 1500^{o}C. The particle size of the synthesized SiC was 30-60 nm. The excess carbon was eliminated by using H_2 gas through the formation of methane ($C + 2H_2 = CH_4$) gas [49].

Furthermore, the SiC powder was prepared from silica sol and resin, where silica sol prepared from ethanol solution of TEOS, deionized water, saccharose and nitric acid. Silica sol was mixed with novolac phenol- formaldehyde resin as carbon resource, and converted to gel at 65^{o}C for 1-5hr, followed by vacuum drying at ~ 40-70^{o}C for at least 36 hrs to increase the viscosity of dried gel. The dried gel was gently crushed and subjected to a carbothermal reduction in a high temperature furnace in an argon atmosphere. The β-SiC formation takes place at 1450 – 1500^{o}C with a particle size of 70-430nm [50].

2.6.4. Microwave heating process

The phase pure submicron silicon carbide particles are formed within a short time of exposure to microwave heating. In this study, silicon powder and amorphous carbon were used as a starting material. First the material was ground for 6hrs with ethanol solution and grinding media. The synthesis experiments were carried out at 1300^{o}C by microwave heating within a very short time of exposure 5-10 min. The reacted powders were calcined in an oxidizing atmosphere at 650^{o}C/8hrs in order to remove excess carbon present in the powder mixture [51]

The drawbacks of the above processes are:

1. The obtained SiC is contaminated with predominant impurity like carbon and followed multistep to achieve pure SiC phase in most of the processes.
2. High temperature is required to complete the reaction process from several sources of precursors.
3. An optimum amount of catalyst is essential for low-temperature conversion, which may persist as an impurity in the final product.

The process mentioned above explains the necessity of multi-steps to achieve pure SiC starts from carbon and silica mixture. In this backdrop, we have motivated to prepare directly useful and economic graphite (carbon) – SiC composite including the different morphology of SiC, which is completely new and innovative approach to the proposed work.

2.7. Role of the graphite-SiC microcomposite

In this study, an attempt has been made to improve the properties by partial replacement of the graphite by silicon carbide (SiC). The material is thermally conducting and mechanically strong, at the same time it has less wettability. It may be possible to improve the thermo-mechanical strength, as well as oxidation resistance. On comparing the physical properties of SiC and graphite, SiC has excellent hardness, elastic modulus and oxidation resistance but has a moderate thermal conductivity. So, the combination of these characteristic properties of SiC could be considered as a hopeful material to strengthen the MgO-C refractory and improve the thermo-mechanical properties. It is advantageous to take both SiC and graphite as they both have unique properties to satisfy the current problem by preparing graphite-SiC microcomposite. Also, of Graphite/SiC microcomposite on MgO-C refractories is supposed to be improved the properties like corrosion resistance and thermo-mechanical properties and oxidation resistance with the addition of partial amount.

2.8. Summary

The brief literature survey shows that several research works regarding the improvement of properties and performance of MgO-C refractories are well documented. Among these, properties improvement by variation of raw materials are common, like

- ✓ Purity, size and type of MgO grains (Fused MgO, dead burn MgO and seawater MgO, etc.)
- ✓ Grade, quality & quantity and purity of the binders (pitch, resins, etc.)
- ✓ With changing of anti-oxidants (Al, Mg and Si)
- ✓ The addition of different types of non-oxide additives (SiC, Al_4C_3, B_4C)

In the consequence of above findings, still there is a scope for further improvement in the properties and appearance of magnesia carbon refractory due to the needful application for the production of high-quality steel.

Literature review depicts that, no attempts have been made to the development of MgO-C refractories by the addition of perform synthesized graphite/SiC microcomposite. The micro composite has a combination of graphite and SiC. Herein, the purpose of graphite/SiC microcomposite addition in MgO-C refractory is to improve the thermo-mechanical properties, as well as corrosion and oxidation resistance due to the superior properties of SiC. To take advantage of the superior properties of Graphite/SiC without alteration of unique properties of graphite, it has been decided to use the graphite/SiC microcomposite for partial replacement of graphite in the conventional MgO-C brick composition. In this perspective, the research work of this current study has been discussed in two major sections:

Part-I: Synthesis of the graphite/SiC microcomposite by using of microfine silica and flake graphite under different conditions.

Part-II: Properties evaluation of the MgO-C brick with the addition of graphite/SiC micro-composite by replacing a part of the graphite.

a. Properties evolution under laboratory scale conditions
b. Properties evolution under pilot plant (Tata Krosaki Refractories Limited, Belpahar, Odisha) investigations

2.9. Scope and Objective of Thesis

The basic objective of the thesis work will be an attempt to reduce the carbon content in conventionally used MgO-C refractory composition by partial / full replacement of graphite by graphite/ SiC micro-composite. The investigation will be carried out in following steps:

- To prepare graphite/SiC microcomposites through variation of precursor compositions, heating atmosphere and varying temperature with time.
- To analyse the influence of processing conditions on the morphology and phase of the developed microcomposites.
- To partial replacement of pure graphite by different grade of graphite/SiC microcomposites in equivalent to conventional MgO-C refractory brick composition.
- To study the compaction mechanical, thermo-mechanical, oxidation resistance and slag corrosion behaviour of developed MgO-C refractory on the addition of synthesized graphite/SiC microcomposite.
- To fabricate pilot scale production of MgO-C bricks from optimized compositions and evaluation of detailed properties with respect to the refractory application.

References

[1] A Richard, Landy and Charles A. Schacht, "Magnesia Refractories", U.S.A. (2004). pp. 109-150.

[2] E. Mohamed, M. Ewais, Carbon based refractories, Journal of the Ceramic Society of Japan 112 (10) (2004) 517–532

[3] H. Barthel. "Effect of carbon in tar-impregnated burnt magnesia brick on the wear of basic oxygen furnace linings". Stahl und Eisen; 86 (1966) 81–88.

[4] A.P. Luz, F.C. Leite, M.A.M. Brito, V.C. Pandolfelli "Slag conditioning effects on MgO–C refractory corrosion performance", Ceramics International 39 (2013) 7507–7515.

[5] E. Ruh "Refractories: Magnesia–Carbon Refractories, History, Development, Types and Applications", International Ceramic Monographs 1(1994) 772-793.

[6] B. Hashemi, Z.A. Nemati, M.A. Faghihi-Sani, "Effects of resin and graphite content on density and oxidation behavior of MgO-C refractory bricks", Ceramics International 32 (2006) 313–319.

[7] E. V. Krivokorytov, N.A. Makarov, "Effect of antioxidants on the properties of unfired carbon-bearing refractories", Refractories and Industrial Ceramics, Vol. 40 (1999) 11-12,

[8] S. K. Nandy, N. K. Ghosh G. C. Das, "Oxidation kinetics of MgO-C in air with varying ash content", Advances in applied ceramics, vol. 104, No.6 (2005) 306-311.

[9] Hunold, Ing. Klaus "Boron compounds in carbon-bonded refractories". Ceramic Industry, Vol. 144 (1995) 47–50.

[10] C. G. Aneziris, J. Hubalkova, R. Barabas, "Microstructure evaluation of MgO-C Refractories with TiO_2 - and Al - additions", Journal of the European Ceramic Society 27 (2007) 73-78.

[11] I. Ganesh, S. Bhattacharjee, B.P. Saha, R. Johnson, K. Rajeshwari, R. Sengupta, M.V. Ramana Rao, Y.R. Mahajan, "An efficient $MgAl_2O_4$spinel additive for improved slag erosion and penetration resistance of high-Al_2O_3 and MgO–C refractories". Ceramics International 28 (2002) 245–253.

[12] M. Bag, S. Adak, R. Sarkar, "Nano carbon containing MgO-C refractory: Effect of graphite content", Ceramic International 38, 4909-4914(2012).

[13] Tianbin Zhu, Yawei Li, Shaobai Sang, Shengli Jina, Yuanbing Li, Lei Zhao, Xiong Liang, "Effect of nanocarbon sources on microstructure and mechanical properties of MgO–C refractories", Ceramics International 40 (2014) 4333–4340.

[14] Y. Xuejun, Q. Zheming, H. Liangquan, "The Influence of Nanometer Carbon Black on the Mechanical Properties of Phenolic Resin", Processing of aircraft materials, 33 [4] (2003) 34-38.

[15] LI Lin, TANG Guang-sheng , HE Zhi-yong , LID Kai-qi, PENG Xiao-yan, "Influences of black carbon addition on mechanical performance of low-carbon MgO-C composite", Journal of Iron and Steel Research, International. 2010, 17(12) 75-78.

[16] Mohammad Hassan Amin, Mohsen Amin-Ebrahimabadi, and Mohamad Reza Rahimipour, "The effect of nanosized carbon black on the physical and thermo-mechanical properties of Al_2O_3–SiC–SiO_2–C composite", Journal of Nanomaterials. Volume 2009, Article ID 325674, 5 pages.

[17] B. Han, N. Li, "Preparation of β-SiC/Al2O3 composite from kaolinite gangue by carbothermal reduction", Ceramics International 31, 227–231(2005).

[18] B.Ma, Q. Zhu, Y Sun, J. Yu and Y Li, "Synthesis of Al_2O_3-SiC-Composite and its Effect on the Properties of Low-carbon MgO-C Refractories", J. Mater. Sci. Technol., 26(8), 715-20 (2010)

[19] Lidong Teng. "Refractory corrosion during steelmaking operations - Treatise on process metallurgy, Hand book, volume –II", pp- 283-304, (2014).

[20] Stefan Feichtinger, Susanne K. Michelic, Youn-Bae Kang and Christian Bernhard, "In Situ Observation of the Dissolution of SiO2 Particles in CaO–Al2O3–SiO2 Slags and Mathematical Analysis of its Dissolution Pattern". J. Am. Ceram. Soc., 97 [1] (2014) 316–325.

[21] Mörtl et al. Berg- und Hüttenmännische Monatshefte 137 (1992) pp. 196

[22] R. R. Das, B. B. Nayak, S. Adak, A. K. Chattopadhyay, "Effect of spinel addition in MgO-C refractory for slag zone of steel ladle", 8th IREFCON Feb 6-8, Kolkata, page 155 – 159 (2010).

[23] R.R. Das, M.Tech (Research) Thesis, "Effect of micron and nano $MgAl_2O_4$ spinel addition on the properties of magnesia-carbon refractories", National Institute of Technology, Rourkela, (Oct.2010).

[24] M. Bavand-Vandchali, F. Golestani-Fard, H. Sarpoolaky, H.R. Rezaie, C.G. Aneziris, "The influence of in situ spinel formation on microstructure and phase evolution of MgO–C refractories". Journal of the European Ceramic Society 28 (2008) 563–569.

[25] M. Tanaka, Maekawa, A., Hokii, T., Asano, K., and Ohtsuka, K., "Relationship between MgO aggregate purity and properties of MgO-C brick after firing in a reducing atmosphere", Taikabutsu Overseas, 21 (2001) pp. 215 **ISSN:**0285-0028.

[26] W.E. Lee, S. Zhang, "Direct and indirect slag corrosion of oxide and oxide refractories", VII International Conference on Molten Slags Fluxes and Salts, The South African Institute of Mining and Metallurgy, 2004.

[27] Huang Yi, Guoping Xu, Huigao Cheng, Junshi Wang, Yinfeng Wan, Hui Chen, "An overview of utilization of steel slag" Procedia Environmental Sciences 16, (2012) 791-801

[28] Fusao Kawano, Minamata, "Magnesia Clinker and Method of Producing the Same", US Patent Number: 4721691. Jan. 26, 1988.

[29] M. Sakaguchi, H. Ishii, K. Aratani and Y. Oguchi, "Effect of Graphite Particle Size on Properties of MgO-C Bricks", Taikabutsu Overseas, Vol. 13 No. 1 (1993).

[30] Rita Khanna, John Spink and Veena Sahajwalla, "Role of ash impurities in the depletion of carbon from alumina-graphite mixtures in to liquid iron", ISIJ International, 47 (2007) No.2, pp.282-288.

[31] Marie-Aline Van Ende, Muxing Guo, Peter Tom Jones, Bart Blanpain, Patrick Wollants, "Degradation of MgO–C refractories by MnO-rich stainless steel slags",Ceramics International 35, 2203–2212 (2009).

[32] Arthur H. Gerber, Louisville, Ky, "Phenolic resin solution and magnesia aggregate; ceramics, bricks", US Patent number: 5248707, Sep. 28, 1993.

[33] Tamka P and Baldo J.B, "A new friendly resin with coupled anti-oxidants protectors for carbon containing refractories", UNITCER'07(2007). pp.30.

[34] S. Zhang, N.J. Marriott, W.E. Lee, "Thermochemistry and microstructures of MgO–C refractories containing various antioxidants", J. Eur. Ceram. Soc. 21 (2001)1037–1047.

[35] S. Uchida, K. Niihara, K. Ichikawa, "High-temperature properties of unburned MgO–C bricks containing Al and Si powders", J. Am. Ceram. Soc. 81[11] (1998) 2910–2916.

[36] Carmen Baudin, Carlos Alvarez, Robert E. Moore, Influence of chemical reactions in magnesia–graphite refractories-I. Effects on texture and high-temperature mechanical properties, J. Am. Ceram. Soc. 82[12] (1999)3529–3538.

[37] S. K. Sadrnezhaad, Z. A. Nemati, S. Mahshid, S. Hosseini and B. Hashemi, "Effect of Al Antioxidant on the Rate of Oxidation of Carbon in MgO–C Refractory", J. Am.Ceram. Soc., 90 [2] (2007) 509–515.

[38] E. Mohamed and M. Ewais, "Carbon Based refractories", Journal of ceramic Society of Japan, 112 [10] (2004) 517-532.

[39] A.S. Gokce, C. Gurcan, S. Ozgen, S. Aydin, "The effect of antioxidants on the oxidation behaviour of magnesia–carbon refractory bricks". Ceramics International 34(2008) 323-330.

[40] YE Fangbao, Michel Rigaud, "Effects of boron bearing additives on oxidation and corrosion resistance of doloma-based carbon bonded refractories", China's Refractories, Vol-7, No-2. (1998) 807-815.

[41] M. Badila, G. Brezeanu, J. Millan, P. Godignon and V. Banu, "Silicon carbide Schottky and ohmic contact process dependence", Diamond and Related Materials 11 (2002) 1258–1262.

[42] X.K. Li, L. Liu, Y.X. Zhang, Sh.D. Shen, Sh. Ge, L.Ch. Ling, "Synthesis of nanometre silicon carbide whiskers from binary carbonaceous silica aerogels". Carbon 39 (2001) 159–165.

[43] Luciano Fabbri, Ernesto Scafe & Giancarlo Dinelli, "Thermal and Elastic Properties Alumina-Silicon Carbide Whisker Composites", journal of the European Ceramic Society 14 (1994) 441- 446.

[44] D. Perrone, Ph.D. Thesis on "Process and characterization techniques on 4H- Silicon Carbide", Torino, March 2007.

[45] G. Dhanaraj, B. Raghothamachar, & M. Dudley, "Growth and characterization of silicon carbide crystals". In Springer Handbook of Crystal Growth (2010) pp. 797–820. Springer Books

[46] Lindstad, L. H. (2002). Recrystallization of silicon carbide. Ph.D. thesis, NTH, Trondheim.

[47] Stefan Kavecky, Beata Janekova, Jana Madejova, Pavol Sajgalik, "Silicon carbide powder synthesis by chemical vapour deposition from silane/acetylene reaction system", J.Eur. Ceram Soc., 20 (2000) 1939-1946.

[48] Hans-Peter Martin, Ramona Ecke and Eberhard Muller "Synthesis of nano-crystalline SiC powder by carbothermal reduction". J.Eur. Ceram Soc., Vol.18 (1998) pp.1737-1742.

[49] Yang Zhong, Leon L Shaw, Misael Manjarres, and Mahmoud F. Zawrah, "Synthesis of Silicon Carbide Nano powder Using Silica Fume", J. Am. Ceram. Soc., 93 [10] (2010) 3159-3167.

[50] Zhe Cheng, Michael D, sacks and Chang- Wang, "Synthesis of nano crystalline silicon carbide powders", 2nd IEEE International Nano electronics Conference, pp.23- 32.

[51] L.N. Satapathy, P.D. Ramesh, Dinesh Agrawal, Rustum Roy, "Microwave synthesis of phase-pure, fine silicon carbide powder" Material Research Bulletin, 40 (2005) 1871-1882.

Chapter - 3

Experimental Work

3.1. Raw materials for preparation of graphite/SiC microcomposite

As noted earlier, this research work is focused on the provision of a graphite-silicon carbide micro-composite for possible use as an additive to MgO-C refractory as partial and full replacement of graphite.

The graphite/SiC microcomposite has been synthesized using natural flake graphite (97FC and 94FC) along with a microfine silica (average particle size 380nm and the average particle diameter 150nm) as the starting materials.The chemical compositions of natural flake graphite are tabulated in Table 3.1

Table 3.1: Chemical composition of flake graphite (As received)

Raw material	Carbon (%)	Volatile matter (%)	Ash (%)
Flake Graphite (97FC)	97.05	0.69	2.26
Flake Graphite (94FC)	94.1	0.75	5.15

Table 3.2: Chemical composition of microfine silica

Raw material	Silica (%)	Carbon (%)	Ash (%)
Microfine Silica	90-97	0.69-2.7	2.26 -7

3.2. Synthesis of Graphite/SiC micro-composite

Graphite-silicon carbide microcomposite has been prepared by a relatively simple process, namely the carbothermal reaction between natural flake graphite and a microfine silica. Here the graphite was sieved through 212-micron sieve (70 meshes), +212-micron fraction graphite was used for the preparation of graphite/SiC microcomposite. After that, different weight percentages of graphite and micro silica batches are prepared as mentioned in Table 3.3.

Table 3.3: Composition of microcomposite by varying amounts of graphite and microfine silica

Composition Identification	SiO_2 content (Wt.%)	Graphite content (Wt. %)
A	10	90
B	20	80
C	30	70
D	40	60
E	50	50

A homogeneous mixing of these compositions is carried separately. The mixed batches are filled in different alumina crucibles and then heat-treated in a reducing atmosphere at various temperatures (1600^{o}C, 1650^{o}C and 1700^{o}C).

In the present system, the microcomposites are prepared in two different atmospheric firing conditions those are mentioned below:

1. The different batch of compositions is packed in different alumina crucibles and are placed inside another alumina crucible containing pet-coked bed that was assembled using alumina cement. The assembled crucible was heated in a conventional laboratory, raising hearth furnace (RHF-Okay) in air atmosphere. The sample heating rate during firing was 3^{o}C/min and soaking time at the operating temperature is 4hours. Normal cooling is followed by soaking.

2. The different batches were packed in different alumina crucibles and are placed inside a graphite lined controlled atmospheric furnace (CAF- Nabertherm, Germany) maintained by argon atmosphere. The furnace chamber is evacuated and filled with argon after placing the crucibles inside the chamber. The heating rate and soaking time was kept at 8^{o}C/min and 4hours at the operating temperature. The cooling rate is maintained at 10^{o}C/min for this particular system.

Table 3.4: Synthesized conditions for preparation Graphite/SiC microcomposite

Purity of Graphite	Furnace Used	Silica/ Graphite Ratio and Temperature of Heat-treated															
94FC	RHF	10/90			20/80			30/70			40/60			50/50			
		1600ºC	1650ºC		1600ºC	1650ºC		1600ºC	1650ºC		1600ºC	1650ºC		1600ºC	1650ºC		
	CAF	10/90			20/80			30/70			40/60			50/50			
		1600ºC	1650ºC	1700ºC	1600ºC	1650ºC	1700ºC	1600ºC	1650ºC	1700ºC	1600ºC	1650ºC	1700ºC	1600ºC	1650ºC	1700ºC	
97FC	RHF	10/90			20/80			30/70			40/60			50/50			
		1600ºC	1650ºC		1600ºC	1650ºC		1600ºC	1650ºC		1600ºC	1650ºC		1600ºC	1650ºC		
	CAF	10/90			20/80			30/70			40/60			50/50			
		1600ºC	1650ºC	1700ºC	1600ºC	1650ºC	1700ºC	1600ºC	1650ºC	1700ºC	1600ºC	1650ºC	1700ºC	1600ºC	1650ºC	1700ºC	

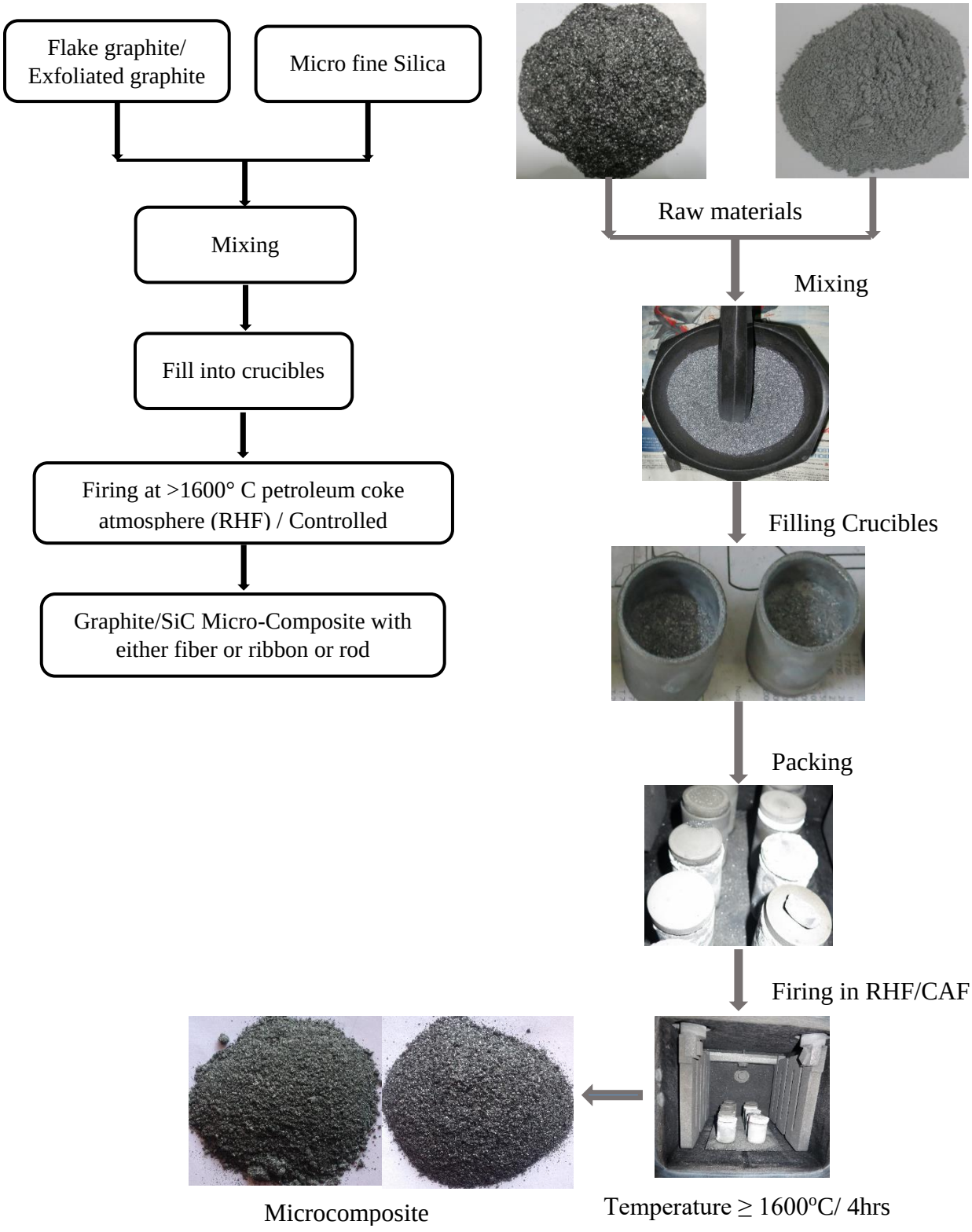

Figure 3.1: Flow chart for the preparation of graphite/SiC microcomposite by natural flake graphite and microfine silica.

3.3. Characterizations of microcomposite

3.3.1. Phase analysis:

Phase formation of sintered powdered samples was studied by Philips X-Ray diffractometer with Ni filtered Cu-K_α radiation (λ= 1.5418 Å). The phase analysis conducted by the Philips X'Pert High score software provided with the equipment. This technique gives some valuable information about crystal structure, the crystallinity of the material, crystallite size, chemical analysis, etc. The voltage and current of the generator set at 35KV and 25mA respectively. The scan rate was 0.05^o/Sec. A powdered sample was packed on a sample stage so that the X-ray can scan it. The diffracted X-rays get detected by an electronic detector placed on the other side of the sample. In order to get the diffracted beams, the sample has rotated through different Bragg's angles. The goniometer keeps track of the angle (θ), and the detector records the detected X-rays in units of counts/sec, and it sends this information to the computer. After the sample scans, the X-ray intensity (counts/Sec) (Y axes) was plotted against the angle theta (2θ) (X-axes). The angle (2θ) for each diffraction peak was then converted to d-spacing, using the Bragg's law.

$$n\lambda = 2d \sin\theta$$

Where λ = Wavelength of x-ray

n = order of diffraction.

3.3.2. Microstructural analysis:

The microstructural analysis is one of the important interpretation tools to study the surface property of microcomposite; which is prepared in RHF and CAF. The microcomposite prepared with different compositions at different firing temperatures /4hrs. Study of the fractured surface of the MgO-C sample after firing in reducing the atmosphere at 1600^oC/ 4hrs.

Morphological characteristics of the powders were carried out by using NOVA NANOSEM FEI 450 system. In Field Emission Scanning Electron Microscopy (FESEM), the source of electrons are liberated from a field emission source and accelerated in a high electrical field gradient. Within the high vacuum column, these so-called primary electrons are focussed and deflected by electronic lenses to produce a narrow scan beam that bombards the object. As a result, secondary electrons are emitted from each spot on the object. The velocity and angle

of these secondary electrons relate to the surface structure of the object. A detector catches the secondary electrons and produces an electronic signal. This signal is amplified and transformed into a video scan image that can be seen on a monitor or to a digital image.

3.3.3. Packing Density:

The Tap density is an increased bulk density attained after mechanically tapping a container containing the powder sample

$$\text{Tap Density} = \frac{W}{V_f}$$

Where W = Weight of the material

V_f = Volume of the material after taping

3.3.4. Oxidation test:

This test method covers the rate of oxidative weight loss per exposed nominal surface area. The test is valid in the temperature range where reaction kinetics limits the rate of air oxidation of graphite and manufactured carbon.

This information is useful for discriminating between material grades with different impurity levels, grain size, pore structure, the degree of graphitization, or anti-oxidation treatments, or both.

Physical measurements of the powder sample were taken before and after oxidation and also after calcining at 1000^{o}C/ 1hr the material loss caused by oxidation.

$$\text{The rate of oxidation} = \text{Weight loss/ Initial weight} \times 100$$

3.4. Fabrication of MgO-C brick

High purity fused magnesia (97FM) was chosen based on parameters like purity, CaO/SiO_2 ratio, low Fe_2O_3 content and having crystallite size in the range of 200μm-6mm. Natural flake graphite (94FC) with low ash content was used. A variation in silica to carbon ratio yields three different morphologies of Graphite-SiC microcomposite after firing which gives different amount of graphite and SiC. Resin (novalac type) is used as the binder and aluminium metal powder (150μ) as the anti-oxidant. The chemical composition of raw materials has been tabulated below.

Table 3.5: Chemical composition of fused magnesia in (%)

Raw materials	**Chemical composition**					
	MgO	Al_2O_3	SiO_2	CaO	Fe_2O_3	Na_2O
Fused magnesia	97.10	0.06	0.50	1.40	0.50	0.50

Table 3.6: Physical and chemical analysis of liquid resin

Property	**Value**
Specific gravity at 25°C	1.2
Viscosity (CPS) at 25°C	8500-9000
Fixed carbon (%)	47.90
Non-volatile matter (%)	80.00
Moisture (%)	~ 4.5

Aluminium metal powder: Purity: 98 %

Particle size: 100% passing through 150 mesh BSS

50-75% passing through 300 mesh BSS

3.4.1. Fabrication of MgO-C samples with the addition of graphite/SiC micro-composite

In order to investigate the effect of the graphite-SiC microcomposite on various properties of MgO-C refractory. The samples were prepared by replacing partial/fully the graphite with different amounts of the microcomposite keeping the concentration of the MgO phase unchanged. MgO-C refractory compositions were imitated under laboratory conditions by preparing specimens of MgO grains together with varying amounts of graphite flakes and graphite-SiC micro-composites (both with ribbon and fiber morphologies). Only finer grades of MgO used in order to facilitate sintering within the available temperature in the laboratory. For industrial investigations, standard size fractions are used. A specific amount of liquid resin used as the binder. A metallic aluminium powder used as the antioxidant. Exact batch compositions of the specimens are presented in Tables 3.7 respectively. But, the industrial investigations carried out by using the partial amount of replaced by graphite with microcomposite.

Table 3.7: Different MgO-C batch compositions for laboratory investigations

Raw materials	**Batch-1***	**Batch-2***	**Batch-3***	**Batch-4***	**Batch-5***	**Batch-6***
MgO grains (0-1mm)	28	26.5	25	28	26.5	25
MgO Dust (~200µ)	66	62.5	59	66	62.5	59
Graphite (94FC)	**5**	**10**	**15**	0	0	0
Liquid Resin	3	3	3	3	3	3
Al metal powder	1	1	1	1	1	1
Graphite-SiC micro composite	0	0	0	**5**	**10**	**15**
Specimen Code	**MHG**			**MHR (**for Ribbon) / **MHF** (for fiber)		

* The above compositions are in weight percentages

All the powders from different batch compositions were prepared by hot mixing at 60-70^{o}C followed by grounding for 20 minutes. The powder mixture was pressed into pellets (12mm in dia. and 5-10mm in height). Pellets were tempered at 280^{o}C/12hrs followed by coking/sintering at 1500^{o}C, 1550^{o}C and 1600^{o}C/4hrs under a reducing atmosphere in the presence of petroleum

coke. The compressive strength measurement was done in a universal testing machine (H10KS, Tinus Olsen, U.K). The samples dimension for strength measurement were 12.5mm in diameter and 10-12mm in height.

3.4.2. Mixing:

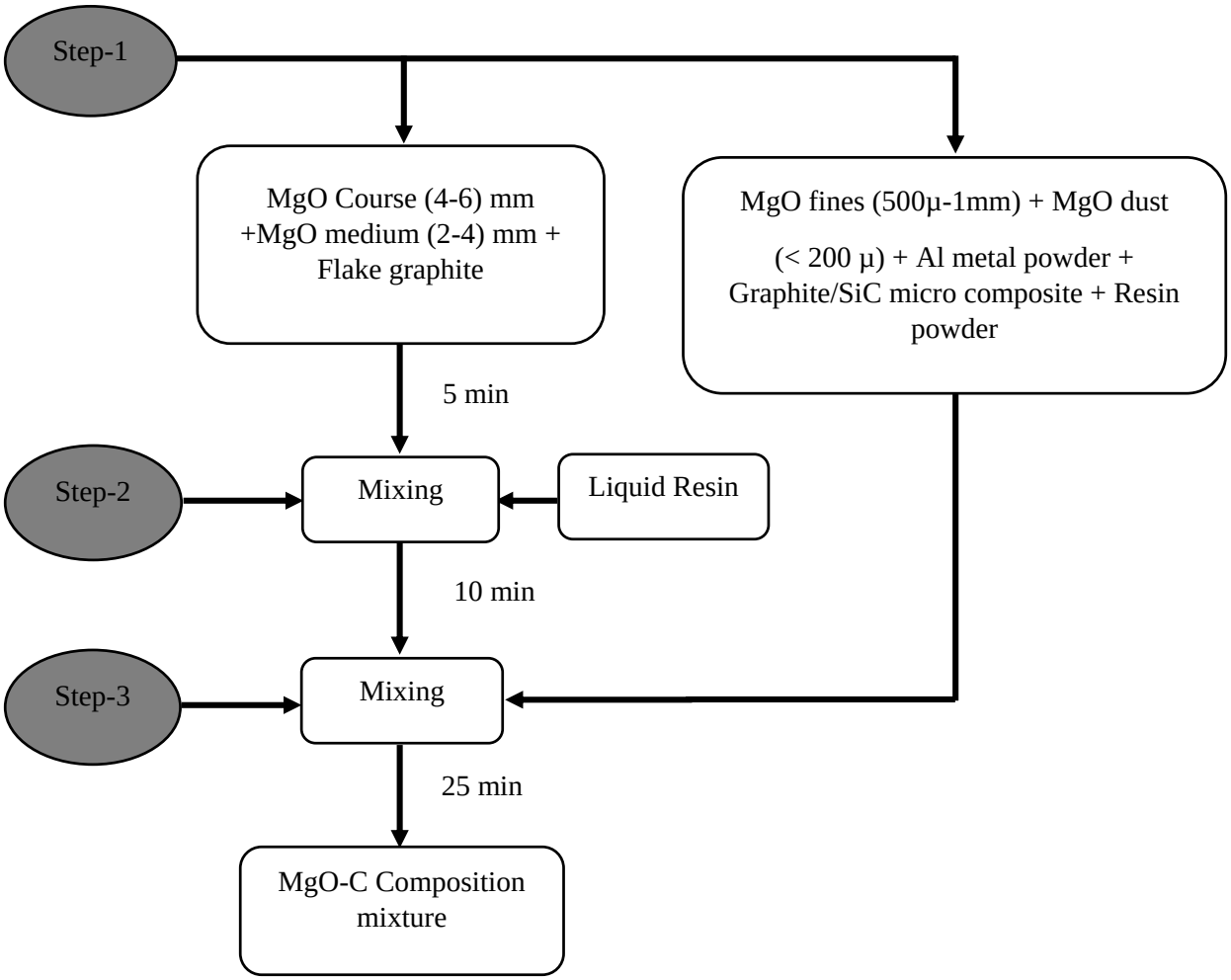

Figure 3.2: Schematic representation of MgO-C brick mixing process

The Figure 3.2 shows mixing sequence of various raw materials during MgO-C brick preparation process. The purpose of mixing the raw materials is to make a refractory batch and transform all the solid components and the liquid additions into a macro homogeneous mixture. The homogeneous mixture can be subsequently moulded or shaped by one of the numerous fabrication methods employed by modern refractory manufacturers. All the raw materials were thoroughly mixed using pan mixer at room temperature for nearly 45 minutes.

3.4.3. Aging:

After homogeneously mixing of the materials, the batches were kept for 2 hours for aging. While aging the polymerization of the resin takes place by developing carbon-carbon bond.

3.4.4. Pressing:

The laboratory scale aged mixtures were used for preparing suitable batches. The sample dimensions were Ø 50 mm and 50 mm in height. To achieve better-filled density and uniform levelling, the mixture was tapped slowly into the mould. Then the top punch was applied slowly. First, the pressing was done in a uniaxial hydraulic press (Carver, USA) with a pressure of 1800 kg/cm^2. The holding time was 60 seconds, and then the pressure was released slowly and then the sample is demoulded. For industrial scale, the aged batches were pressed in a friction screw press (400T FSP, Tata Krosaki Refractories Limited) to form standard bricks of dimensions 220 mm × 110 mm × 75 mm. An appropriate weight of each mixture is taken so as to get the desired green density and the size of the brick. Kerosene is used to avoid the stickiness between the mould and the mixture. In order to avoid lamination in the pressed bricks, the mixtures were filled slowly into the mould cavity and levelled uniformly.

3.4.5. Tempering:

Tempering is the heat treatment process of the refractories at low temperature to remove the volatile matter from the organic green binders and to impart enough green strength. By this process, the chemical bond is developed in the refractory body. Phenolic resin is converted to a brittle solid mass called resist during the curing process (above 200° C.) and then with increasing the temperature it turns to carbonaceous phase (residual carbon). The carbonization of resin is responsible for the final carbon binding and strength development in such bricks. However, certain drawbacks of residual carbon of phenolic resin cause limiting the applications of phenolic resin as a bonding agent. The pressed samples were tempered at 200^{o}C for 12-15 hours in a tempering kiln.

3.5. Characterization of Brick

3.5.1. Apparent Porosity (AP) and Bulk Density (BD):

Apparent porosity (AP) is a measure of the volume of the open pores, into which a liquid can penetrate, as a percentage of the total volume. In green refractory material the pores are all open and, fluids can pass through them. When these materials fired at a particular temperature, some liquid formation due to fusion takes place and, as a result, some pores will be sealed. The apparent porosity (AP) called as such takes the open pores and not the closed pores. (As per the standard of IS: 1528, Part-8, 1974).

$$\text{Apparent porosity (AP)} = \frac{W - D}{W - S} \times 100$$

The test specimen of dried at 110^{o}C after wet cutting. First, the dry weight (D) has to be noted, after that the samples placed in an empty vacuum desiccator. After 30 minute evacuation, water is allowed to enter, and vacuum maintained for 20 minutes.

This process is planned to fill up all voids present in the specimen with water. The suspended weight (S) and the soaked weight (W) were taken.

Where,

D- Dry weight of the specimen

W- The saturated weight of the sample immersed (soaked) in water or kerosene

S -The saturated weight of the soaked sample in the air.

Bulk density (BD) of the material defined as the ratio of the mass of the sample to its bulk volume. The BD was calculated as per the standard of IS: 1528, Part -12 (1974).

$$\text{Bulk Density (BD)} = \frac{\mathbf{D}}{\mathbf{W - S}} \times \text{Density of the liquid (water or Kerosene).}$$

3.5.2. Cold Crushing Strength (CCS):

The cold crushing strength(CCS) is the capability of a refractory to provide resistance to compressive load at room temperature or the material ability to resist the failure under compressive load at room temperature.

$$CCS = \frac{\text{Load}}{\text{Unit volume}} \ (kg/cm^2)$$

The test specimen size (50mm×50mm×50mm) is taken and dried at 100°C. The cold crushing strength of the refractories is measured by placing a suitable refractory specimen in between two flat surface rams. Then after followed by application of the uniform load to it through a bearing block in a standard mechanical, hydraulic compression testing machine. The load at which crack appears in the brick represents the cold crushing strength of the specimen. The load is applied uniformly to the sample in the flat position. The applied is load expressed in terms of MPa.

3.5.3. Hot modulus of rupture (HMOR):

The hot modulus of rupture (HMOR) defined as refractory material ability to resist deformation under load at elevated temperature or over a range of temperature or the flexural breaking strength of a refractory at a chosen elevated temperature in air.

It determines as per ASTM C133-7. The test conducted by three - point bending test using HMOR testing apparatus. For HMOR test, all the specimen sizes were maintained as 150 mm × 25 mm × 25 mm without pre-firing at air atmosphere. The final temperature of HMOR was 1400ºC/30 min. with a heating rate of heating rate of 5ºC/min. The test carried out in an air atmosphere with the loading rate of HMOR was 1.2-1.4 kg/s according to samples.

The following formula calculated the HMOR value:

$$HMOR = \frac{3P \times L}{2b \times d^2} \ (kg/cm^2)$$

Where P = the maximum load required to break the specimen

L = the span length between the lower supporting points.

b = the breadth (cm).

d = the height of the specimen (cm).

3.5.4. Slag corrosion test:

Slag corrosion test by the static crucible test method conducted for the different MgO-C components carried out at 1600°C for 3h. The chemical composition and basicity of the slag composition are given in Table 3.8. The slag corroded samples were cut vertically by diamond

saw, and the depth of slag corroded area (visually distinguishable) were measured with vernier callipers.

Table 3.8: Chemical composition of the synthetic slag.

Tata Steels LD2 Slag composition (wt.%)						
CaO	SiO_2	Al_2O_3	MgO	Fe_2O_3	CaO/Al_2O_3	CaO/SiO_2
54.90	9.11	31.10	3.50	0.99	1.76	6.02

Preparation of synthetic slag:

The above mentioned mineralogical composition data were collected from Tata Steels, LD2 slag composition. The synthetic slag is prepared according to the above-mentioned composition with using of lime powder ($CaCO_3$), fumed silica (SiO_2), calcined alumina (Al_2O_3), MgO dust and Fe_2O_3 in the form of mill scale. In this section, the fine fraction of raw materials were used for the preparation of synthetic slag. Moreover, the mixtures were grounded in XRF grinding machine with tungsten grinding media, after that these slag powder sieved through 200 mesh to separate the coarse particles.

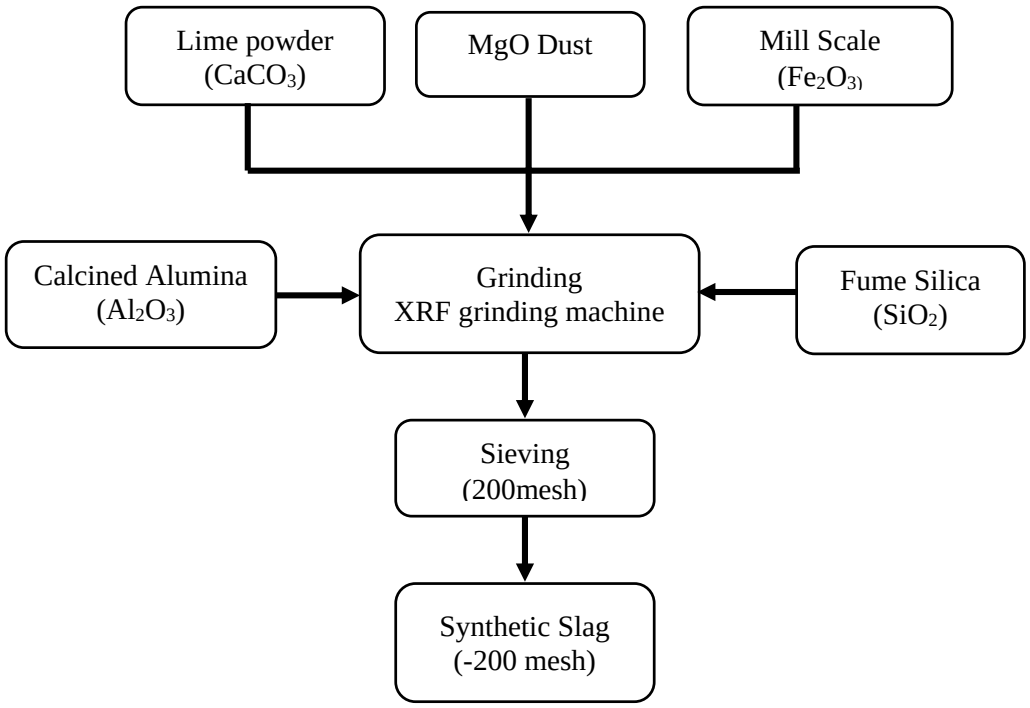

Figure 3.3: Flow chart for preparation of synthetic slag

3.5.5. Oxidation resistance test

For oxidation resistance test, cylindrical samples (Height =50 mm, Diameter =50mm) were prepared by wet cutting from the tempered bricks and then dried at 100^{o}C. These cylindrical samples were placed in an electrically heated furnace (heating rate of 5^{o}C /min) under the ambient condition at 1400^{o}C/5hrs. The furnace is then cooled down at the same rate of 5^{o}C/min. Fired samples were horizontally cut into two pieces.

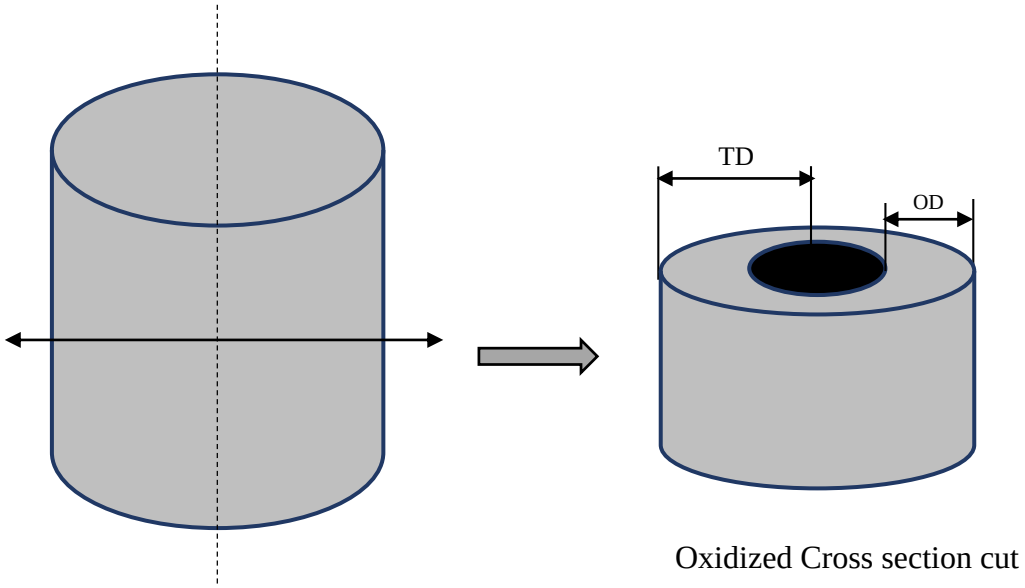

Figure 3.4: Specimen used for oxidation test as per ASTM standards

The remaining black surface was measured at eight different locations. The total diameter of the samples were also noted. The average value of oxidized area is given by,

Oxidation index = (Oxidized diameter (OD)/Total diameter (TD)) ×100

Chapter - 4

Results & Discussion

SECTION – I

Synthesis of Graphite-SiC Microcomposites from Natural Flake Graphite and Microfine Silica at different conditions

4.1. Structure and properties of raw materials used for preparation of microcomposite

In this study, the raw material for microcomposite preparation namely natural flake graphite and a microfine silica has been examined briefly before using it for carbothermal reduction. The properties studied like phase, crystallinity, morphology; particle size and shape is investigated.

4.1.1. Phase analysis & microstructure of graphite

The XRD pattern of 94FC natural flake graphite has been presented in Figure 4.1. Two sharp crystalline peaks appeared at 2θ equals to 26.6172^o (111) and 54.6855^o (222), respectively. These peaks were well matched with JCPDS No. 75-2078, which represents the graphite phase with the rhombohedral crystal structure. Figure 4.2 represents the FESEM image of the natural flake graphite. The individual graphite flake appears like a wedge (Figure 4.2a) but high-resolution SEM at the cross section shows that it has the layer-like structure (Figure 4.2b).

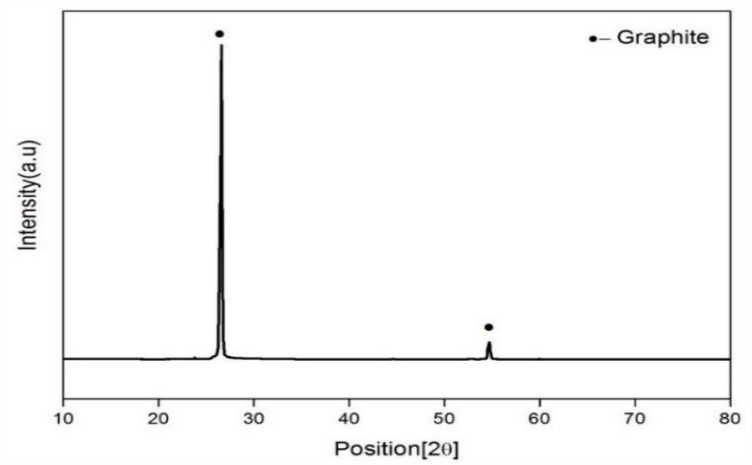

Figure 4.1: X-Ray diffraction pattern of natural flake graphite.

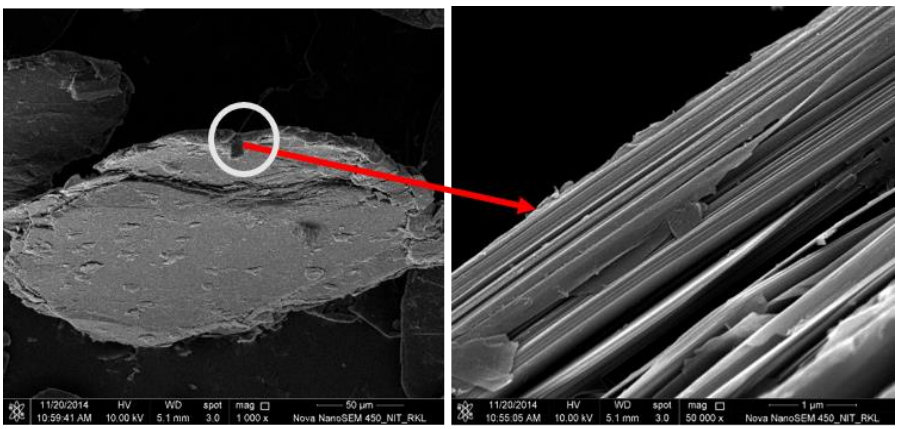

Figure 4.2: Micrographs of natural flake graphite.

4.1.2. Phase analysis, microstructure & particle size distribution of the microfine silica

The XRD pattern of the microfine silica is shown in Figure 4.3(a). It showed a broad peak of silica at 2θ=22° (JCPDS No. 29-0085) attributing to the amorphous nature of the silica raw material. It has also been observed to have some traces of tridymite as an impurity phase in the raw material. The micrographs of microfine silica showed Figure 4.3(b) spherically shaped particles. Particle size has also been analysed as presented in Figure 4.4. The average particle size of the microfine silica was 352nm. A narrow distribution of particles has been observed which shows particles were almost uniform in nature.

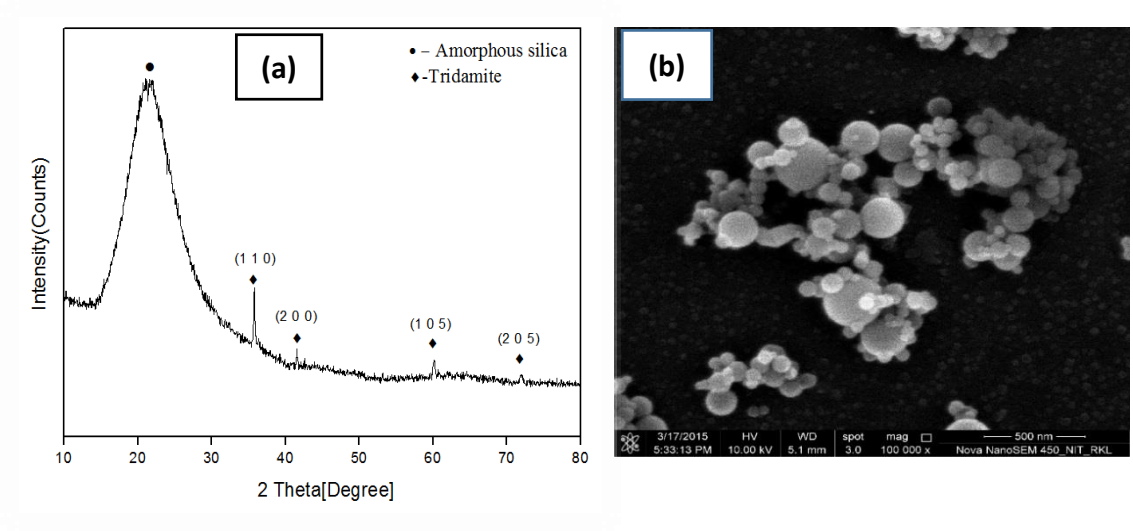

Figure 4.3: Phase analysis and microstructure of the microfine silica

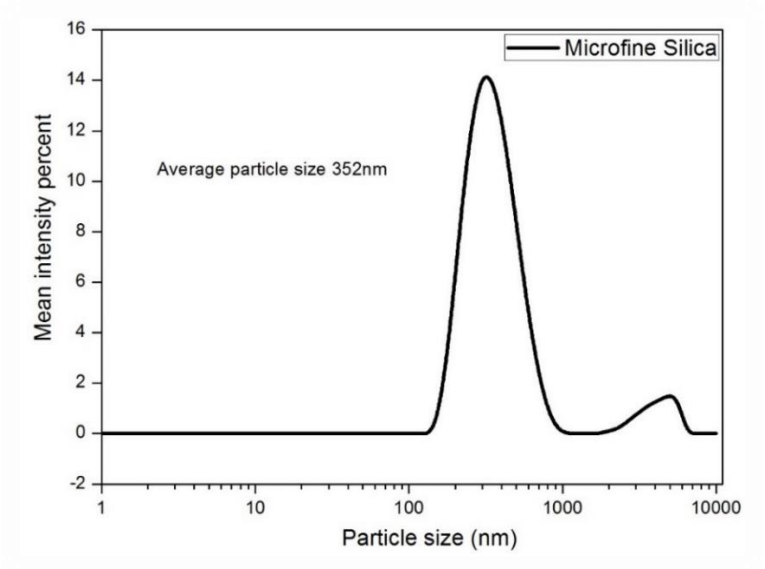

Figure 4.4: Particle size distribution of the microfine silica.

4.2. Characterizations of graphite/SiC microcomposite under different conditions

4.2.1. XRD Analysis

The microcomposite (30:70) prepared by carbothermal reduction between microfine silica and graphite under different atmospheric conditions (CAF and RHF) at different temperatures [1600ºC, 1650 ºC and 1700ºC] has been studied. The XRD pattern of 30/70 (microfine Silica/graphite) microcomposite, after firing at different temperatures has been shown in Figure 4.5. It has been confirmed that all the samples after heat-treatment contain both graphite and β-SiC phases. However, the peaks are of different intensities indicating the quantitative variation of the phases.

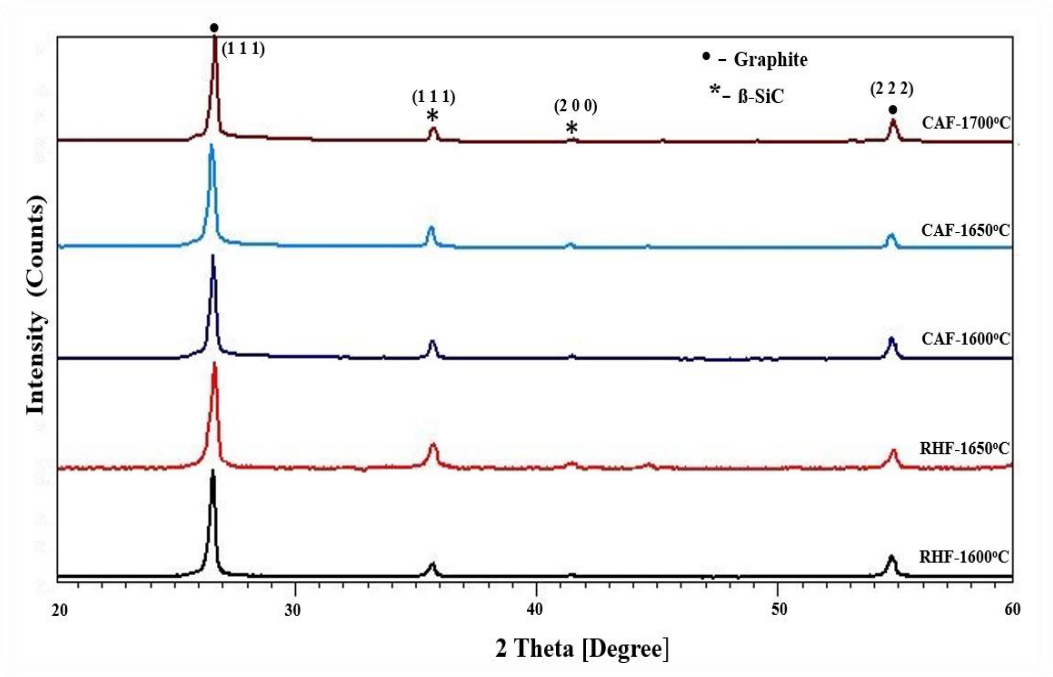

Figure 4.5: XRD patterns of the 30/70 [micro-fine silica/graphite (94FC)] microcomposite, prepared under different atmospheric conditions (CAF, RHF) at various temperatures

The 40/60 (microfine silica/graphite) microcompositions have also been established with the similar processing conditions as 30/70 composition. The XRD pattern of 40/60 microcomposites has been shown in Figure 4.6 which showed that graphite and β-SiC phases are obtained irrespective of calcination temperature and atmosphere in either CAF or RHF. However, a distinct intensity variation along with different morphologies are noticed, which are discussed in Section 4.2.2.

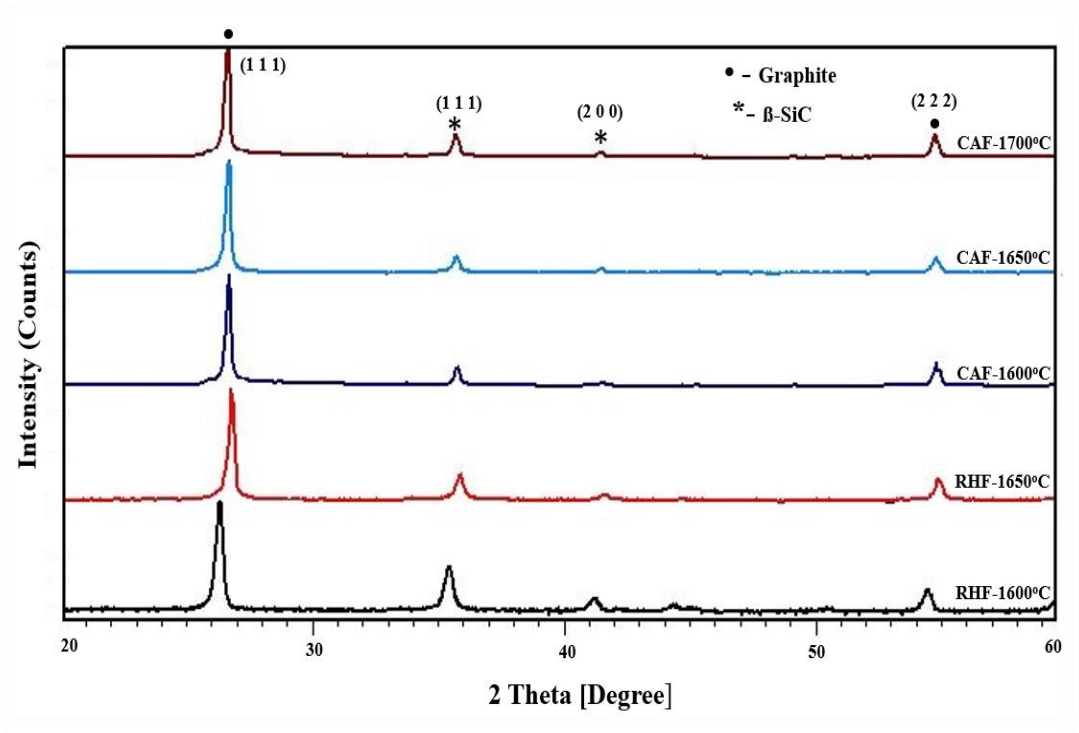

Figure 4.6: XRD patterns of the 40/60 [microfine silica/graphite (94FC)] micro-composite, prepared under different atmospheric conditions (CAF, RHF) at various temperatures

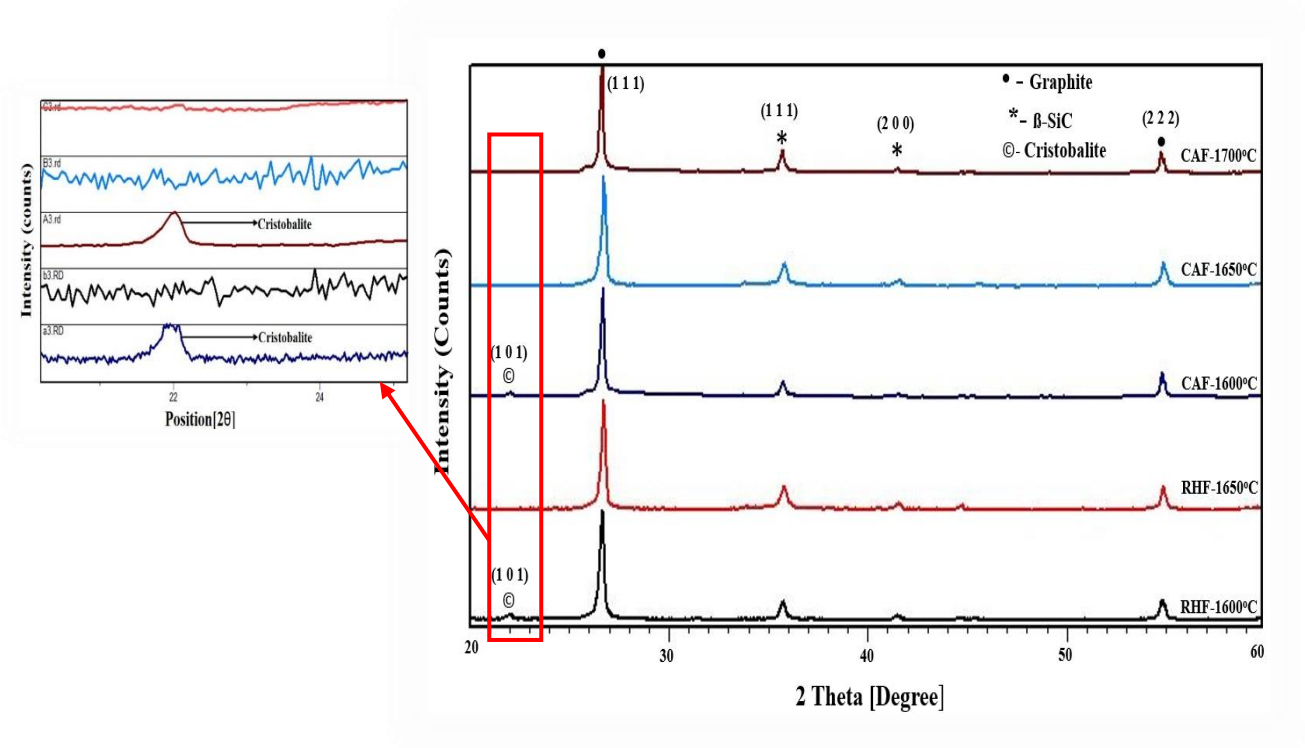

Figure 4.7: XRD patterns of the 50/50 [microfine silica/graphite (94FC)] micro-composite, prepared under different atmospheric conditions (CAF, RHF) at various temperatures

The XRD patterns of 50/50 wt% [microfine silica/graphite] component after heat treated at various firing conditions and temperatures are shown in Figure 4.7. These samples contain graphite and SiC, but the sample fired at 1600^{o}C contained a trace amount of unreacted silica in the form of cristobalite. The presence of other phases could be attributed to the tendency of incomplete reaction between the raw materials and presence of unreacted silica (upon addition of >40% silica content at lower temperature firing). However, detailed analysis of the XRD pattern from 2θ = 21-24^{o} revealed the presence of unreacted silica in the form of cristobalite as shown in Figure 4.7. The phases obtained under different temperature has been tabulated in Table 4.1.

Table 4.1. The phases present in a few selected micro-composites as a result of XRD analysis

Composition	Condition and Temperature	Phases identified from X-ray diffraction pattern
Microcomposite Prepared with (50/50) wt% (Microfine silica/graphite)	CAF/1700^{0}C/4hrs	Graphite, Silicon Carbide
	CAF/1650^{0}C/4hrs	Graphite, Silicon Carbide
	CAF/1600^{0}C/4hrs	Graphite, Silicon Carbide, Cristobalite
	RHF/1650^{0}C/4hrs	Graphite, Silicon Carbide
	RHF/1600^{0}C/4hrs	Graphite, Silicon Carbide, Cristobalite

4.2.2. Morphology of the Micro-composite

Detailed microstructural analysis by FESEM of most of the micro-composite samples synthesized under this investigation is presented in Figures 4.8 - 4.15. It is confirmed from these micrographs that two distinctly different morphologies namely (a) ribbon and (b) fibre /rod type β-SiC are produced under various conditions of heat treatment and composition (silica to graphite ratio). In general, higher the temperature more is the tendency of ribbon formation. On the other hand lower temperature and the higher silica content is fibre formation predominates. However, in many of the samples, both fibre and ribbons are normally present. Their relative amounts vary with the temperature and silica content. Another interesting feature of the microstructure is that the ribbons normally form on the outside surfaces of the graphite flakes strongly adhering to the flat

surface of the flakes while the fibres are preferably grown in interlamellar spaces of the flakes. Such spaces appear to act as reaction chambers for the following gas phase reaction to take place [1, 2].

$$SiO + 3CO \rightarrow SiC + 2CO_2 \quad \ldots\ldots\ldots\ldots (4.1)$$

It is well-known that a gaseous phase like SiO is formed when SiO_2 is heated to more than 1500°C under a reducing condition. The gas phase reaction mentioned above leads to the formation of SiC fibres within the interlamellar spaces of the graphite flakes. On the other hand, a gas-solid reaction on the surface of the graphite flakes such as the following one possibly leads to the formation of SiC ribbons, which gets adhered to the surface of the flakes.

$$SiO + 2C \rightarrow SiC + 2C \quad \ldots\ldots\ldots\ldots\ldots (4.2)$$

It is also noted that the fibers are relatively large diameter (may be described as rods rather than fibres) when the heat-treatment is carried out inside the Controlled Atmosphere Furnace (CAF) with graphite heating elements than when the same composition is heated in a Raising Hearth Furnace (RHF). Impurity content of the graphite flakes, particularly Fe_2O_3 content also has an influence on the nature of the SiC rods formed, possibly due to a catalytic effect of the impurities. SiC rods are formed in larger quantities when an impure variety of the graphite (94FC) is used (compared to 97FC). Another interesting feature of the microstructure is that most of the rods are attached to a spherical ball at one of the ends.

The SiC whiskers/fibres and rods were formed due the vapor-liquid-solid (VLS) process. Here the Fe_2O_3 impurity in the flake graphite is acting as a catalyst for the growth of whiskers and fibres. A catalyst droplet was formed on the tip of the all the rods in Figure 4.9c. Whiskers show smooth surfaces and no ramifications. They have a uniform diameter (500nm-1.25µm) and lengths between 50 to 300µm. When SiO gas transported through flake graphite structures, the impurity iron phase inside the graphite helped SiO generators for growth to take place through the vapor phase. The whisker growth rate depends on the presence of Fe droplets of appropriate size and SiO available in great quantity [3, 4].

1600°C/4hrs - 30% SiO_2 + 70% Graphite (94FC) CAF	(a)	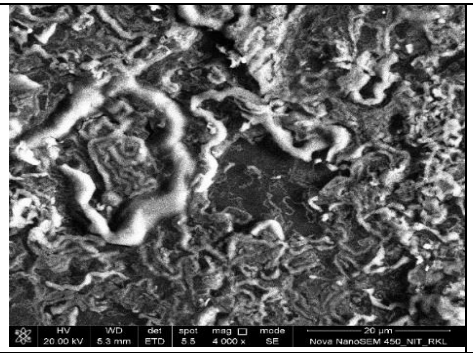	(b)	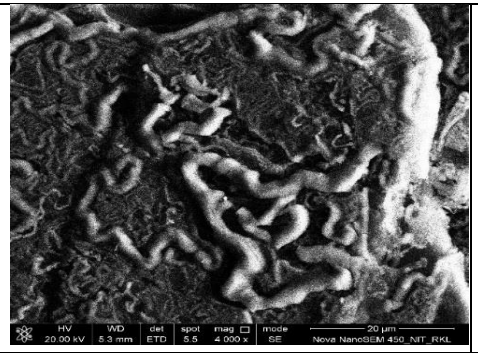	(c)	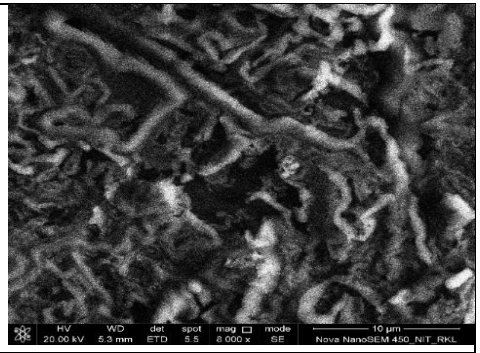
1600°C/4hrs - 40% SiO_2 + 60% Graphite (94FC) CAF	(a)	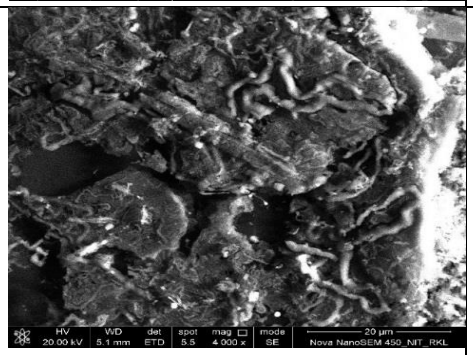	(b)	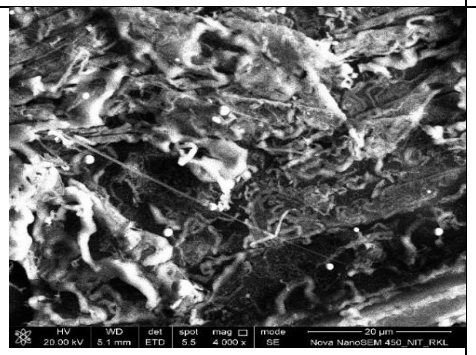	(c)	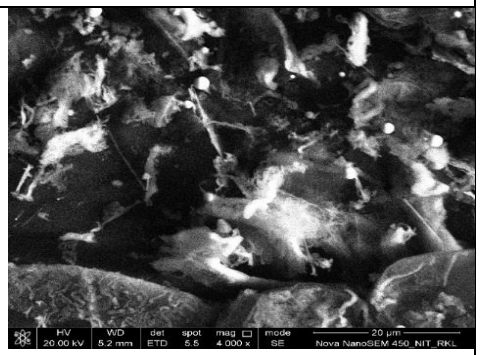
1600°C/4hrs - 50% SiO2 + 50% Graphite (94FC) CAF	(a)	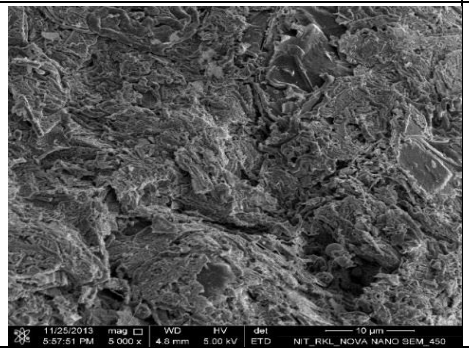	(b)	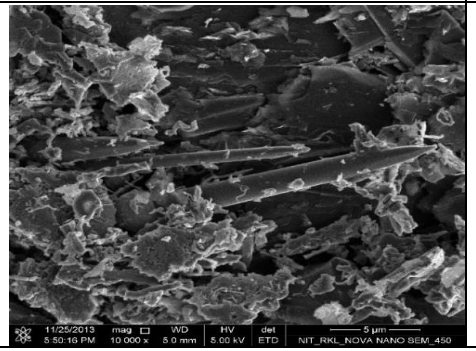	(c)	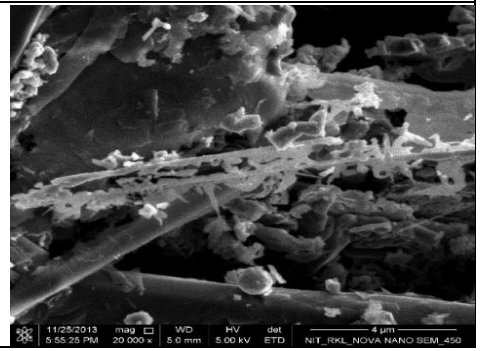

Figure 4.8: FESEM images of micro composite having 30/70, 40/60 and 50/50wt.% of SiO_2/ graphite, fired at 1600°C/4hrs in CAF using 94FC graphite (+212µ) flakes. Pictures at (a), (b) and (c) represent micrographs of the same specimen with increasing magnification

1650ºC/4hrs - 30% SiO2 + 70% Graphite (94FC) CAF	(a)	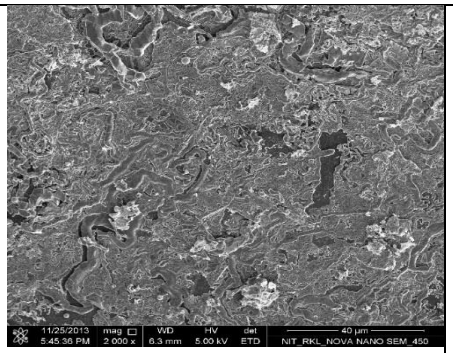	(b)	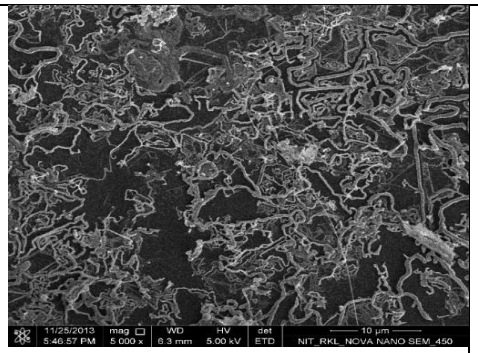	(c)	
1650ºC/4hrs - 40% SiO2 + 60% Graphite (94FC) CAF	(a)	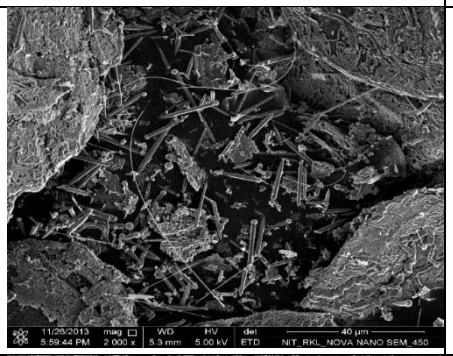	(b)	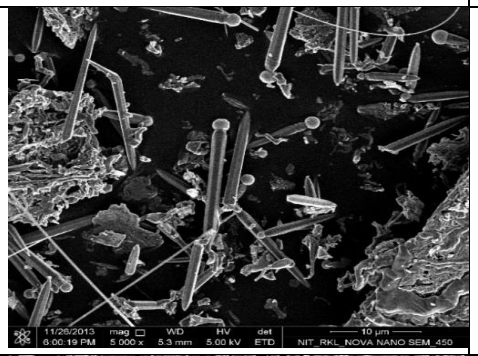	(c)	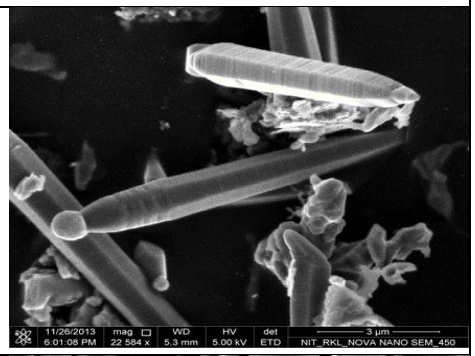
1650ºC/4hrs - 50% SiO2 + 50% Graphite (94FC) CAF	(a)	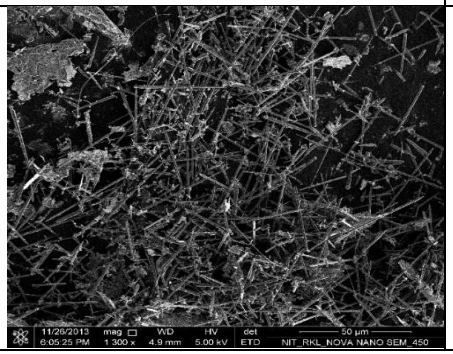	(b)	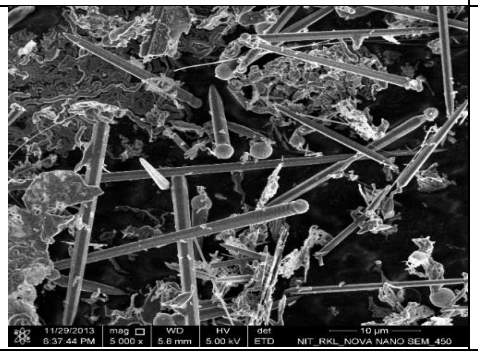	(c)	

Figure 4.9: FESEM images of micro composite having 30/70, 40/60 and 50/50wt% of SiO_2/ graphite, fired at 1650ºC/4hrs in CAF using 94FC graphite (+212µ) flakes. Pictures at (a), (b) and (c) represent micrographs of the same specimen with increasing magnification.

1700ºC/4hrs - 30% SiO2 + 70% Graphite (94FC) CAF	(a)		(b)	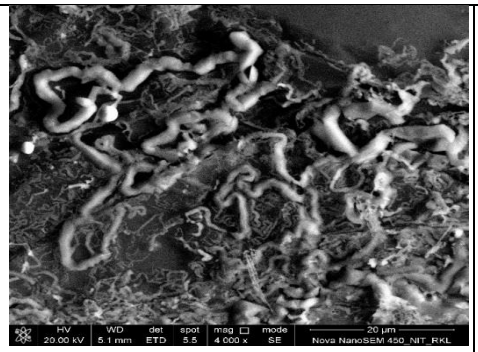	(c)	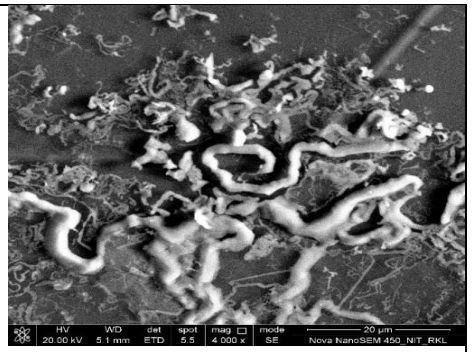
1700ºC/4hrs - 40% SiO2 + 60% Graphite (94FC) CAF	(a)	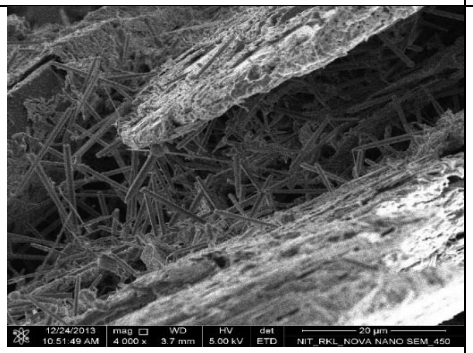	(b)	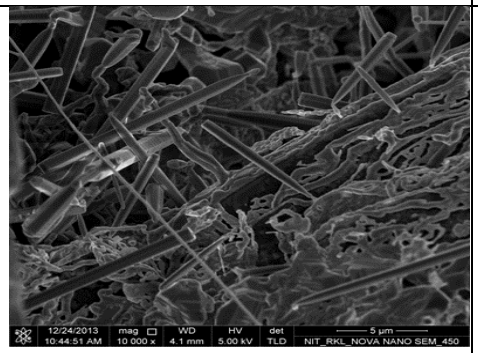	(c)	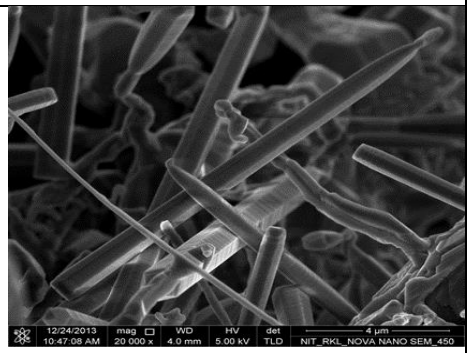
1700ºC/4hrs - 50% SiO2 + 50% Graphite (94FC) CAF	(a)	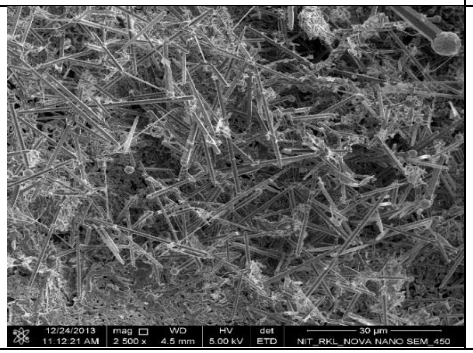	(b)	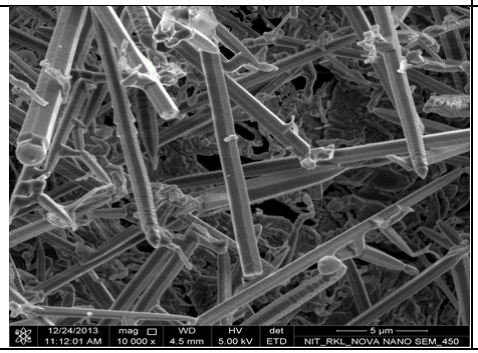	(c)	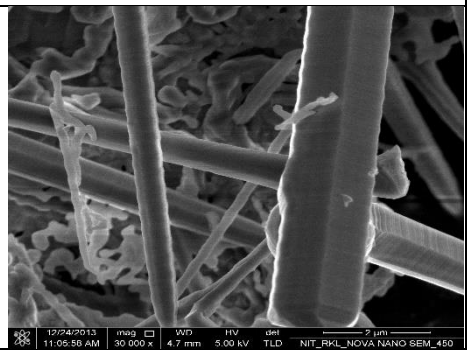

Figure 4.10: FESEM images of micro composite having 30/70, 40/60 and 50/50wt.% of SiO_2/ graphite, fired at 1700ºC/4hrs in CAF using 94FC graphite (+212µ) flakes. Pictures at (a), (b) and (c) represent micrographs of the same specimen but with increasing magnification.

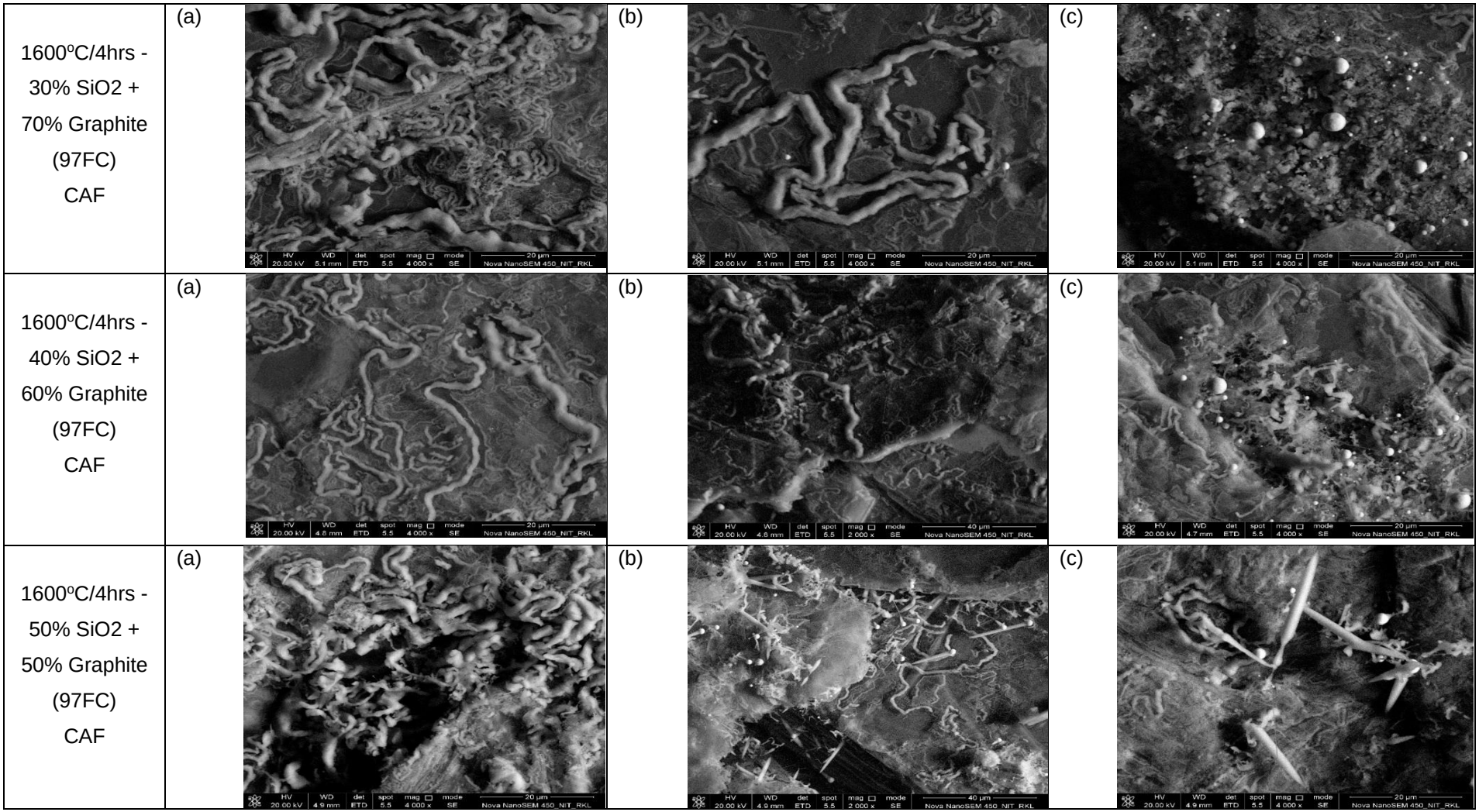

Figure 4.11: FESEM images of micro composite having 30/70, 40/60 and 50/50wt.% of SiO_2/ graphite, fired at 1600°C/4hrs in CAF using 97FC graphite (+212µ) flakes. Pictures at (a), (b) and (c) represent micrographs of the same specimen with increasing magnification.

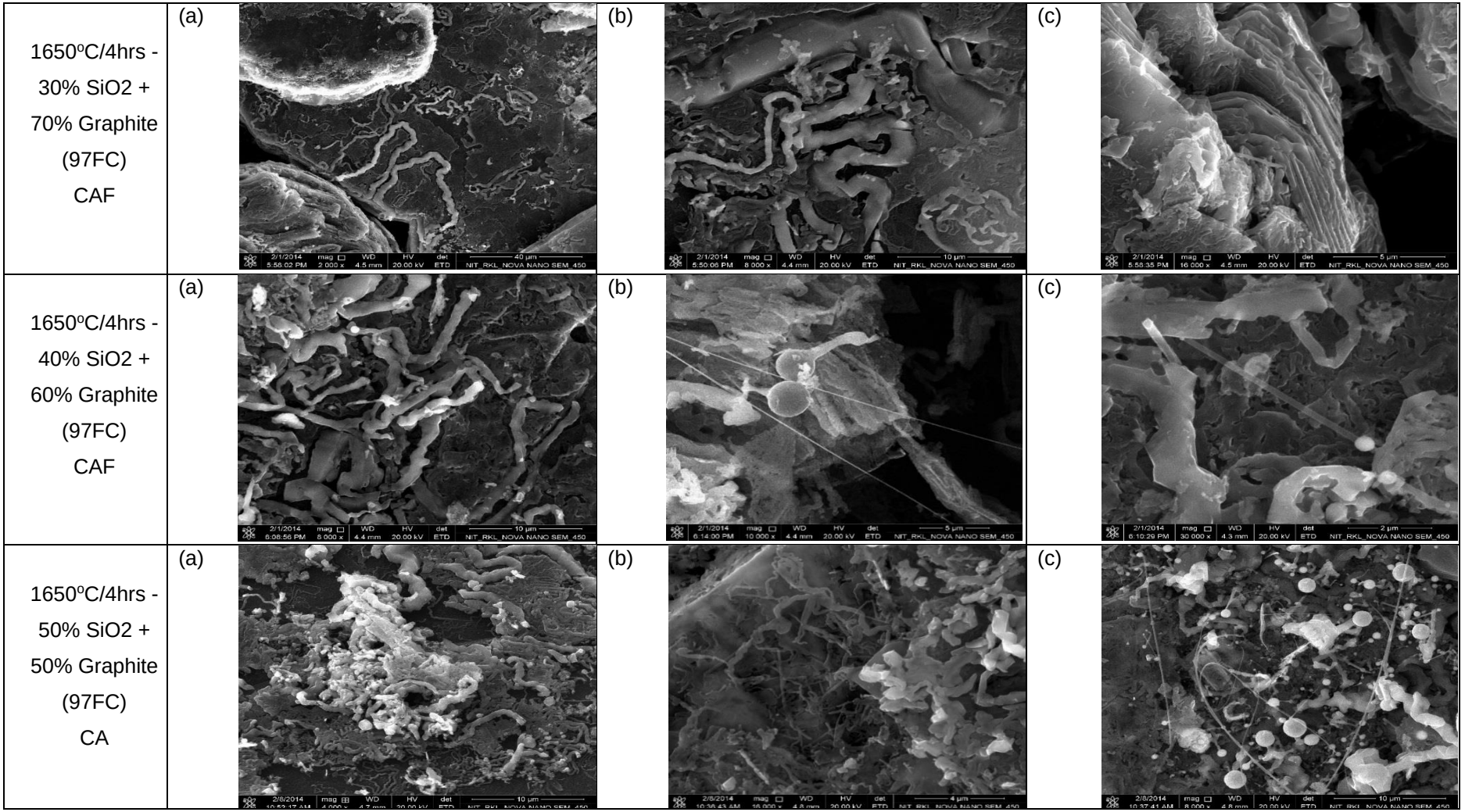

Figure 4.12: FESEM images of micro composite having 30/70, 40/60 and 50/50wt.% of SiO_2/ graphite, fired at 1650°C/4hrs in CAF using 97FC graphite (+212µ) flakes. Pictures at (a), (b) and (c) represent micrographs of the same specimen with increasing magnification.

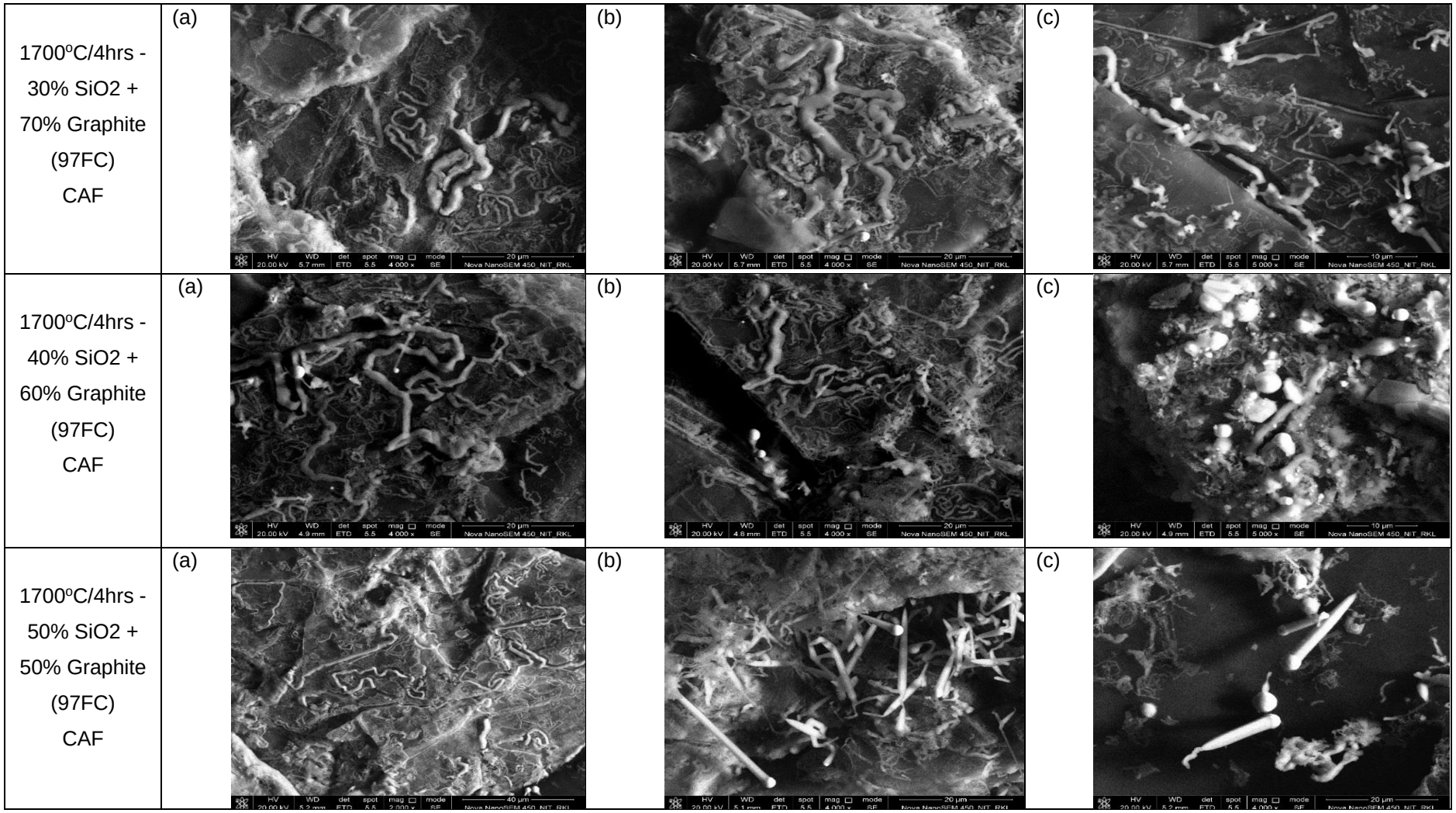

Figure 4.13: FESEM images of micro composite having 30/70, 40/60 and 50/50wt.% of SiO_2/ graphite, fired at 1700°C/4hrs in CAF using 97FC graphite (+212µ) flakes. Pictures at (a), (b) and (c) represent micrographs of the same specimen with increasing magnification.

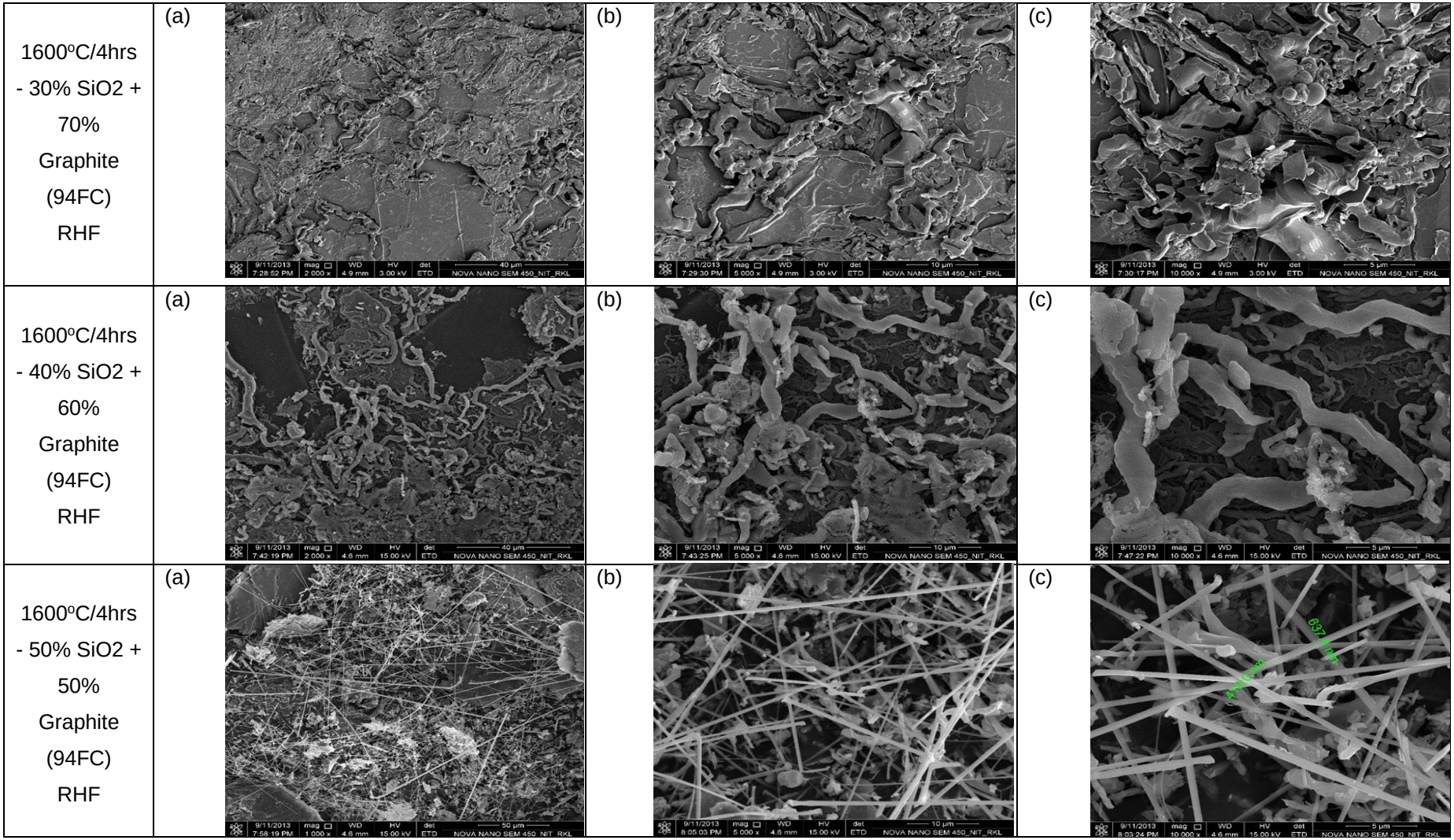

Figure 4.14: FESEM images of micro composite having 30/70, 40/60 and 50/50wt. % of SiO_2/ graphite, fired at 1600ºC/4hrs in RHF using 94FC graphite (+212µ) flakes. Pictures at (a), (b) and (c) represent micrographs of the same specimen with increasing magnification.

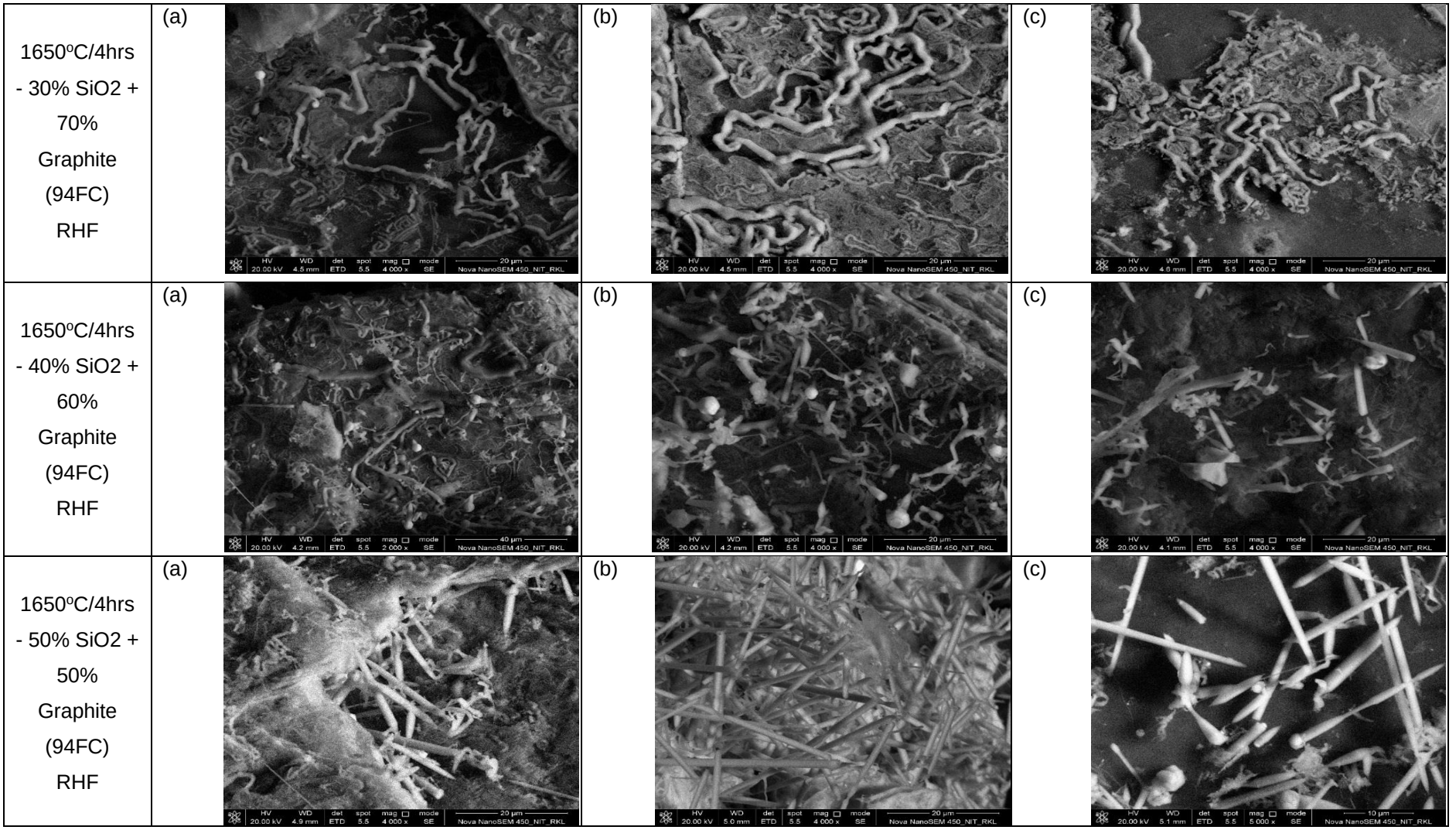

Figure 4.15: FESEM images of micro composite having 30/70, 40/60 and 50/50wt. % of SiO_2/graphite, fired at 1650°C/4hrs in RHF using 94FC graphite (+212µ) flakes. Pictures at (a), (b) and (c) represent micrographs of the same specimen with increasing magnification.

Energy dispersive spectrometer (EDAX)

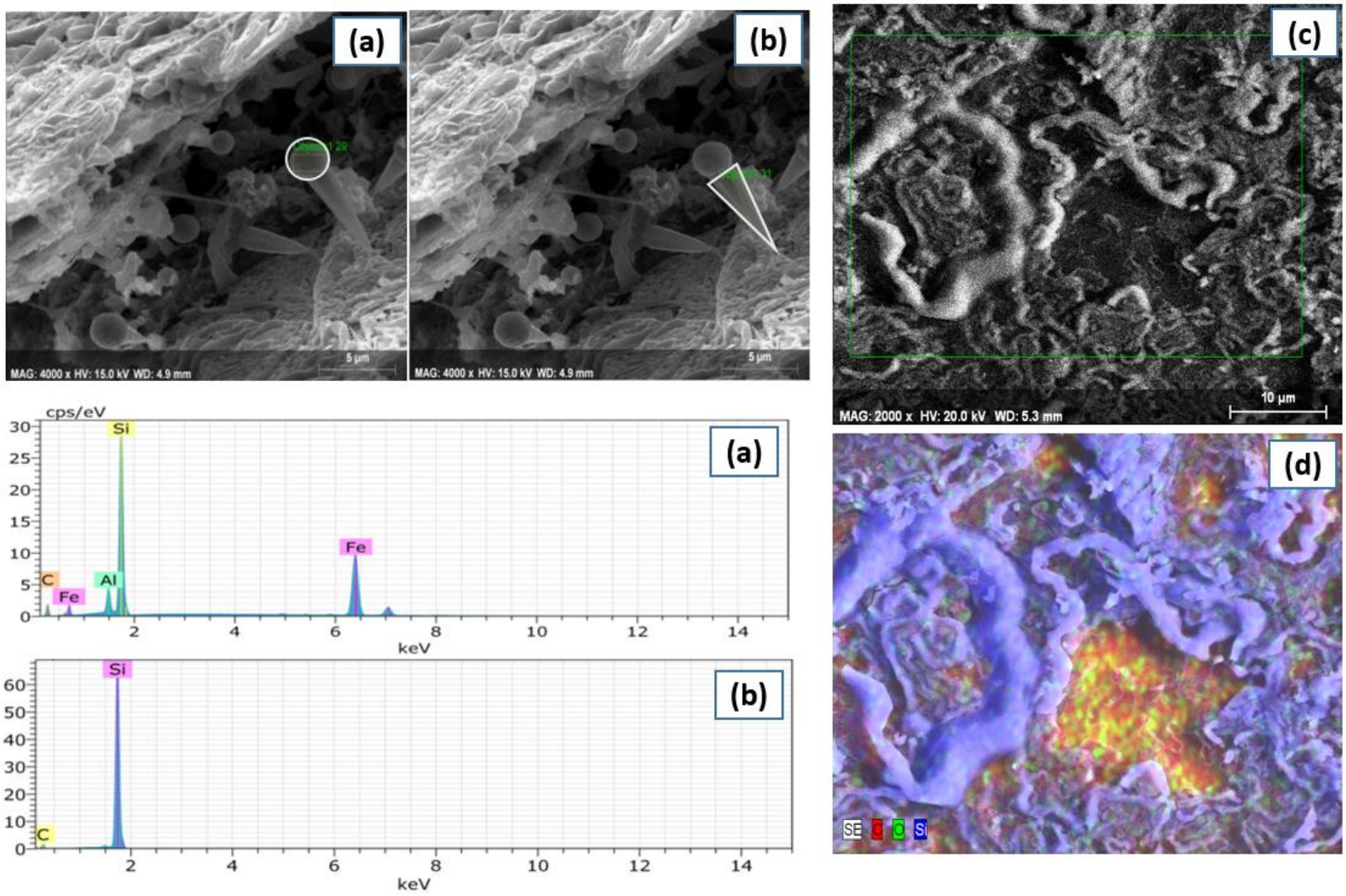

Figure 4.16: Energy dispersive spectrometer (EDS) of ball headed rod (a & b) and (c & d) elemental mapping of microcomposite.

The microstructure is shown in Figure 4.16 (a) & (b) the rods are attached to a spherical ball at one of the ends. EDAX analysis has confirmed that these are SiC balls but with a significant quantity of Fe and rod body contains SiC. This observation leads to a conclusion that Fe possibly acts as a catalyst for the growth of the SiC rods. The elemental mapping shows Figure 4.16 (c) & (d) elements present in the microcomposite confirmed through colour marking [4].

4.2.3. Tap Density

The effect of the change in morphology of SiC with varying percentage of silica followed by heat treatment under different atmosphere can also be obtained through measurement of tap density of the synthesized micro-composite powder. It can observed that with an increment of fibre content, the composite powder becomes fluffier resulting in less tap density as presented in Figure 4.17.

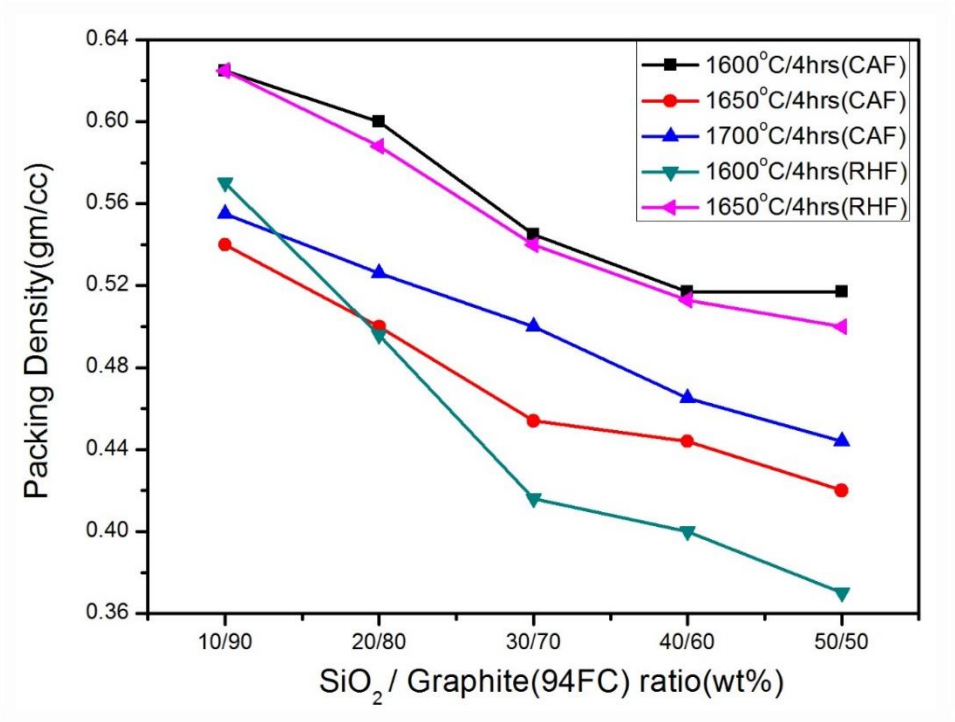

Figure 4.17: The variation in tap density of microcomposites by changing the amount of silica/graphite (94FC), after heat treated at different conditions.

The above figure indicates that the tap density monotonically decreases with increasing silica content irrespective of the atmosphere of heat-treatment and furnace type used. The above result confirms the formation of more amount SiC fibre with increasing of silica to

graphite but with decreasing temperature. These observations compare well with the FESEM analysis presented earlier.

For any specific silica content, with higher temperature, ribbon formation is more under a particular furnace atmosphere. It may also be noted that the effect of temperature is more significant in RHF than in CAF. This is possibly due to the fact that in CAF there is a tendency to formation of a rod-like morphology having larger diameter resulting in better packing compared to curled fibres formed under RHF conditions.

4.2.4. Estimation of SiC content in the synthesized microcomposite

In order to get an idea of the quantity of the SiC phase, the synthesized micro-composite is heated under an oxidizing atmosphere in chamber furnace at temperature 1000^{o}C/1hr to oxidize the unreacted graphite present in the composite. Before carrying out the oxidation experiments with the composite, pure graphite samples having two different purity (94FC and 97FC) has been heated to the same temperature under identical length of time to ensure complete oxidation and to determine the ash content in each case. Results of this initial experiments are presented in Figure 4.18. After oxidation, only 2.5 wt% residue is obtained for pure variety 97FC graphite whereas 4 wt% ash content is observed in 94FC impure graphite.

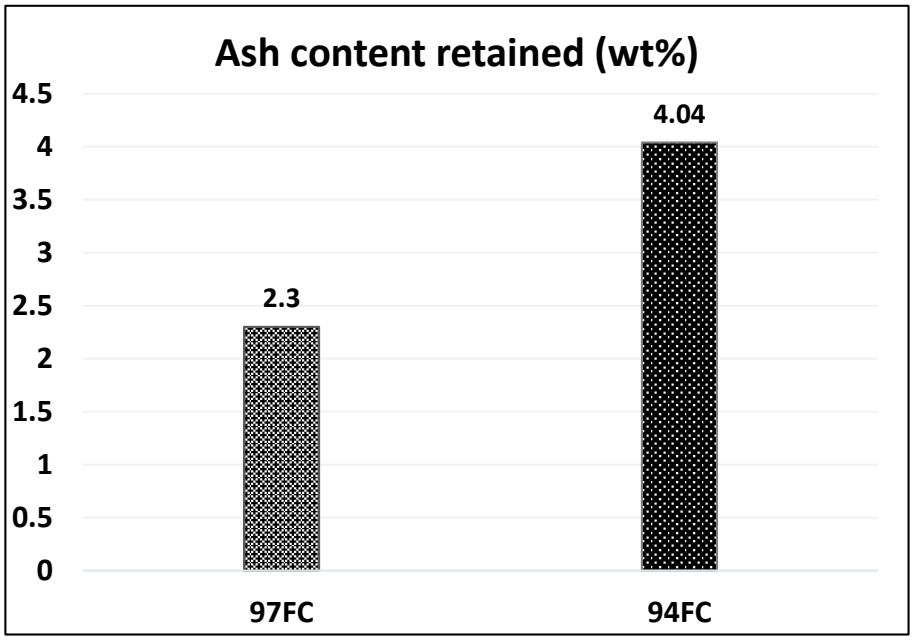

Figure 4.18: Residue (ash) of two different grades of graphite retained after oxidized at 1000^{0}C/1hr.

The mineralogical constituents of the residual ashes collected are determined by XRD measurement and presented in Figure 4.19. It is observed that both the samples contain oxide phases like cristobalite (SiO_2), Al_2O_3, Fe_2O_3 and $FeSiO_3$ in addition to a small amount of unoxidized graphite. As expected, the quantities and the peak intensities of all the oxidized phases are relatively smaller in the purer variety of the graphite (97FC).

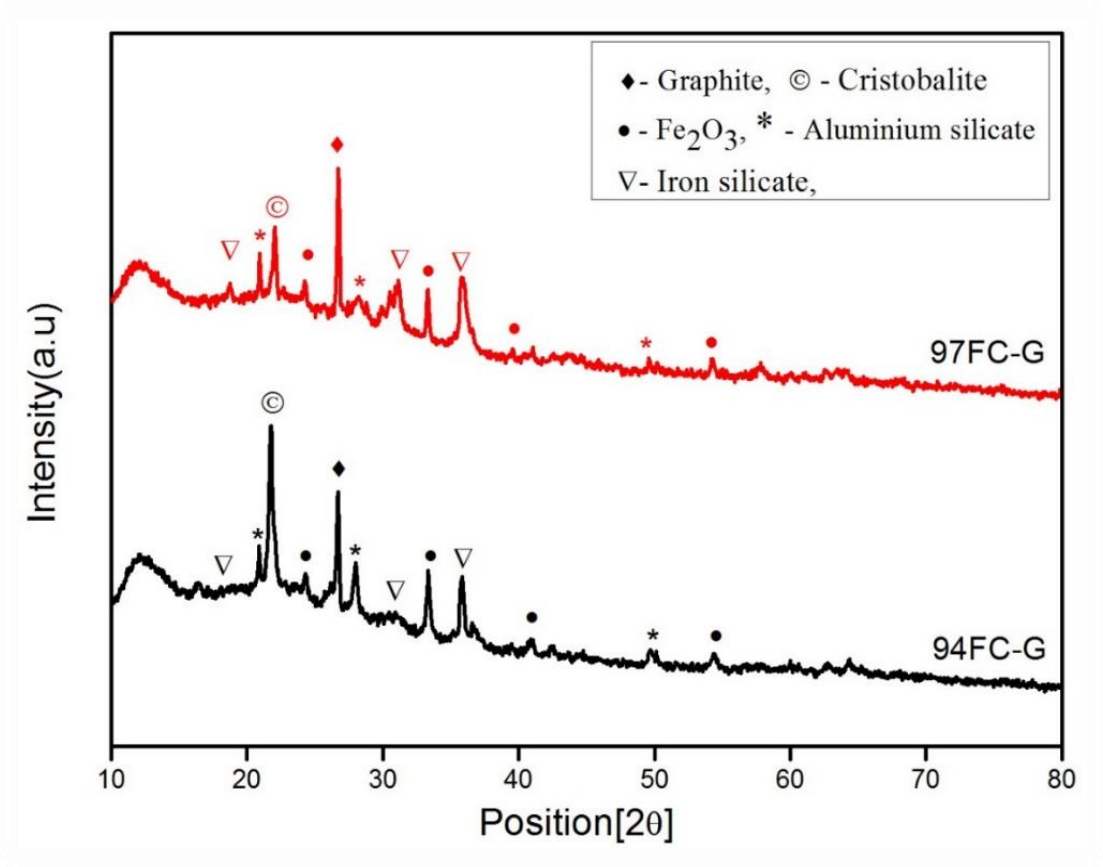

Figure 4.19: XRD patterns of the residue (ash) obtained by oxidation of 97FC & 94FC graphite.

The determination of the SiC content in the synthesized micro-composite is investigated by oxidizing the graphite component of the micro-composite. The remaining material after the heat-treatment is assumed to be the SiC content in the micro-composite. Also, a supportive XRD pattern is also provided in Figure 4.20 to understand the formation of SiC during this process.

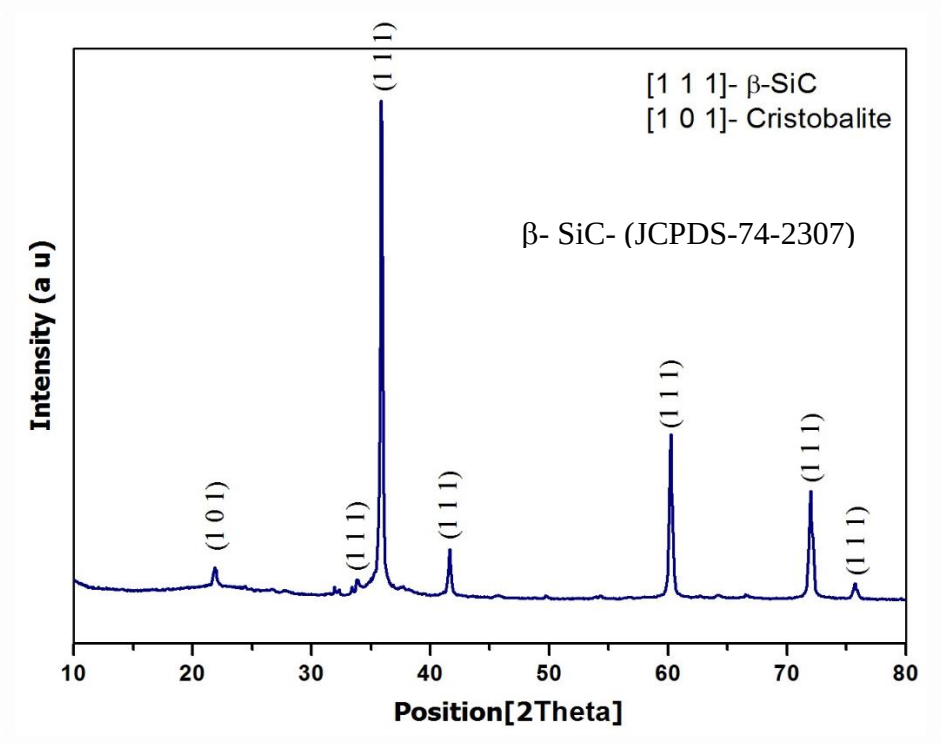

Figure 4.20: XRD pattern of microcomposite after oxidized at 1000°C/1hr.

The SiC content of all composites prepared under different conditions is plotted against silica content of the original mixture heat-treated at various temperatures. The results are presented in Figure 4.21(a) & (b) for 94FC & 97FC graphite. It is interesting to note that irrespective of heat treatment conditions like temperature (>1600^{0}C), purity of the graphite (94FC or 97FC) and the type of the furnace (RHF or CAF), the quantity of SiC formed is primarily depend on the percentage of silica addition during microcomposite preparation. At 10% silica addition, SiC content is slight below 10% and this value increases almost linearly with increasing silica content, finally reaching a value of around 60% when the silica content is increased up to 50%.

The microcomposite powder was characterized by XRD (JCPDS-74-2307) analysis, which confirmed the formation of β-SiC. The Si-C phase diagram reports that the β-SiC phase formation is thermodynamically favourable at 1500°C < β-SiC > 2000°C. As the temperature increases beyond 2000°C, there is a possibility to α-SiC phase predominates [5].

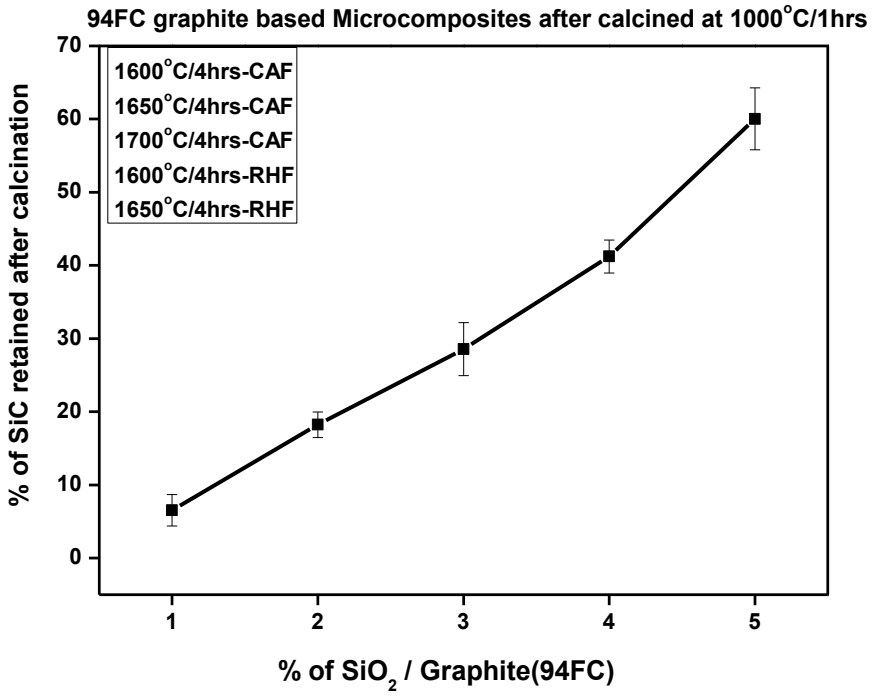

Figure 4.21(a): Estimation of SiC present in microcomposite (94FC) after heat treated at 1000°C/1hr (Composite prepared by variation in temperature).

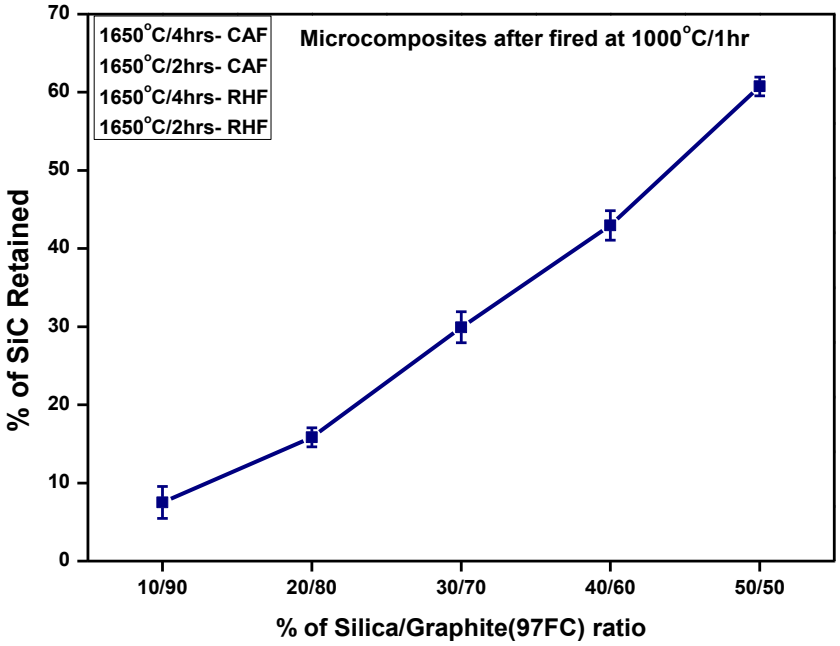

Figure 4.21(b): Estimation of SiC present in microcomposite (97FC) after heat-treated at 1000°C/1hr (Composite prepared by variation in time)

4.2.5. Oxidation behaviour of microcomposite

The effect of temperature on microcomposite formation is more distinctly observed by plotting the percentage of SiC formed against temperature for a fixed amount of silica content of the composite as shown in Figure 4.22. It observed that the amount of SiC formed, increases up to a temperature of 1650°C and after that remains constant. In the below figure, the data for 50/50 SiO_2/Graphite has been presented. However, a similar trend is observed for all the compositions investigated irrespective of the type of the furnace used.

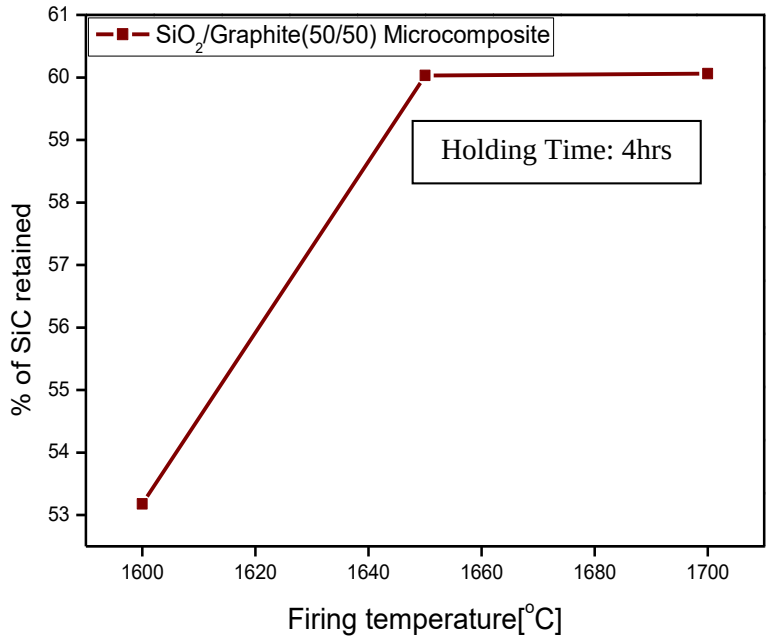

Figure 4.22: Estimation of SiC present in microcomposite after heat-treatment at 1000°C/1hr. (Composite prepared at different temperature with equal composition)

Table 4.2: Characteristics of the graphite/SiC microcomposite prepared under different conditions

Type of Graphite	Atmosphere	Properties studied	Temperature and materials ratio (Graphite /silica)														
			10/90			20/80			30/70			40/60			50/50		
			1600°C	1650°C	1700°C	1600°C	1650°C	1700°C	1600°C	1650°C	1700°C	1600°C	1650°C	1700°C	1600°C	1650°C	1700°C
94FC	CAF	Tap density	0.62	0.54	0.55	0.60	0.50	0.53	0.54	0.45	0.5	0.52	0.44	0.46	0.52	0.42	0.44
		Phases	C, S	C, S	C, S	C, S	C, S	C, S	C, S	C, S	C, S	C, S, Cy	C, S	C, S	C, S, Cy	C, S	C, S
		Morphology	GSI	GSI	GSI	GSI	GSI	GSI	GSI	GSI	GSI	GSI	GSR	GSR	GSR	GSR	GSR
		SiC retained after calcination (wt %)	6.45	6.57	8.11	17.0	18.27	16.28	28.60	25.95	27.0	41.63	41.27	40.12	55.22	60.07	59.64
	RHF	Tap density	0.57	0.62		0.496	0.59		0.416	0.540		0.4	0.513		0.370	0.5	
		Phases	C, S	C, S		C, S	C, S		C, S	C, S		C, S	C, S		C, S, Cy	C, S	
		Morphology	GSI	GSI		GSI	GSI		GSI	GSI		GSI	GSI		GSF	GSF	
		SiC retained after calcination (wt %)	7.96	6.67		19.23	18.56		32.43	39.55		48.34	48.41		67.39	63.45	
97FC	CAF	Tap density	0.652	0.638	0.682	0.625	0.625	0.652	0.612	0.577	0.6	0.577	0.555	0.578	0.566	0.517	0.545
		Phases	C, S	C, S	C, S	C, S	C, S	C, S	C, S	C, S	C, S	C, S, Cy	C, S	C, S	C, S, Cy	C, S	C, S
		Morphology	GSI	GSI	GSI	GSI	GSI	GSI	GSI	GSI	GSI	GSI	GSI	GSI	GSI	GSI& GSR	GSI& GSR
		SiC retained after calcination (wt %)	7.81	7.95	6.423	16.14	18.430	17.134	30.22	28.58	27.463	43.27	43.595	42.756	61.05	63.10	62.572

Phases: C - Graphite, S - Silicon carbide, Cy – Cristobalite

Morphology: GSR - Graphite-SiC_{rod}, GSF - Graphite-$SiC_{fiber,}$ GSI - Graphite-SiC_{ribbon}

Conclusion

Based on the experiments carried out so far, both in the laboratory at NIT, Rourkela and also by the industrial partner (TRL-Krosaki Refractories Ltd), following conclusions are drawn.

- Graphite/β-SiC microcomposite can be synthesized either in a raising hearth furnace in which a reducing atmosphere is maintained by packing the samples inside a pet-coke bed. (Or) In a controlled atmosphere furnace with graphite heating elements. (Or) In a tunnel kiln by maintaining reducing atmosphere by the use of pet coke as in the first case.
- A minimum heat-treatment temperature of 1600^{o}C is necessary for the completion of the reaction. Morphology of the SiC phase differs significantly depending on the temperature of heat-treatment, composition (silica/ graphite ratio) and also the type of furnace. With pet-coke packing, lower silica content and higher temperature give ribbon type morphology adhering strongly to the surface of the graphite flakes. Higher silica content and lower temperature favor the formation of free-standing SiC fibres/rods typically within the interlamellar spacing of flakes.
- Heat-treatment inside a graphite furnace with argon atmosphere give rise to the formation of "nail" type SiC rods (1-1.5µ in diameter) instead of fibres (100-200nm in diameter). Spherical "head" of these SiC nails consist of metallic iron together with SiC. On oxidation at 1000^{o}C, the metallic iron gets oxidized to Fe_2O_3 and the spherical shape gets destroyed. It appears that Fe_2O_3 present as an impurity in natural graphite has a role to play in the formation of this SiC rod type morphology. This distinctive feature is less prominent when pure (97%FC instead of 94%FC) variety of natural graphite is used for the synthesis of the composite.
- As expected, higher is the fibre content of the composite; lower is its tap density. Therefore, simple measurement of tap density provides an indication of the extent of SiC fibre formation.
- Heat-treatment of the micro-composite at 1000^{o}C/1hr in the air is sufficient to oxidize the graphite part entirely and is quite useful for quantitative determination of the SiC content of the composite. Interestingly, there is nearly 1:1 correspondence between the silica content of the original mixture and the SiC content of the composite irrespective of the heat-treatment temperature and the morphology of the SiC Phase.

SECTION II

Investigations carried out at Laboratory Scale- I

4.3. Properties of Graphite/SiC microcomposite containing MgO-C samples

The compressive strength, bulk density and oxidation behaviour of MgO with the micro-composite has been studied on a laboratory scale. The MgO-C batch compositions are presented in Table 3.7 of the experimental section.

4.3.1. Specific strength of MgO-C samples containing graphite and graphite-SiC micro-composite

The specific strength results of the MgO-C (with the addition of graphite & microcomposite) samples are presented in Figure 4.23. In order to get an idea of the room temperature mechanical properties, the compressive strength of all the samples mentioned in Table 3.7 is measured. Samples are prepared conditions as referred to in section 3.4.1. The densities of the samples were measured by Archimedes principle. The bulk densities, values are low and varied significantly between the different samples. All the compressive strength data have been normalized by dividing the strength data by respective density values and the resultant values and referred to as “specific strength”(Specific Strength = Strength/ Density). These results have been plotted against the percentage of graphite or the micro-composite added on magnesia.

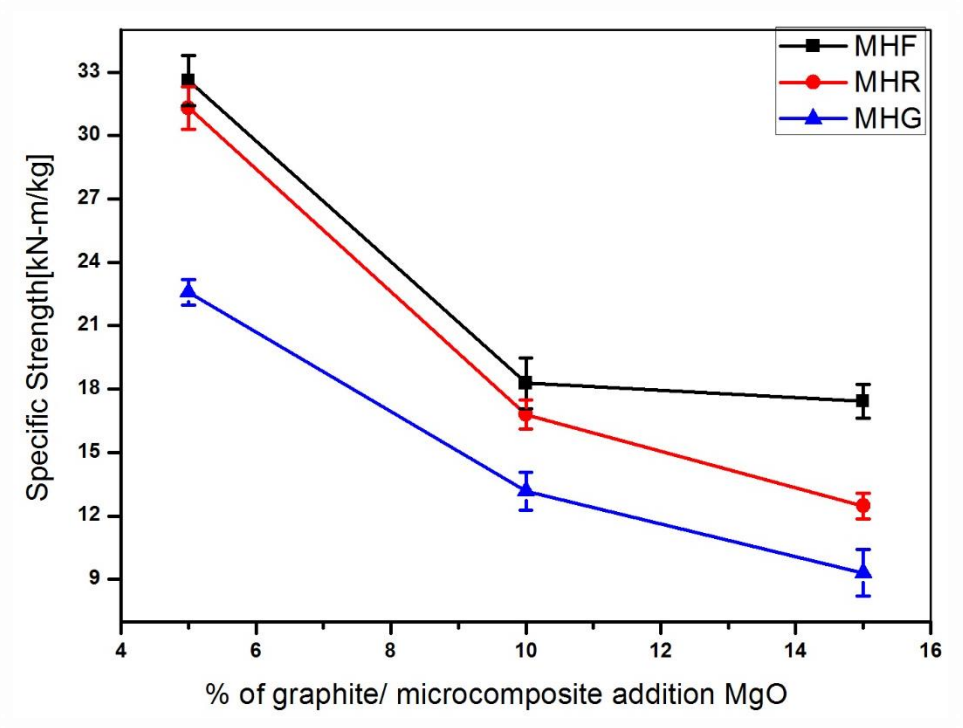

Figure 4.23: Specific Strength of the sintered samples of MgO-C and MgO-C/SiC composites (with both fibre and ribbon morphologies) with different (5, 10 and 15) wt% additives.

The following points can be inferred from figure 4.23

a) The specific strength decreases monotonically with increases in addition to either pure graphite or the graphite-SiC composite (both fibre and ribbon morphologies) on MgO.
b) The strength values are lowest in case of pure graphite addition and highest for the addition of the composite with fibre morphology. The samples with a ribbon morphology have the intermediate strength values.

Importantly we can conclude that the graphite-SiC composite with fibre morphology is more effective in enhancing the cold crushing strength of the MgO-C compositions due to the better-reinforcing effect of the SiC fibres.

4.3.2. Effect of the micro-composite on the mechanical properties of sintered MgO-microcomposite samples

The sample preparation is similar to the conditions mentioned in section 3.4.1. However, the micro-composites were prepared with different ratios of graphite and silica at varying temperatures. The conditions of synthesis were as follows:

a) Microfine silica to graphite was 40/60 and 50/50.
b) Temperatures of heat-treatment used were 1650^{o}C and 1700^{o}C in CAF

The magnesia samples were prepared with the addition of 5& 10wt% of the micro-composites and only graphite (for comparison) to magnesia samples, which is fired at 1600^{o}C/4hrs in presence of petroleum coke atmosphere in raising hearth furnace. The specific strength of these specimens, prepared under different conditions are presented in Figure 4.24.

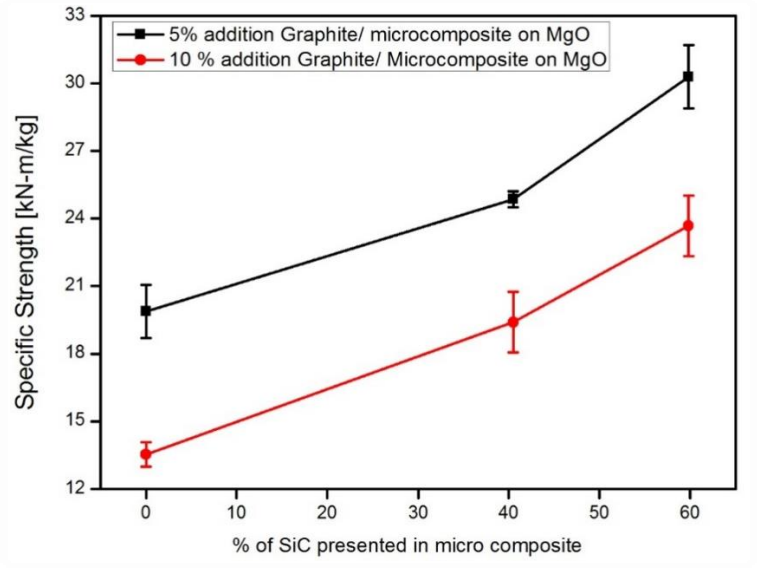

Figure 4.24: Specific Strength of the MgO-C and MgO-graphite/SiC micro-composite samples.

The samples with only graphite possess the lowest strength for both the compositions (5 and 10wt %). At the same time, the strength decreases as the graphite content increases (from 5 to 10 wt %). Similarly, strength decreases with increase in the amount of the micro-composite. However, the strength increases with increasing SiC content of the microcomposite (from 40 to 50 wt %) and also with increasing the heat-treatment temperature (from 1650 to 1700^{0}C). Both these parameters are expected to increase the SiC content of the micro-composite and therefore, it may be concluded that SiC content has a direct influence on the CCS of the MgO-C refractory.

4.3.3. Weight change during heat-treatment

The pellets of selected compositions from Table 3.7 was prepared, and their weight change measurement was carried out after firing at 1600^{o}C/4hrs. The weight change behavior is plotted and presented in Figure 4.25 along with the values tabulated in Table 4.3.

Table 4.3: Weight change of the samples after heat-treatment at specified temperatures.

Temperature(^{o}C)	% Initial weight (at room temperature)		
	MHG	MHF	MHR
280	97.38	97.64	99.90
1500	94.62	103.67	102.0
1550	--	100.42	95.24
1600	--	95.13	90.60

In figure 4.25, the weight change behavior of three different categories of MgO-C samples is plotted. The three different categories are: i) samples with only graphite flakes (without the micro-composite); ii) samples with the micro-composite having ribbon type morphology; iii) samples with the micro-composite having fiber morphology. It may be further noted that the specimens with only graphite flakes (first category) lose their weight continuously till a sintering temperature of 1500^{o}C which corresponds to the normal behavior of MgO-C refractories. On the other hand both second and third categories of samples, which contain the micro-composite of either of the morphologies, lose their weight till 280^{0}C (the tempering temperature). Secon & third category of samples gained weight (2% & 4% respectively) till 1500^{o}C and finally lost weight till 1600^{o}C, it is similar to the first category of the samples.

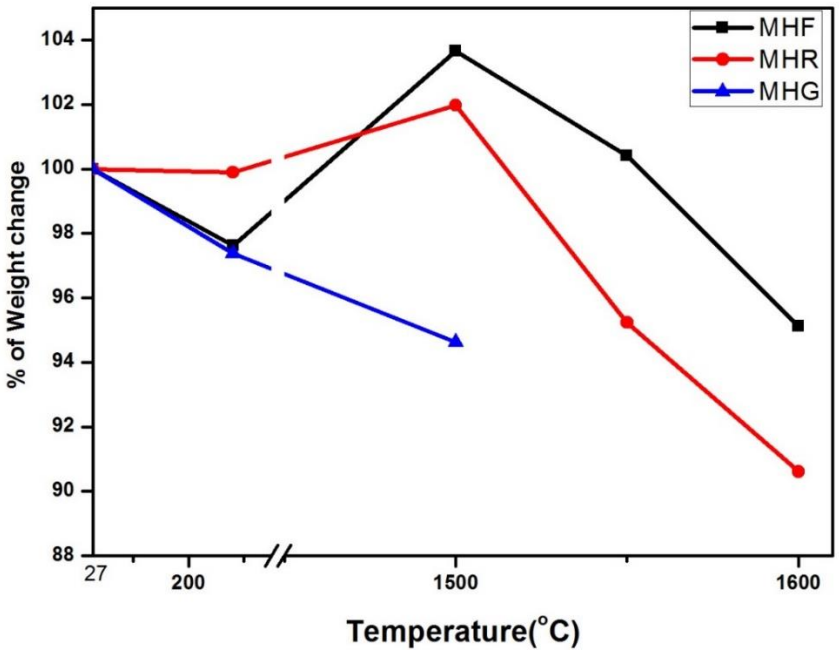

Figure 4.25: Weight change behaviour of MgO-C and MgO-graphite/SiC micro-composite samples.

For samples containing only graphite (MHG), the weight loss is initially due to the removal of the volatile matters from the resin during the tempering operation. After that, partial oxidation of the graphite flakes in the presence of a reducing atmosphere is observed. For samples containing the fibrous composite (MHF), the weight-loss is nearly identical with the first category of samples till 280°C followed by significant weight gain till 1500°C. Plausible reason for this weight gain is the partial oxidation of SiC to form SiO_2 according to the following reaction [6]

$$SiC + 2O_2 = SiO_2 + CO_2\uparrow \text{ ---------- (4.4)}$$

The theoretical weight gain according to this reaction is around 50%. However, actual weight changes are much less because the quantity of the added SiC is very less, and the whole of it might not have been oxidized. Another point to be noted is that the weight change (both loss and gain) for the samples containing the fibre composite (MHF) is relatively greater than that of the samples containing the composite with ribbon type morphology (MHR). The weight change indicates that the reaction kinetics for the fibre composite is relatively high due to the porous structure and higher surface area of composite compared to that of the ribbon type morphology in the composite. It may be noted that the overall change in weight for the samples with ribbon morphology (MHR), is much less in comparison to those containing only graphite flakes (MHG).

From the above observation, it may be concluded that, volatilization of the added resin and oxidation of both graphite and silicon carbide, the ribbon type composite has an edge over both the fibre type composite and pure graphite.

4.3.4. Phase Analysis of the Sintered MgO-C Samples

Phase analysis of the sintered samples with 10wt% of MHR, MHG and MHF added to MgO has been analysed by X-ray diffraction. The composite XRD patterns of the samples are presented in Figure 4.26.

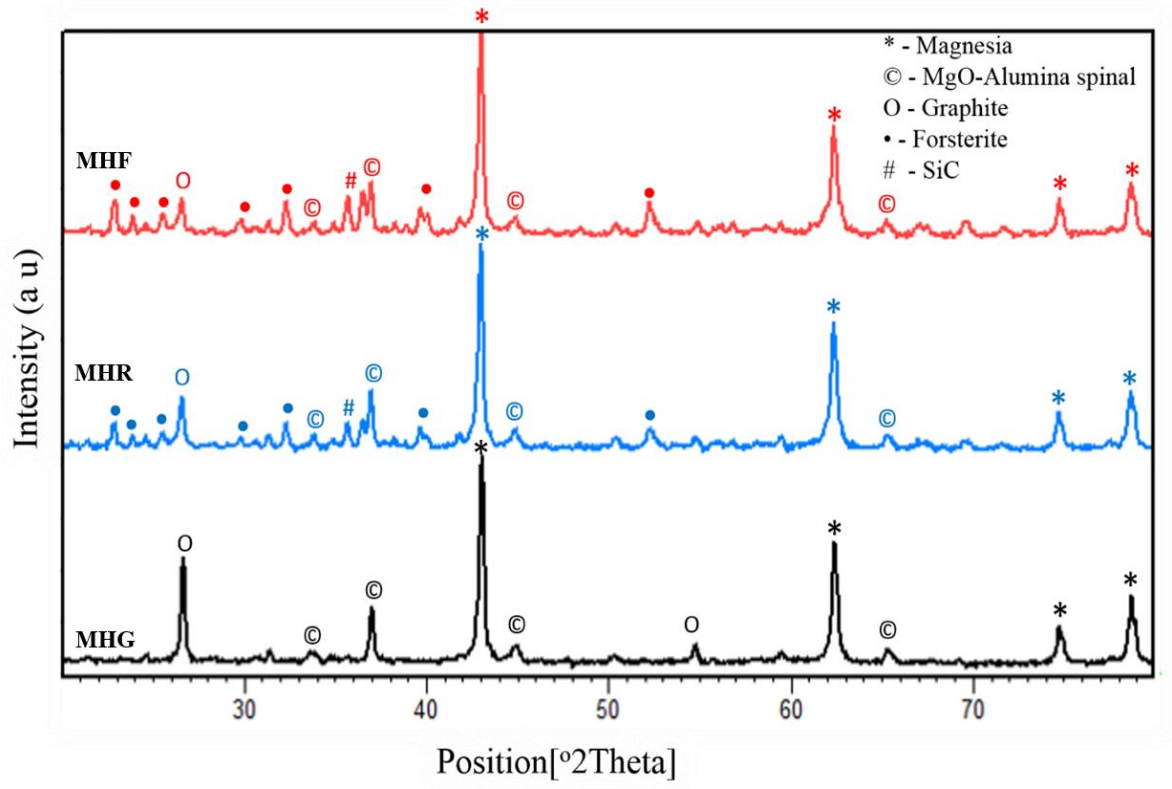

Figure 4.26: XRD patterns of sintered MHG, MHR and MHF samples (with a 10wt. % addition in each case).

The major phases in all the specimens are MgO and graphite. In addition, all the samples contain a small amount of MgO-Al_2O_3 spinel. The origin of spinel is possibly; some amount of alumina might have reacted up from the alumina crucible used during the sintering process. On the other hand, the samples containing MHR and MHF indicated the presence of additional minor peaks corresponding to β-SiC and forsterite ($2MgO.SiO_2$). Thus, it can be concluded that the SiC phase in the micro-composite gets decomposed to form SiO_2 during the sintering process and reacts with MgO to form the forsterite phase. This has become one of the major problems of having SiC phase in MgO-C refractories.

Therefore, it is essential to quantify the optimum SiC phase in the micro-composite so as to take advantage of the presence of this phase in terms of cold crushing strength, oxidation resistance as well as thermal conductivity. The same has been done during the next phase of the investigation.

Conclusion

a) With the addition of microcomposite, a few properties of the MgO-C samples is improved, but a higher amount of microcomposite addition degrades properties like corrosion and oxidation. The presence of more SiC is caused by formation of forsterite at higher temperature (According to CaO-MgO-SiO_2 phase diagram the C/S ratio should not exceed 3 vol%).

b) The SiC content of the micro-composite has to be restricted up to a certain level to limit the formation of forsterite at high temperature and thereby deteriorating the slag corrosion property of the brick.

Pilot Plant Investigations - II

4.4. Properties of Commercial Grade MgO-C Bricks for Steel Ladle

The prime objective of this section is to understand and evaluate the properties of MgO-C prepared from synthetic graphite/SiC composites. A comparison is made between the existing properties of microcomposite containing MgO-C bricks and commercially used (pure graphite) standard bricks. The different properties of the commercial MgO-C brick are presented in Table 4.4. For the present condition, three types of MgO-C bricks are selected namely: i) Ladle Metal Zone Brick, ii) Ladle Slag Zone Brick and iii) Ladle Bottom Zone Bricks. Initially, different grade of bricks were collected from the shop floor and tested at TKRL lab, by ASTM method.

Table 4.4: Properties required for MgO-C brick used at different application zones in steel ladle

Application Zone	Tempered Bricks (Before Coking			Coked Bricks (After Coking)			HMOR (kg/cm^2)	Oxidation (% area)
	AP (%)	BD (gm/cc)	CCS (kg/cm^2)	AP (%)	BD (gm/cc)	CCS (kg/cm^2)		
Ladle metal zone brick	1.91	3.05	420	8.9	2.98	177	29	61.40
Ladle slag zone brick	2.65	2.98	341	8.4	2.91	192	40	52.51
Ladle bottom zone brick	2.25	3.04	436	10.1	2.95	180	37	55.81

From the Table 4.4, it is evident that the properties of the bricks are slightly different in comparison with various zones of steel ladle. In general, the slag zone bricks possess relatively better properties particularly bulk density, CCS (after coking), HMOR and oxidation resistance than bricks of the bottom zone and metal zone. The HMOR, oxidation and CCS after coking varied in the range 30-40 kg/cm^2, 50-60% and 175 – 195 kg/cm^2, respectively.

The above-mentioned bricks properties are compared with the bricks prepared by using of present graphite/SiC microcompositions, which are synthesized either in the controlled atmospheric furnace (CAF- laboratory) or tunnel kiln (TK-industrial) conditions. The compositions are partly replaced with 1wt% & 3wt% in place of graphite without changing MgO proportion. The particular compositions of the bricks are presented in Table 4.6.

These bricks are labelled according to the variation of composition, firing condition (10/90, 20/80, 30/70, 40/60 and 50/50 & CAF, TK. A few microcompositions are prepared by using two different grades of graphite (94FC and 97FC); these compositions are labelled as MC31A, MC33A and MC31B, MC33B. The different MgO-C brick compositions and their batch codes are shown in Table 4.5.

Table 4.5: Sample codes used in this investigation for MgO-C bricks.

Controlled Atmospheric Furnace(CAF) NIT		**Tunnel Kiln(TK) TKRL**	
MC00	No composite used	MC41TK	40/60(94FC)- 1wt.% addition
MC11	10/90(94FC)- 1wt.% addition	MC43TK	40/60(94FC)- 3wt.% addition
MC13	10/90(94FC)- 3wt.% addition	MC51TK	50/50(94FC)- 1wt.% addition
MC21	20/80(94FC)- 1wt.% addition	MC53TK	50/50(94FC)- 3wt.% addition
MC23	20/80(94FC)- 3wt.% addition		
MC31A	30/70(94FC)- 1wt.% addition		
MC33A	30/70(94FC)- 3wt.% addition		
MC31B	30/70(97FC)- 1wt.% addition		
MC33B	30/70(97FC)- 3wt.% addition		
MC51	50/50(94FC)- 1wt.% addition		
MC53	50/50(94FC)- 3wt.% addition		

The standard bricks with the mentioned compositions in Table 4.6 are prepared under industrial conditions to understand the effects of partial substitution of natural flake graphite by varying amounts of Graphite-SiC microcomposite prepared under different conditions (CAF & TK). The “MC00” represents that the standard conventional brick (without any addition of the micro-composite). The rest of bricks were prepared by using microcompositions with different amounts replacing by a part of graphite (94FC).

The mentioned raw material composition after mixing, pressed under a friction screw press were subjected to standard heat treatment conditions (tempering).

Table 4.6: Composition of MgO-C bricks with the addition of different amounts of microcomposite

Raw material		CAF, NIT (1650ºC/4hrs)										TK, TKRL (1680ºC/2hrs)			
	MC00 No composite	MC11 10/90	MC13 10/90	MC21 20/80	MC23 20/80	MC31A 30/70	MC33A 30/70	MC31B 30/70	MC33B 30/70	MC51 50/50	MC53 50/50	MC41 40/60	MC43 40/60	MC51 50/50	MC53 50/50
		94FC						97FC		94FC					
FMLC97 (4-6)	10	10	10	10	10	10	10	10	10	10	10	10	10	10	10
(2-4)	40	40	40	40	40	40	40	40	40	40	40	40	40	40	40
(0-1)	27	27	27	27	27	27	27	27	27	27	27	27	27	27	27
Dust(200µ)	12	12	12	12	12	12	12	12	12	12	12	12	12	12	12
Al metal powder	1	1	1	1	1	1	1	1	1	1	1	1	1	1	1
Graphite 94FC	10	9	7	9	7	9	7	9	7	9	7	9	7	9	7
Microcomposte * (C+SiC)	0	1	3	1	3	1	3	1	3	1	3	1	3	1	3
Liq. Resin	2.75	2.75	2.75	2.75	2.75	2.75	2.75	2.75	2.75	2.75	2.75	2.75	2.75	2.75	2.75
Carborose	0.5	0.5	0.5	0.5	0.5	0.5	0.5	0.5	0.5	0.5	0.5	0.5	0.5	0.5	0.5

Different sizes of specimens prepared from the tempered bricks; 150×25×25(mm) for HMOR, 50Ø × 50 (mm) height are used for CCS, BD, AP, Oxidation test. The schematic representation of the following test specimens is shown in Figure 4.27.

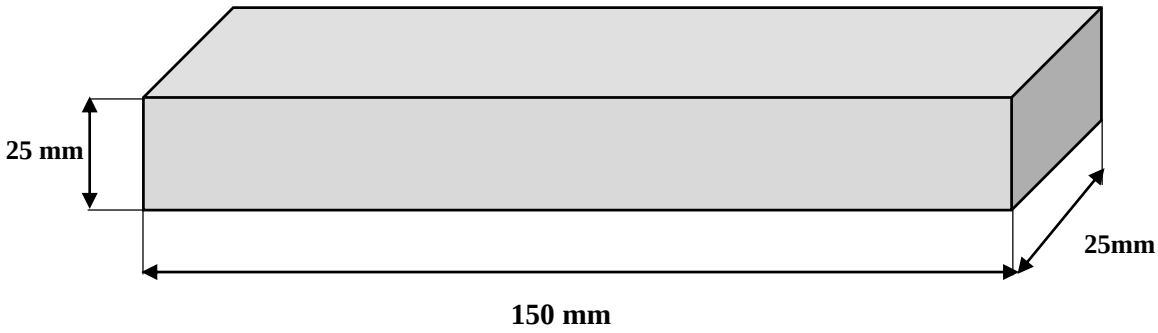

Specimen (150× 25×25) mm cut from the standard brick used for HMOR test

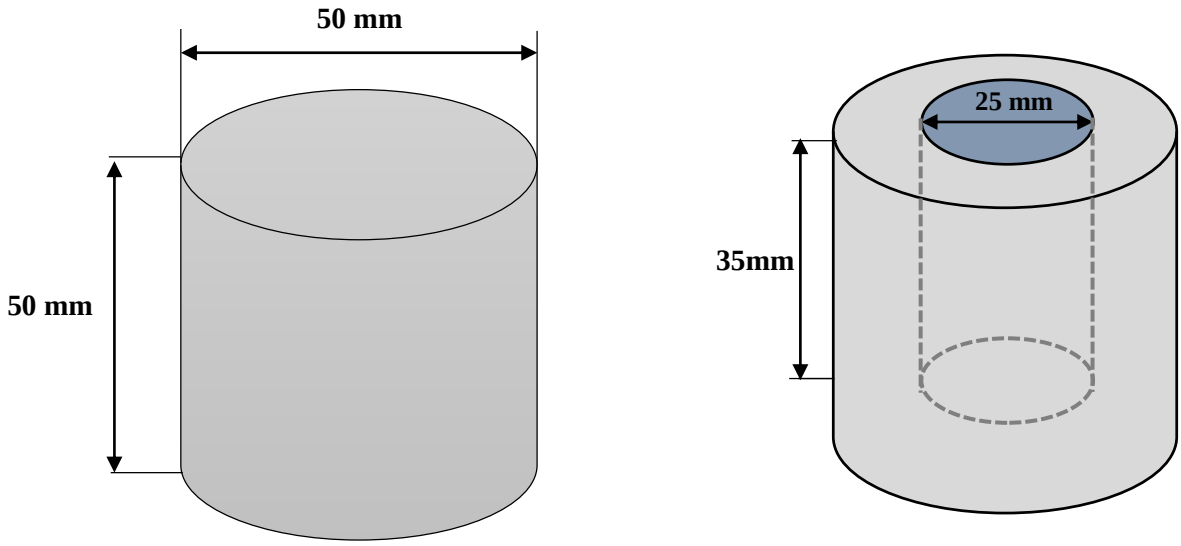

Specimen used for AP, BD, CCS, Oxidation test

Specimen used for Slag corrosion test

Figure 4.27: Specimens used in this investigation for different characterization

4.5. Pilot plant comparative study: Pure graphite versus partial replacement of graphite by graphite/SiC microcomposites in MgO-C bricks

Different compositions including 10wt% pure graphite and their partial replacement by synthesized graphite/SiC microcomposites have been used to fabricate MgO-C bricks under industrial conditions. The physical, mechanical, thermomechanical, oxidation and slag corrosion test of different compositions were studied systematically. The nomenclature of different set of bricks are defined as MC00 only 10wt% graphite (without composites); CAF 01 & CAF 03 - 1 and 3wt% addition of microcomposites (10/90, 20/80 and 30/70) with different weight percentage of β-SiC. Another set of bricks namely MC 40/50 bricks are prepared with the addition of 1 and 3wt% microcomposites; made from 40/60 and 50/50 (silica/graphite) either in TK or CAF.

4.5.1. Physical Properties of MgO-C brick with addition of microcomposite

(a) Bulk density before coking

The calculated bulk density (BD) of the magnesia carbon brick is shown in Figure 4.28(a). The calculated bulk density of conventional MgO-C brick (without microcomposite) is 3.01gm/cc. With the addition of microcomposites, the BD of CAF 01 and CAF 03 set of bricks gradually increased. However, the addition of ribbons containing composite (CAF 01, CAF03 set of bricks) in MgO-C brick provides additional compatibility and, flowability resulting in better packing density and it gives better bulk density.

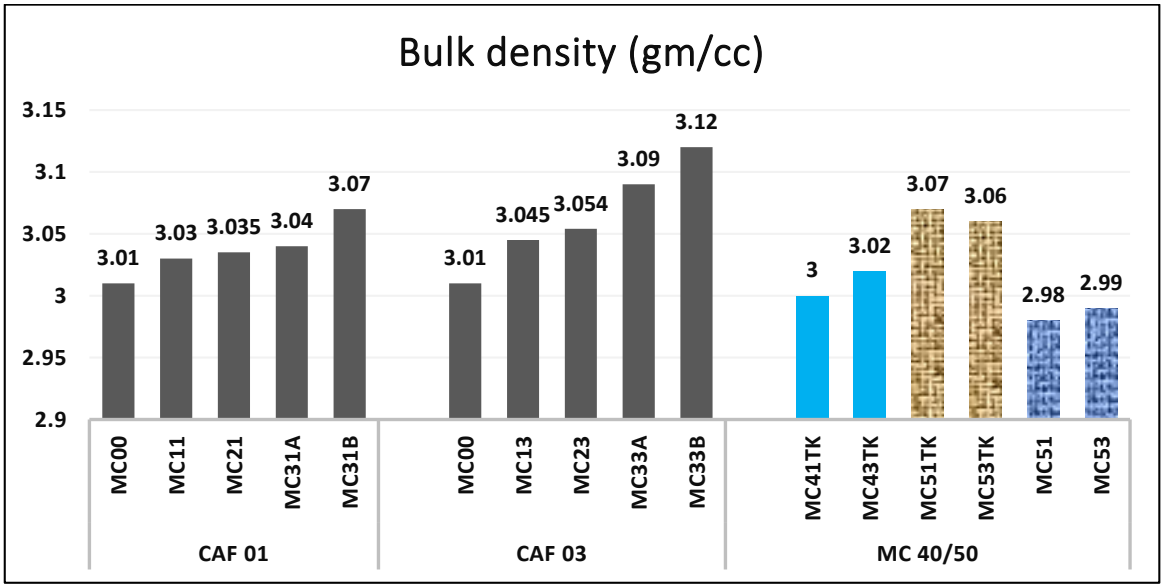

Figure 4.28(a): Bulk density of the different grades of MgO-C bricks, before coking.

From figure 4.28(a), it is observed that the 30/70 microcomposite attains maximum density in both 1 and 3wt% addition. Moreover, the BD of MgO-C brick increased with the purity of graphite used for the preparation of microcomposite. The MC 40/50 set of samples is followed the uncertain trend, which may be due to the incompressibility of a higher amount of fiber/ rods containing microcomposite causing reduction in density of MgO-C brick. However, further study is required in the perspective of the industrial application.

(b) Bulk density after coking

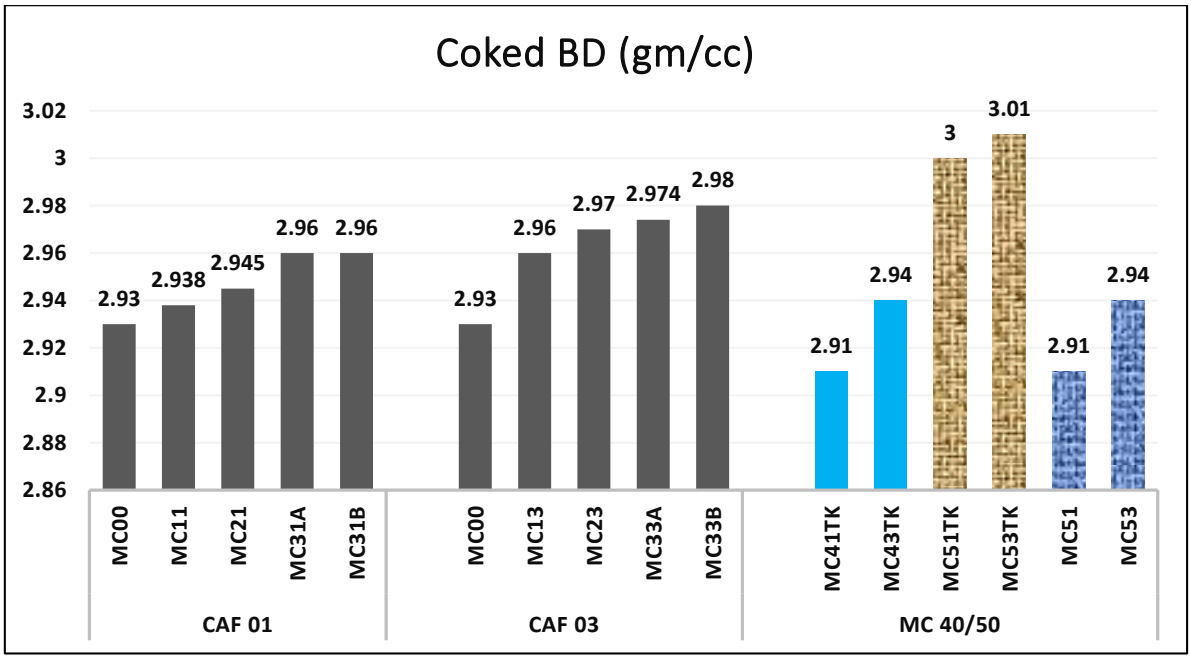

Figure 4.28(b): Bulk density of the different grades of MgO-C bricks after coking at 1000°C/5hrs.

The bulk density (BD) of the coked MgO-C bricks at 1000°C/5hrs is shown in Figure 4.28(b). The BD of coked MgO-C bricks slightly declined due to the burning out of organic matter and volatile matter by the presence of resin in the brick; at a high temperature. In figure 4.28(b), CAF 01 and CAF 03 set of bricks followed systematic variation, irrespective of different amount addition of microcomposites. Additionally, MC 40/50 set of MgO-C bricks followed an uncertain trend after coking.

(c) Apparent porosity before coking

The apparent porosity (AP) of the magnesia carbon bricks is shown in Figure 4.29(a). Herein, the apparent porosity is measured as minimum as 2.5% for conventional MgO-C brick (without microcomposite). The addition of microcomposite on MgO-C brick composition provides better

pore filling due to the finer particles attained lesser porosity, but the an additional amount of microcomposite tends to decrease in porosity. The apparent porosity of the bricks (CAF 01 and CAF 03) decreases with the increasing amount of microcomposite. Minimum apparent porosity is obtained by the incorporation of 3 wt%, 30/70 microcomposite. The High degree of apparent porosity is observed in the MC 40/50 set of bricks due to fluffy nature caused by the presence of enriched SiC fibre/rod in the microcomposite.

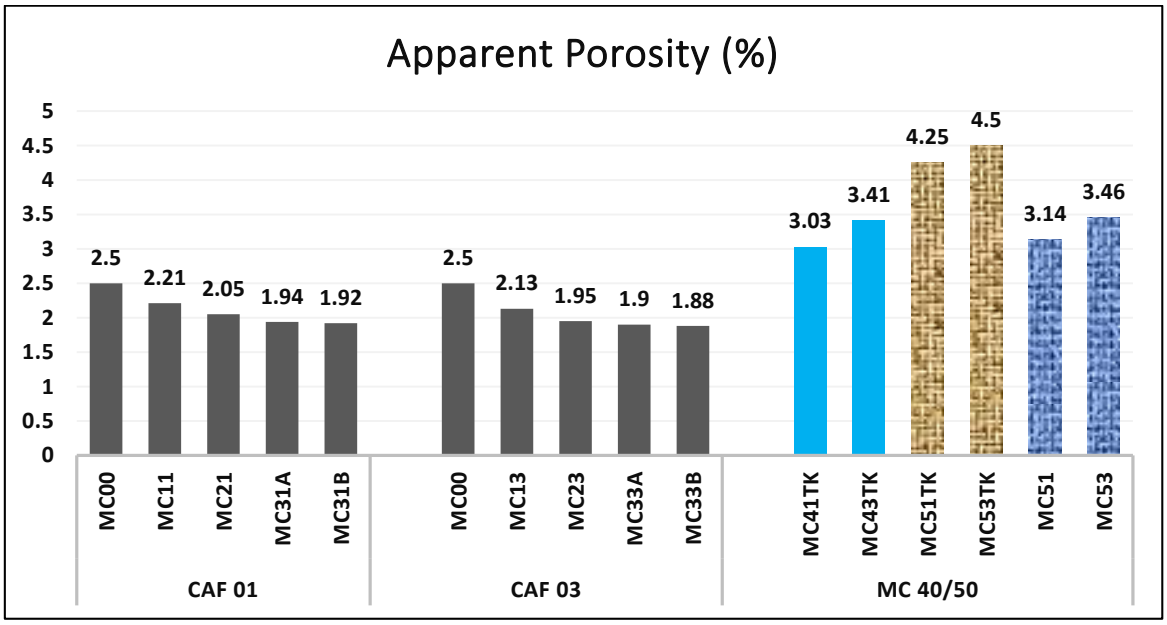

Figure 4.29(a): Apparent porosity of the different grades of MgO-C bricks, before coking.

(d) Apparent porosity after coking

The apparent porosity of coked MgO-C bricks are shown in Figure 4.29(b). During coking, the resin present in the brick burn out at high temperature, it leads to the formation of micropores resulting increases in apparent porosity. MC00 brick has attained the maximum apparent porosity (~9.5%). The apparent porosity of the MgO-C brick decreases with increase in the addition of microcomposite due to the filling of spaces between coarse refractory particles. A similar trend of apparent porosity can be observed in a CAF01 and CAF03 set of bricks. The least apparent porosity is observed in the bricks made of 30/70 (SiO_2/graphite) micro composite (1 wt% and 3 wt%). The MC 40/50 set of (40/60 & 50/50 microcompositions TK and CAF prepared) bricks have more porosity due to the presence of more amount of SiC fibers/rods in the microcomposite makes it fluffy than other bricks.

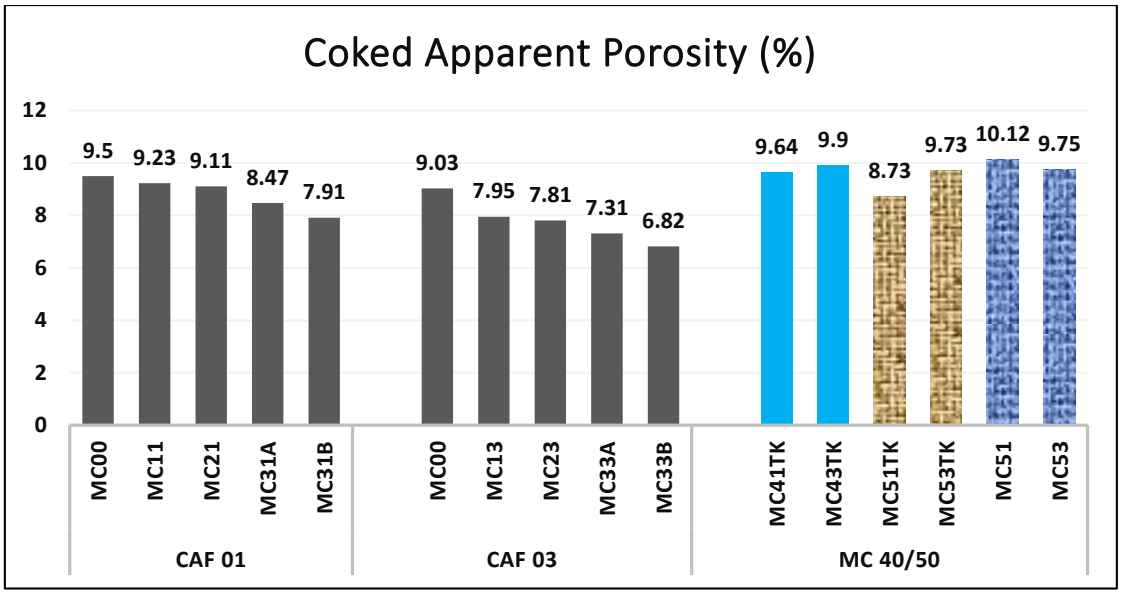

Figure 4.29(b): Apparent porosity of the different grades of MgO-C bricks, after coking at 1000°C/5hrs.

4.5.2. Cold Crushing Strength (CCS)

(a) CCS before coking

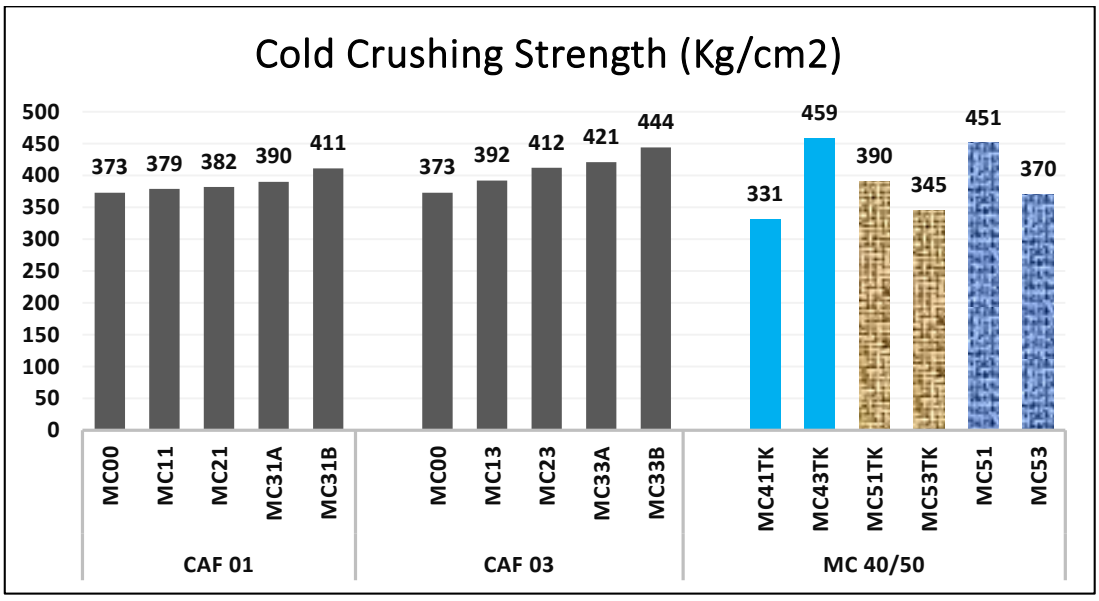

Figure 4.30(a): Cold crushing strength of the different grades of MgO-C bricks, before coking.

The cold crushing strength (CCS) of the MgO-C bricks is shown in Figure 4.30(a). The CCS of the standard conventional MC00 brick attains a lower value (~373 Kg/cm^2) due to the poor mechanical property of graphite. The CCS value of both CAF 01 and CAF 03 set of bricks is

gradually increased with the addition of microcomposite. This is because of the presence of β-SiC in microcomposite, which gives better packing of particles improving the mechanical strength. The bricks prepared with the addition of 1 and 3 wt% of 30/70 microcomposite attains higher CCS value of 411 and 444kg/cm^2 respectively. The addition of 3wt% of 30/70 microcomposite enhances the CCS value by 20%. However, the CCS value increased with the purity of graphite used (97FC than 94FC) for the preparation of microcomposite. Moreover, the MC 40/50 bricks attained better CCS value but it followed an uncertain trend with the variation of microcomposites. The CCS value followed the consistent trend up to 3wt% addition of micro composite, further addition degrades the mechanical properties.

(b) CCS after coking

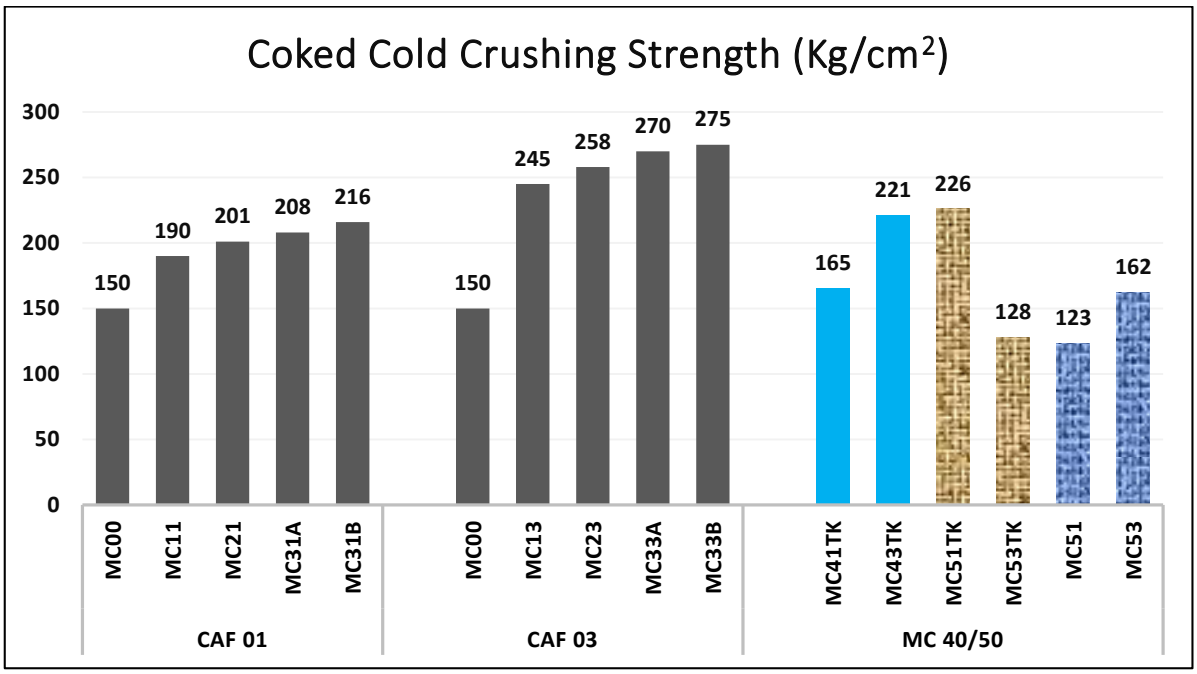

Figure 4.30(b): Cold crushing strength of the different grades of MgO-C bricks, after coking at 1000^{o}C/5hrs.

The cold crushing strength (CCS) after coking at 1000^{o}C/5hrs of MgO-C bricks is shown in Figure 4.30(b). There is a decrease in value of CCS due to the breaking of interlocking texture that is created by the polymerization of the phenolic resin at a higher temperature. The coked commercial MgO-C brick (MC00) attains a maximum CCS value of 150kg/cm^2. However, the microcomposite containing bricks (CAF 01 and CAF 03) gave better-coked strength due to the presence of SiC. The addition of (20/80 & 30/70) microcomposites enhances the coked CCS value by 70-80% in

the case of CAF 03 set of bricks. CCS values decreased with an uncertain trend after coking in case of MC 40/50 set of bricks due to the presence of an excess of SiC fiber/rods containing microcomposite.

4.5.3. Hot Modulus of Rupture (HMOR)

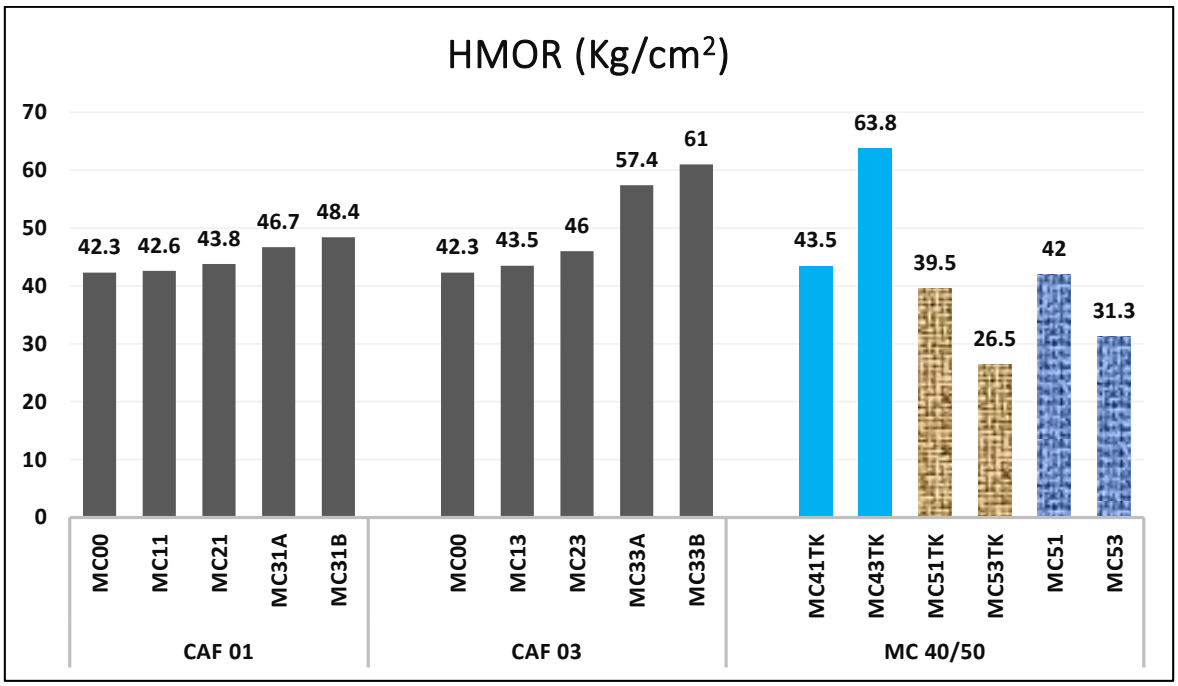

Figure 4.31: Hot modulus of rupture (HMOR**)** of different grades of MgO-C bricks, conducted at 1400^{o}C/30 min.

Variation in the hot modulus of rupture (HMOR) of the MgO-C bricks is shown in Figure 4.31. The HMOR test is performed at 1400^{o}C/30min in an oxidising atmosphere by varying load. The conventional MC00 (without composite addition) brick attained a minimum value of 42.3 Kg/cm^2 due to oxidation of carbon at higher temperatures. However, the HMOR value is gradually increased in both CAF 01 and CAF 03 set of bricks by the addition of microcomposite. The bricks are containing 30/70 microcomposite attained better HMOR value with the addition of 1 and 3wt%. The HMOR value is enhanced by 35 - 40% on the addition of 3 wt% of 30/70 microcomposite. The HMOR value is increased with the purity of graphite used for the preparation of microcomposite. The presence of β-SiC in the microcomposite give better thermo-mechanical strength due to filling with spaces between bigger particles. However, the HMOR results of MC 40/50 set of bricks decreases with an uncertain trend with the addition of microcomposite, because of fluffy nature in the bricks. The presence of silica beyond 40 % in the microcomposite is

responsible for the degradation of thermo-mechanical properties. The optimum value of microcomposite addition can be considered as 3 wt% because further addition decreases the HMOR value.

4.5.4. Oxidation Resistance Test

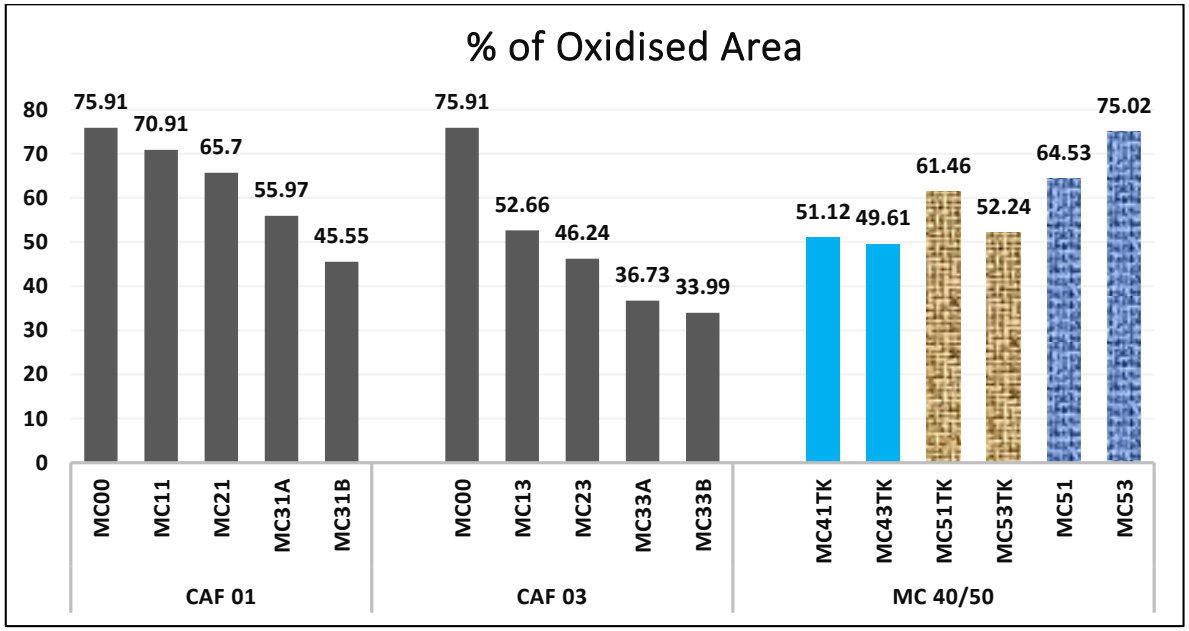

Figure 4.32: Oxidation resistance of different grades of MgO-C bricks, after oxidation at 1400°C/5hrs.

Figure 4.32 depicts the oxidation resistance of various MgO-C bricks. These bricks are prepared with the addition of varying amounts of microcomposite in place of graphite. The oxidation of the brick is measured after oxidising at 1400°C/5hrs. From figure 4.32, the oxidation of standard brick (MC00) takes place up to 75.91% area due to the oxidization of graphite at higher temperatures. Improved oxidation resistance is observed in the case of CAF 01 and CAF 03 set of bricks with the addition of microcomposite. Better oxidation resistance is attained by the addition of 30/70 microcomposite with 3wt%. The presence of ß-SiC in the microcomposite reduces the oxidation of graphite by decreasing the penetration of oxygen through filling of pores. Thus, the addition of 3wt% of 30/70 microcomposite is considered as the optimum amount for improving oxidation resistance. The oxidation resistance is decreased in the case of MC 40/50 MgO-C bricks owing to the incompressibility of the fiber/rods containing microcomposite causing more porosity.

The cross-sectional view of different magnesia carbon bricks, after oxidized to 1400^{o}C/5hrs, are shown in Figure 4.33. Its colour clearly separates the oxidized layer (yellow) and unoxidized region (black). The standard conventional MC00 (without the addition of microcomposite) brick oxidized more due to the presence of excess carbon. Carbon oxidizes at high temperature in the oxidizing atmosphere, and the extent of oxidation increases with increasing the carbon content. However, the oxidation resistance increases in case of CAF 01, CAF 03 set of bricks with the addition of microcomposite. Moreover, MC33A and MC33B shows better oxidation resistance with the addition of 3 wt% of (30/70-SiO_2/graphite) microcomposite. The oxidation resistance of MgO-C bricks (MC 40/50) decreased, beyond the 40/60 (SiO_2/graphite) microcomposite composition.

Oxidized MgO-C sample

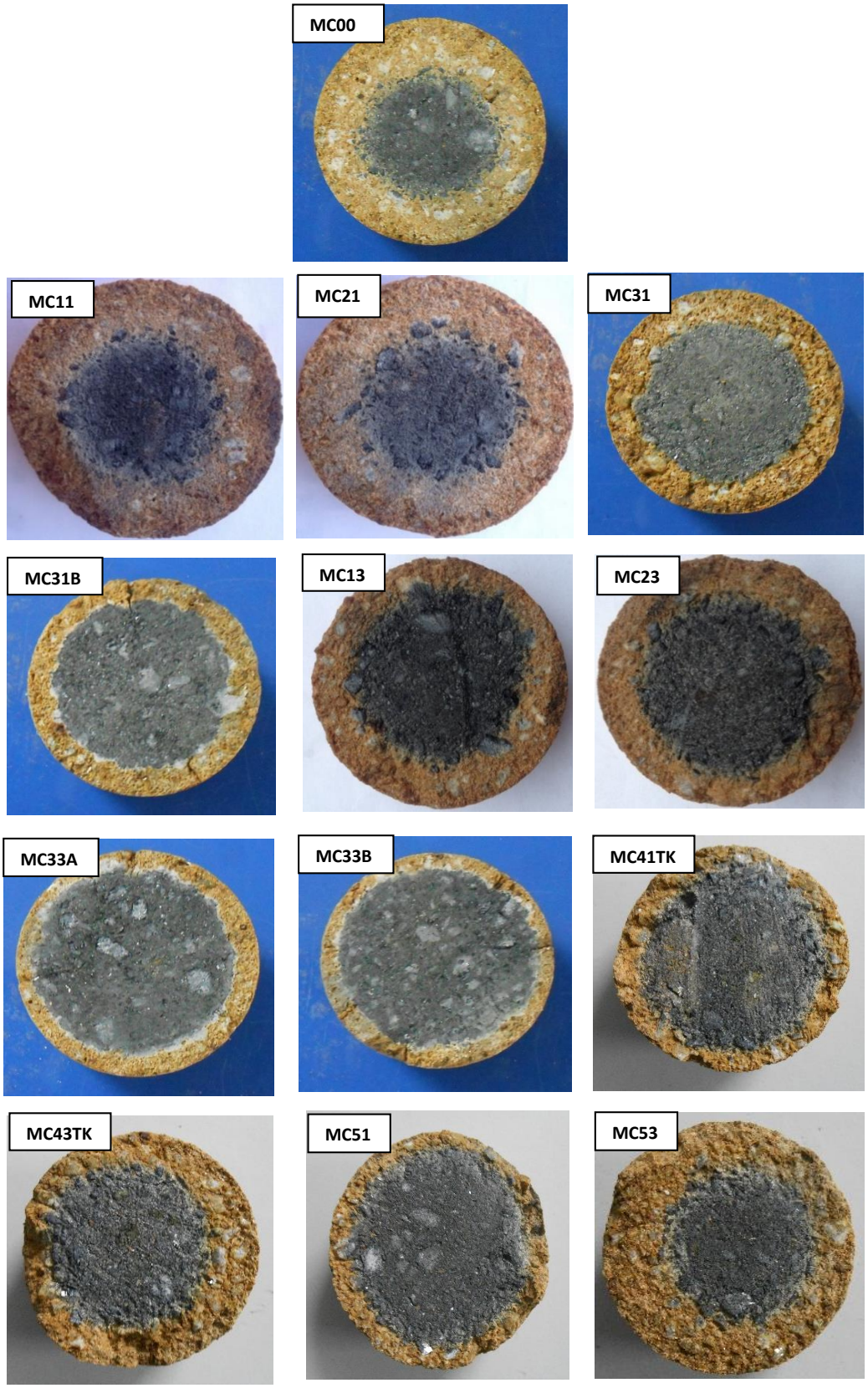

Figure 4.33: Photographs of the cut cross sections of the oxidized samples

4.5.5. Slag corrosion test:

In commercial steel making furnaces, slag attacks on refractories phenomenon involve not only chemical wear (corrosion), but also physical/ mechanical wear (erosion/ abrasion) that act in an interactive manner. The refractories are chemically attacked by liquid slag emphasizing both penetration and reaction of slag by dissolution. The penetration rate of slag can be measured by poiseulle's law which, even though ignoring much of the influence on the microstructure of the refractories, does include the effect of slag viscosity indirectly includes the temperature. The slag penetration can be suppressed by increasing slag viscosity (contact angle) by decreasing the surface tension. The slag corrosion resistance of MgO-C refractory reduces with the rise of temperature and the content of FeO/MnO in melting slag, and also reduces with the decrease of alkalinity [7, 8]. Improving the working life of MgO-C refractory has become the focus of researchers in recent years. Much effort has been made to improve the performance of MgO-C refractories.

The slag resistance test was carried out by static crucible method shown in Figure 4.34. In the beginning, we collected the "TATA Steels LD2 converter" slag analysed and prepared the synthetic slag according to their composition for maintaining the consistent slag chemistry (Table 3.8). The slag test is performed at 1600^{o}C/5hrs in an oxidising atmosphere. The cross-sectional view of slag corroded MgO-C bricks (with and without microcomposite addition) is shown in figure 4.34. Incorporation of different amounts of microcomposite is used to study the slag corrosion mechanism. The effect of microcomposite in the brick is more prominent because it contains fine ß-SiC particles which seal the pores. Hence, the slag corrosion resistance is improved by preventing its infiltration. Better corrosion resistance is observed in the bricks (MC13, MC23, MC33A, and MC33B) containing 3 wt % microcomposite.

Slag corrosion tested samples

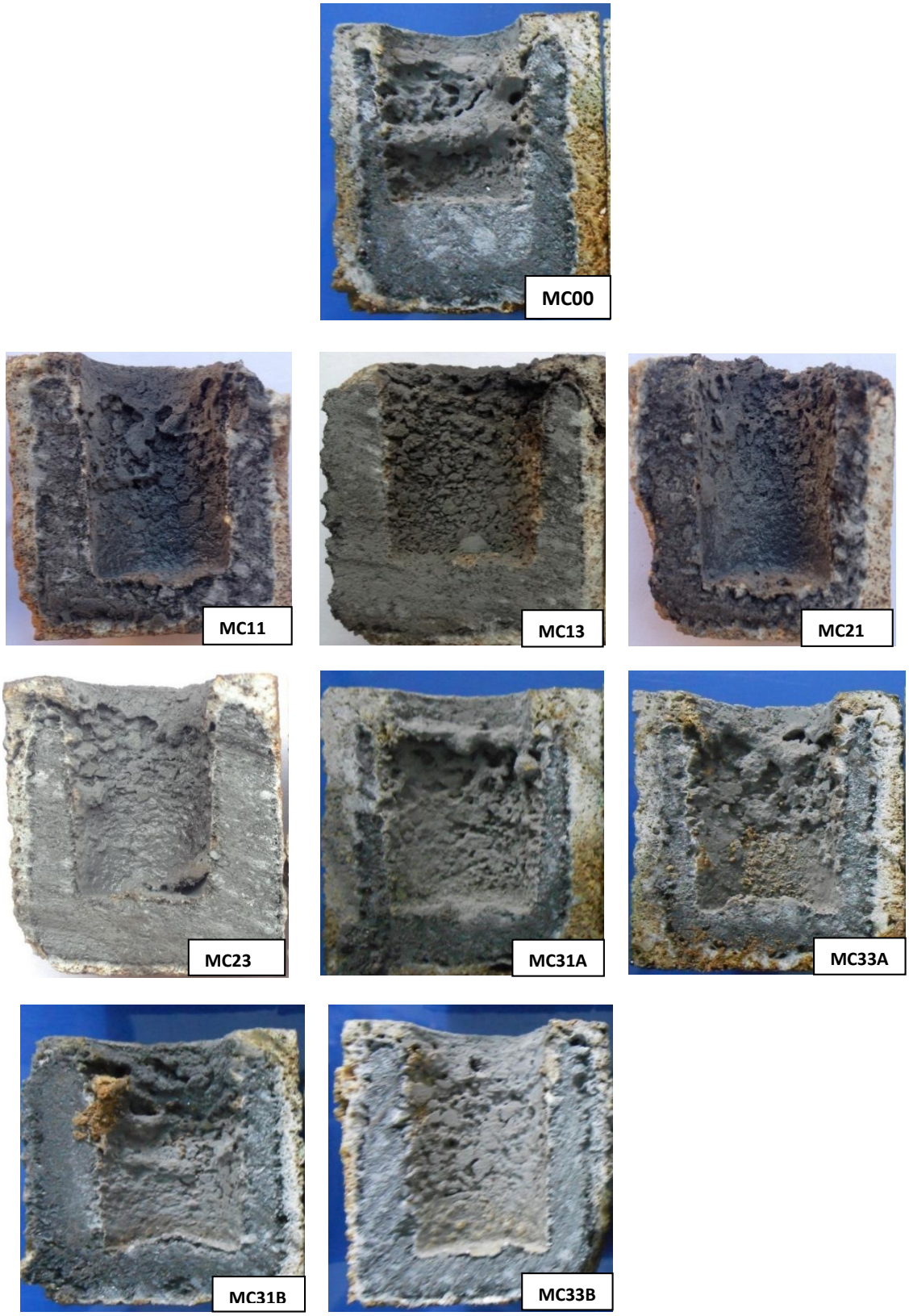

Figure 4.34: Photographs of the cross sectional view of samples after static slag test

Figure 4.35 shows the schematic representation of probable slag corrosion mechanism during brick slag interaction. The carbon present in the MgO-C brick plays a vital role in improving slag corrosion resistance. Benefits of carbon include its non-wettability by slag and its high thermal conductivity that facilitates the use of cooling systems and improves thermal shock resistance [9]. Here, the carbon is used in two forms; a) Flake graphite as an aggregate form b) Resin binders (pitch or resin) used as binder for matrix formation & for reducing porosity, which prevent slag penetration. The poor oxidation resistance of carbon causes micropores in the brick structure when it interacts with the atmospheric oxygen during BOF operation. Dissolution of the brick occurs due to the penetration of liquid slag/metal through the micropores as shown in Figure 4.35(b) &(c)

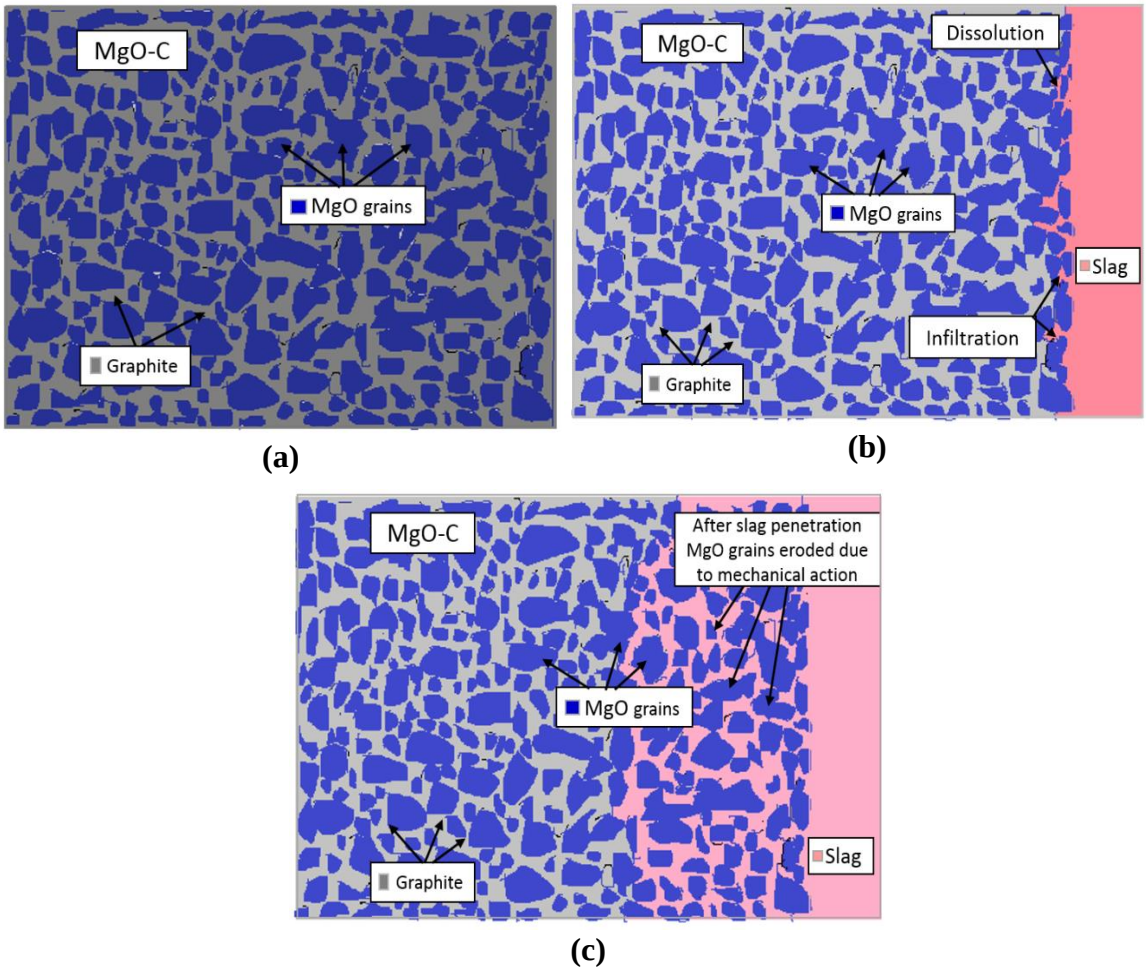

Figure 4.35: Slag corrosion mechanism of graphite containing MgO-C brick.

The Figure 4.36 shows that, the slag corrosion mechanism of Graphite/SiC microcomposite containing MgO-C brick. Antioxidants are used to improve the oxidation resistance of MgO-C bricks. The presence of more carbon is not desirable in a refractory due to its poor oxidation resistance. In the current exertion, a proportion of graphite is replaced with graphite/SiC microcomposite to enhance the life of the brick by improving its oxidation and corrosion resistance. The microcomposite acts as CO reducing agent contributing to carbon oxidation inhibition and developing hot strength by forming high temperature ceramic bonds. The non-oxide ceramic additives, on other hand, block the open pores to reduce the oxidation of the carbon. As a result of this, corrosion resistance and hot strength of the brick is improved [10, 11]. This detailed description is schematically shown in Figure 4.36(b) & (c).

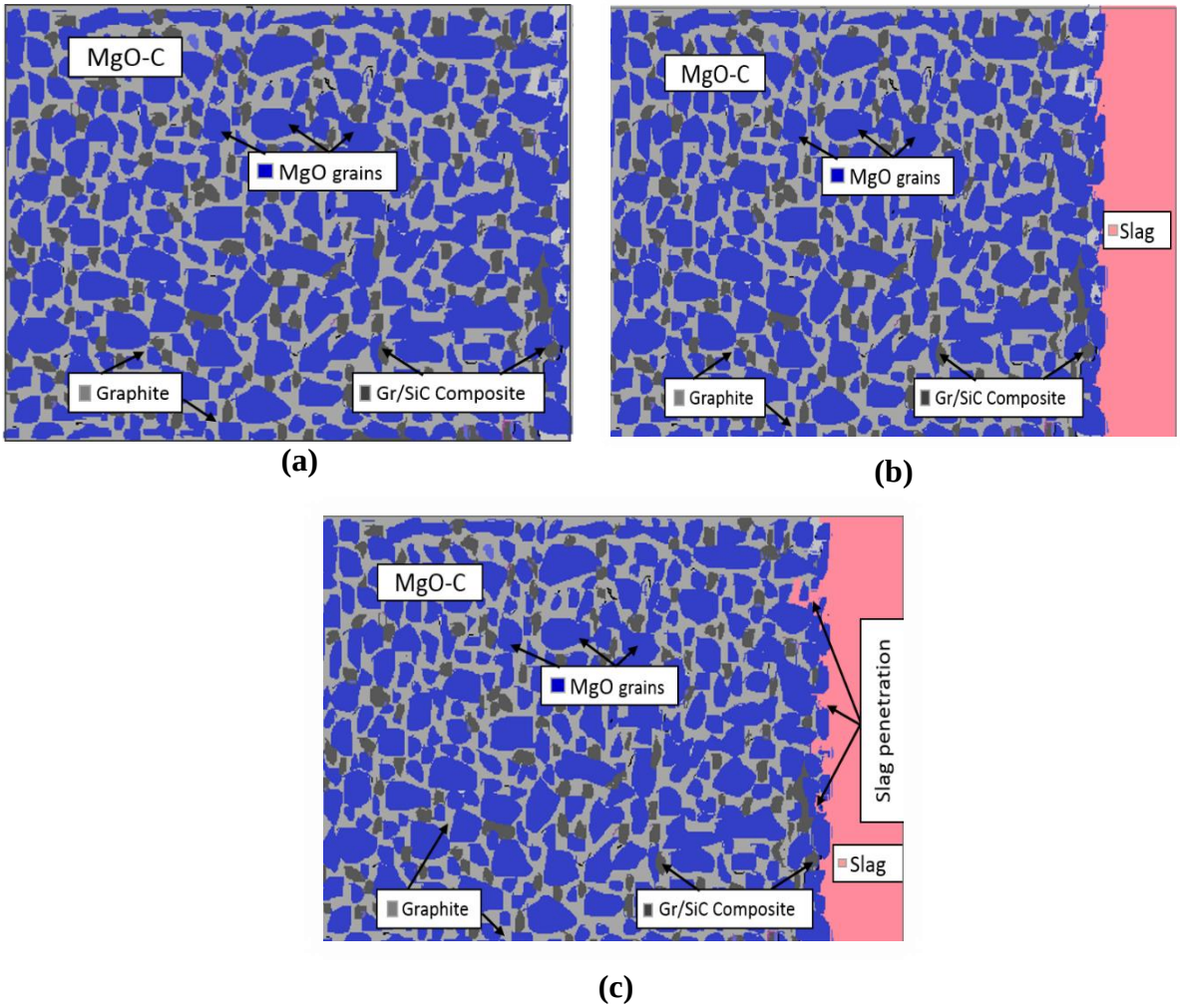

Figure 4.36: Slag corrosion mechanism of microcomposite containing MgO-C brick

4.6. Comparing properties of commercial ß-SiC containing MgO-C brick with commercial brick and microcomposite containing magnesia carbon refractories.

In being Figure 4.37 compared the properties of three different types of MgO-C bricks (MC00, MCCS and MC33A). Here, MC00 brick is prepared with pure graphite (standard commercial composition as mentioned in Table 4.6). The MCCS and MC33A bricks were made by the addition of commercially available free ß-SiC with the addition of 1wt% as well as by addition of 30/70 (silica/ graphite) microcomposite with 3wt%, respectively. The microcomposite consists of 30wt% of SiC and rest as graphite. Here, 94FC based graphite was used for both microcomposites preparation and brick fabrication.

4.6.1. Bulk Density (BD)

The bulk density of the three different types of MgO-C bricks (MC00, MCCS and MC33A) before and after coking is plotted in Figure 4.37. The standard conventional MgO-C brick (MC00) attained a BD of 3.01gm/cc. Moreover, the slight increment of BD is observed for MCCS brick with the addition of ß-SiC, but a high value of BD is measured for MC33A brick in the presence of the 3wt% addition of microcomposite. The MCCS brick achieved less density after coking at 1000ºC/5hrs due to the increased porosity level and decreased density values associated with the increased bulk volume of the sample in the presence of ß-SiC.

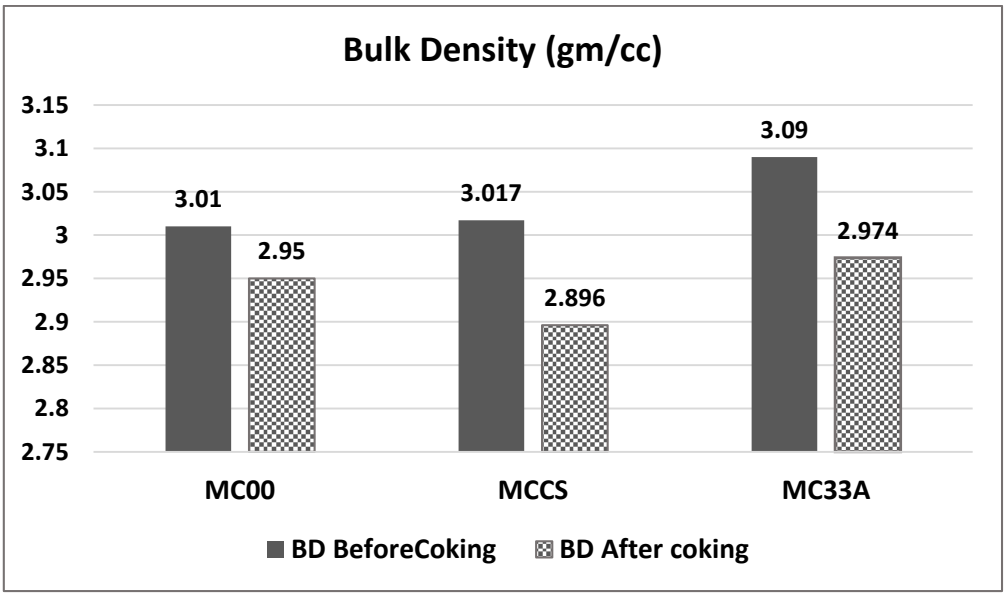

Figure 4.37: BD of the three different types of MgO-C refractories before and after coking

4.6.2. Apparent Porosity (AP)

The variation in the apparent porosity of different kinds of MgO-C bricks before and after coking is plotted in Figure 4.38. Before coking, apparent porosity of MC00 and MC33A bricks is 2.5% and 1.9% respectively. Higher apparent porosity can be observed in MCCS brick due to the incompressibility of the β-SiC. The porosity is slightly increased after coking at 1000°C/5hrs because of the removal of organic and volatile matter.

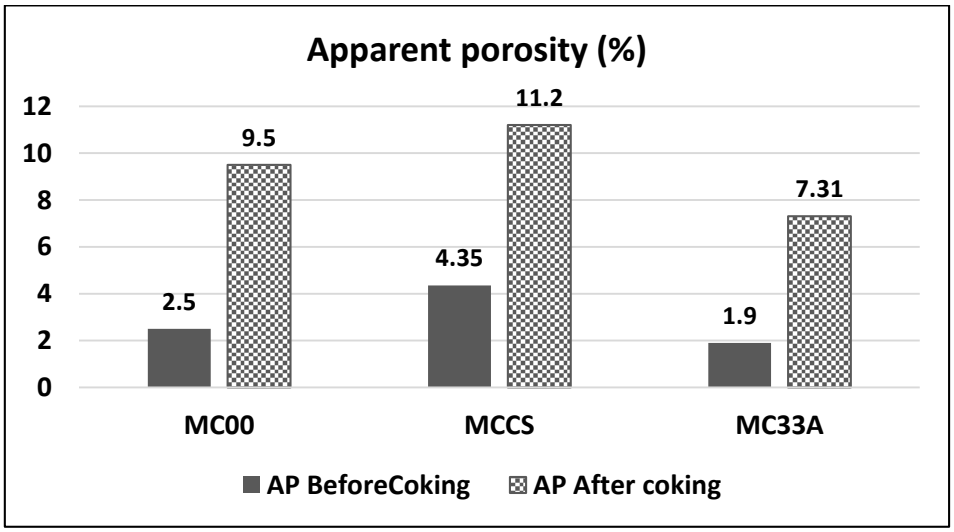

Figure 4.38: AP of the three different types of MgO-C bricks before and after coking.

4.6.3. Cold crushing strength (CCS)

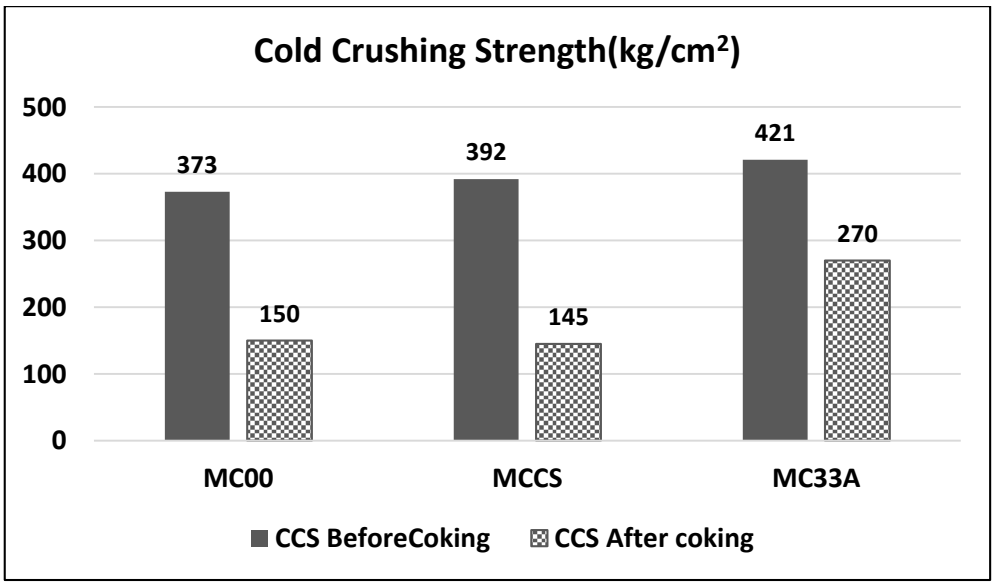

Figure 4.39: CCS of the three different types of MgO-C bricks before and after coking.

Before and after coking, the cold crushing strength (CCS) of the three different types of bricks are shown in Figure 4.39. The CCS of MC00 (standard commercial) brick attained a value of 373kg/cm^2. Moreover, CCS value increased with the addition of commercial β-SiC and graphite/SiC microcomposite. But, the graphite/SiC containing (MC33A) brick achieved higher strength due to the compressibility and flowability of the composite. After coking the CCS is lowered, because of breaking of the organic bonds between the particles which are formed by resin. The lowest CCS value is observed in the MCCS brick due to higher porosity caused by the addition of commercial β-SiC.

4.6.4. Hot Modulus of Rupture (HMOR)

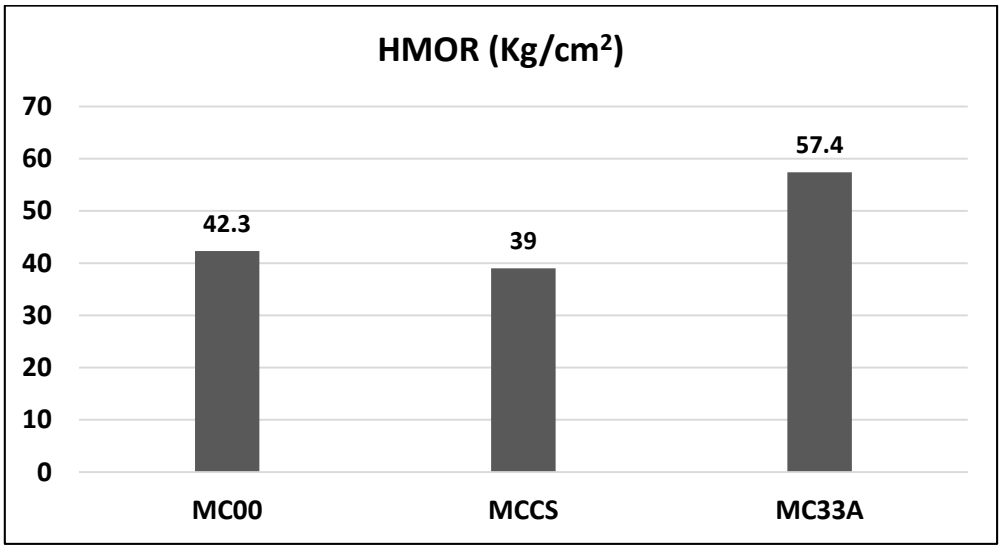

Figure 4.40: Hot modulus of rupture of the three different types of MgO-C refractories after 1400^{o}C/30 min.

In particular, for every refractory system such as MgO–C brick, the hot modulus of rupture is an important property. HMOR results of the three different types of MgO-C bricks are shown in Figure 4.40. The commercial (MC00) brick attained an HMOR value of 42.3 kg/cm^2. However, the brick with the addition of microcomposite has higher HMOR value. Incorporation of microcomposite reduces the residual porosity, which in turn enhances the oxidation resistance, resulting in higher HMOR value. But MCCS brick attained poor HMOR value due to the addition of commercial ß-SiC. However, the addition of ß-SiC causes the brick more porous by oxidation of graphite at higher temperatures, ensuring lower HMOR value.

4.6.5. Oxidation resistance

The oxidised area of the different types of magnesia carbon refractories, after oxidation at 1000°C/5hrs, is shown in Figure 4.41. MC33A brick has greater oxidation resistance in contrast to MC00 and MCCS bricks. This is due to deposition of SiC on the graphite flakes, which enhances the oxidation resistance.

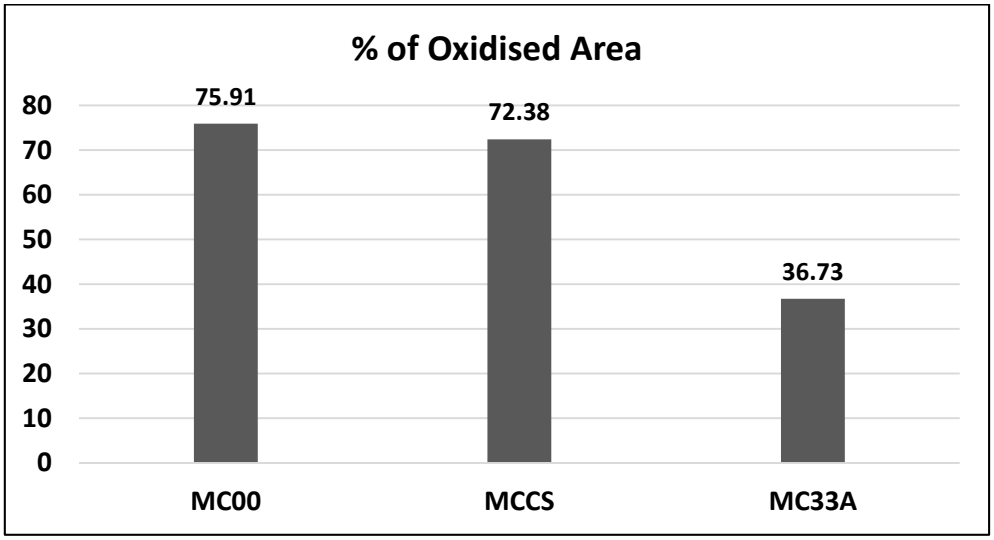

Figure 4.41: Oxidation resistance of the three different types of MgO-C refractories after oxidizing at 1000°C/5hrs.

The Figure 4.42 shows the cross-sectional view of the oxidised bricks after oxidation test. Its colour clearly separates the oxidized layer (yellow) and unoxidized region (black). The thickness of the oxidized layer is more in case of MC00 and MCSS bricks due to the exhaustion of a large amount of graphite. However, the MC33A brick possesses the thinnest oxidised layer and the brick cross-section has the smoothest surface. The cross-sectional surface of the MCCS brick appears as rough due to oxidation of graphite.

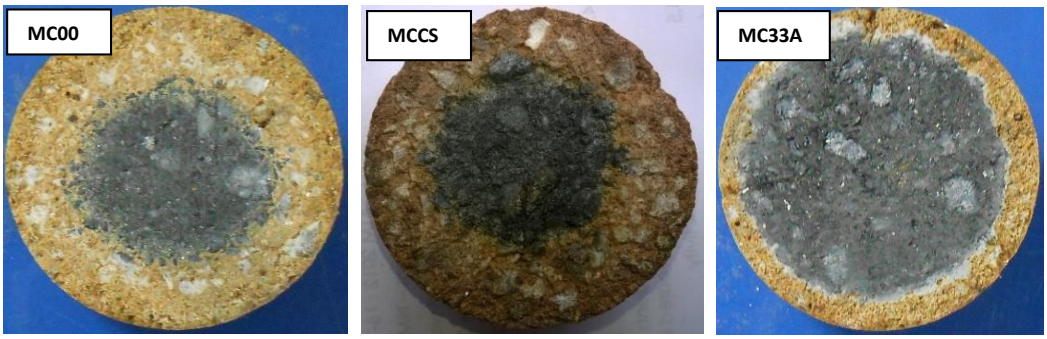

Figure 4.42: Photographs of the cut cross sections of the oxidized MgO-C bricks

Conclusion

Both laboratory investigation in small scale and industrial experiments on relatively large scale confirm the beneficial effects of addition of the micro-composite to the MgO-C brick composition replacing a part of flake graphite.

- There is a consistent improvement in most of the physical properties of the MgO-C particularly up to an addition of 3wt% micro-composite prepared from 30/70 ratio of SiO_2/Graphite. However, for higher percentages of silica (40 and 50wt%) the results are not so consistent possibly due to the presence of unreacted silica (cristobalite) and also due to formation of SiC fiber instead of more compact ribbons.
- Lowest AP (1.9%) was observed for the addition of 3wt% composite prepared from a precursor ratio of 30/70.
- Improvement in the purity of the flake graphite (97FC compared to 94FC) results in enhancement of all the properties. Lowest porosity, highest CCS and HMOR together with best oxidation resistance have been obtained when 3wt% of the composite prepared from 97FC graphite (30/70 ratios) is added.
- The addition of 3wt% composite prepared from 30/70 silica-graphite ratio enhances the HMOR of the bricks by 35%. This value becomes 45% with the better quality of graphite used for the preparation of the composite (97FC).
- Industrial level experiments have definitely demonstrated that the addition of the micro-composite in the appropriate amount leads to 20% enhancement of the CCS value and around 55% reduction in oxidation property of the bricks.
- The MgO-C brick properties are degrading with the addition of 1wt% commercial free ß-SiC compared to the addition of 3wt% microcomposites in which in-situ developed ß-SiC is near to 30wt%.
- However, SiC content of the micro-composite has to be restricted up to a certain level to restrict the formation of forsterite at high temperature and thereby deterioration of the slag corrosion property of the brick. The exact limit is still to be determined. Nonetheless as per the current status of the investigation, overall SiC content of the brick may have to be limited to ~3wt%.

Future work

An extensive study on the synthesis of graphite/SiC microcomposites and their utility to improve the MgO-C refractory properties has opened up a tremendous scope for further research. However, several important and the following information are needed to deliver for the commercial viability in future.

- Estimation of thermal conductivity of the developed bricks and their correlation with corrosion behaviour with respect to time.
- Estimation of the dynamic slag corrosion test and understand their mechanism through microstructural and phase studies.
- Fabrication of an appreciable number of bricks from proposed composites, and compare their performance in steel ladle (minimum two layers in slag zone) with respect to existence MgO-C brick composition.

References

[1] X.K. Li, L. Liu, Y.X. Zhang, Sh. D. Shen, Sh. Ge, L.Ch. Ling., Synthesis of nanometre silicon carbide whiskers from binary carbonaceous silica aerogels. Carbon 39, 159–165 (2001).

[2] Z. G. Cambaz, G. N. Yushin, and Y. Gogotsi., Formation of carbide-derived carbon on ß-silicon carbide whiskers. J. Am. Ceram. Soc., 89[2] 509–514 (2006).

[3] E. Karamian, H. Amini, A. Monshi, A. Bataille, "The role of silicon doped carbon powder on the formation ß-sic whiskers nano sized diameter in silicon-carbon-resole composite materials" ECCM15 - 15TH European conference on composite materials, Venice, Italy, 24 -28 (2012).

[4] Brian D. Bertram and Rosario A. Gerhardt, "Properties and applications of ceramic composites containing silicon carbide whiskers", ISBN 978-953-307-201-2, (2011).

[5] Jens Erik Davidsen, "Formation of Silicon Carbide in the Silicomanganese Process (Ref: Lindstad, 2002; Nederland, 1986).

[6] Xinfa Qiang, Hejun Li, Yulei Zhang, Linjun Guo, Jianfeng Wei, "Microstructure and anti-oxidation property of Si–W–Cr coating for SiC coated carbon–carbon composites", Journal of Alloys and Compounds509 L249–L253 (2011).

[7] C. G. Aneziris, J. Hubalkova, and R. Barabas, "Microstructure evolution of MgO-C refractories with TiO_2 and Al- additions," J. Eur. Ceram. Soc., 27(1) 73-78 (2007).

[8] F.Q. Ma, and L. Jing, "Experimental study on optimization of slag splashing modifiers with magnetic trailing," Applied Mechanics and Materials, 395, 302-307 (2013).

[9] W.E. LEE and S. ZHANG, "Direct and indirect slag corrosion of oxide and oxide-C refractories". VII International Conference on Molten Slags Fluxes and Salts (2004).

[10] S. Zhang, W.E. Lee, "Influence of additives on corrosion resistance and corroded microstructures of MgO–C refractories". Journal of the European Ceramic Society 21 2393–2405 (2001).

[11] Chen-Feng Chan, Bernard B. Argent, and William E. Lee, "Influence of Additives on Slag Resistance of Al_2O_3–SiO_2–SiC–C Refractory Bond Phases under Reducing Atmosphere". J. Am. Ceram. Soc., 81[12] 3177–88 (1998).

Publications originating from M.Tech (Research) work

Journal Publication

1. **Raju Mula**, Tapas Mahata, Debasish Sarkar, Himadri Sekhar Maiti, "Synthesis of graphite-SiC microcomposite by carbothermal reduction process **(to be communicated after patent filing)**.

2. **Raju Mula**, Tapas Mahata, Debasish Sarkar, Himadri Sekhar Maiti, "Effect of graphite/SiC micro composites on physicochemical properties of MgO-C refractory compositions" **(to be communicated after patent filing)**.

Patents:

3. **Raju Mula**, Tapas Mahata, Debasish Sarkar, Himadri Sekhar Maiti, "Preparation Process of Graphite-SiC Microcomposite from Graphite and Microfine Silica" (Indian patent to be filed)

4. **Raju Mula**, Tapas Mahata, Debasish Sarkar, Himadri Sekhar Maiti, "High-Grade MgO-C Brick by Graphite-SiC Microcomposite" (Indian patent to be filed)

Curriculum Vitae

Mula Raju,

C/o - R. Babu Rao,

Gavarammapeta (Vil), Piruvada (Post),

Polaki Mandal, Narasannapeta (Taluk),

Srikakulam Dist**,** AP-532421

Mobile. No: 09490391373, 09040868966

E-Mail: rajumula8@gmail.com

Date of Birth: 20-06-1990

Educational Qualification:

M.Tech (Research) in Ceramic Engg. (2015) NIT Rourkela, Odisha, India

B. Tech in Ceramic Engg. (2011), Andhra University Visakhapatnam, AP, India

Industrial Experience:

- ✓ Worked as a GET at **WS Industries (India) Limited**, Visakhapatnam in "Glazing & Quality in Process Inspection" department.
- ✓ Worked as a graduate trainee at **TRL Krosaki Refractories**, Belpahar in "R&D" department.

Publications & Patents:

1. **Raju Mula**, Tapas Mahata, Debasish Sarkar, Himadri Sekhar Maiti, "Synthesis of graphite-SiC microcomposite by the carbothermal reduction process.
2. **Raju Mula**, Tapas Mahata, Debasish Sarkar, Himadri Sekhar Maiti, "Effect of graphite/SiC micro composites on physicochemical properties of MgO-C refractory compositions."
3. **Raju Mula**, Tapas Mahata, Debasish Sarkar, Himadri Sekhar Maiti, "Preparation Process of Graphite-SiC Micro Composite from Graphite and Microfine Silica" (Indian patent to be filed)
4. **Raju Mula**, Tapas Mahata, Debasish Sarkar, Himadri Sekhar Maiti, "High Grade MgO-C Brick by Graphite-SiC Microcomposite" (Indian patent to be filed)

Department of Ceramic Engineering

National Institute of Technology, Rourkela

Rourkela-769008, Odisha, India